The Dissertation Committee for Sara Marie Nowinski Certifies that this is the approved version of the following dissertation:

Mitochondrial uncoupling links lipid catabolism to Akt inhibition and blockade of skin tumorigenesis

Committee:

Edward M. Mills, Supervisor

Shawn B. Bratton

John DiGiovanni

Karen M. Vasquez

Casey W. Wright

Mitochondrial uncoupling links lipid catabolism to Akt inhibition and blockade of skin tumorigenesis

by

Sara Marie Nowinski, B.A.

Dissertation

Presented to the Faculty of the Graduate School of

The University of Texas at Austin

in Partial Fulfillment

of the Requirements

for the Degree of

Doctor of Philosophy

The University of Texas at Austin

August 2014

Dedication

To my grandparents, Jim and Claudia.

I wish you could be here to see it.

Acknowledgements

First, I would like to thank my mentor, Dr. Ted Mills, for the endless support and countless opportunities he has provided throughout my time in his laboratory. Over the past six years, you have become not only a trusted adviser, but also my biggest advocate, and a good friend. As I continue my career in science, I hope to emulate your enthusiasm, to have many more opportunities to talk about science together, and to think of you when I need a reminder that sometimes "cowboy" experiments do work.

I also owe many thanks to Dr. Sue Fischer and Dr. John DiGiovanni. Although not official Co-mentors, you both opened your labs and your guidance to me and were instrumental in guiding this project to completion. Similarly, I do not know what I would have done without Dr. Joyce Rundhaug and Dr. Okkyung Rho. Each of you has taught me so much, and I am so grateful that our collaboration gave us the opportunity to work together. I would also like to express my gratitude to my other committee members, Drs. Shawn Bratton, Karen Vasquez, and Casey Wright, for their criticism, advice, and encouragement.

Additionally, I need to thank Dr. Matt Rand for convincing me that I did not want to go to medical school. You were right.

I am incredibly grateful to have shared my time in graduate school with the other members of the Mills lab, past and present. Thank you for your help with experiments, and perhaps more importantly, your friendship. I would especially like to thank Dr. Cory Lago, for starting this project and passing it off to me, for answering the hundreds of questions I asked as a brand new grad student, and for the advice that if I don't split the keratinocytes that need to be split today, no one else will do it for me, and they'll be dead tomorrow. It was a good lesson, and one I'll continue to carry forward.

I also particularly want to thank Ashley Solmonson for admitting me to joke school and for always being willing to walk a little further to get good coffee. I know it's a cliché, but I honestly can't imagine sharing this project with anyone else, and there is no doubt in my mind that this project would not be where it is today without you. I feel incredibly lucky to have worked side by side with you on "Team Cancer" for the past three years, and there are about 459 reasons I'll miss you. Good luck with everything, and if you get stuck, call me, I'm probably stuck too.

To my parents, and my family: Thank you for understanding my need to walk the road less traveled through all these years of school. From the math/science center, to the tiny frozen college in the middle of nowhere, to the biggest university in the Lone Star state, you have always supported my decisions, even if they didn't seem to make sense. I love you, and I hope to be closer to home soon.

And finally, I would like to thank my husband, John Nowinski, for still being willing to listen to how my day went each night when I get home. You've been there throughout all the ups and downs, and you always remind me what really matters at the end of the day. I can't wait to start our next adventure together.

Mitochondrial uncoupling links lipid catabolism to Akt inhibition and blockade of skin tumorigenesis

Sara Marie Nowinski, Ph.D.

The University of Texas at Austin, 2014

Supervisor: Edward M. Mills

In order to support rampant cell growth, tumor cells must reprogram metabolism to simultaneously drive macromolecular biosynthesis and energy production. Mitochondrial uncoupling proteins (UCPs) oppose this phenotype by inducing futile mitochondrial respiration that is disengaged from ATP synthesis. We found that uncoupling protein 3 (UCP3) was normally expressed in follicular and epidermal keratinocytes and that its levels were augmented by calcium-induced differentiation *in vitro*. Over-expression of a UCP3 transgene targeted to the basal epidermis by the keratin-5 promoter (K5-UCP3) led to increased differentiation of both epidermal and bulge stem cells, the progenitors of most squamous carcinomas. Consistent with this phenotype, K5-UCP3 mice were completely protected from chemically induced skin carcinogenesis.

To define the mechanisms by which UCP3 conferred such strong tumor resistance, we interbred K5-UCP3 mice with a "pre-initiated" mouse model, and found that UCP3 over-expression blocked tumor promotion. Uncoupled epidermis displayed

reduced proliferation after treatment with tumor promoter, along with diminished activation of Akt signaling. This effect corresponded to decreased Akt activation by epidermal growth factor (EGF) in K5-UCP3 cells, along with UCP3 overexpressing primary human keratinocytes. Mechanistic studies revealed that uncoupling drove global lipid catabolism, along with impaired recruitment of Akt to the plasma membrane. Over-expression of wild type Akt rescued tumor promoter-induced proliferation and two-stage chemical carcinogenesis in bi-transgenic mice. Collectively, these findings demonstrate that mitochondrial uncoupling is an effective strategy to limit cell proliferation and tumorigenesis through inhibition of Akt, and suggest a novel mechanism of crosstalk between mitochondrial metabolism and growth signaling.

Table of Contents

List of Tables

List of Figures

List of Illustrations

List of Abbreviations

Ψ	Mitochondrial membrane potential
3-PG	3-phosphoglycerate
4EBP-1	Eukaryotic translation initiation factor 4E binding protein 1
7AAD	7-Aminoactinomycin D
AAALAC	Association for Assessment and Accreditation of Laboratory Animal Care
ACL	ATP citrate lyase
AML	Acute myeloid leukemia
AMPK	AMP-activated protein kinase
AMS	4-acetamido-4'-maleimidylstilbene-2,2'-disulfonic acid
ATP	Adenosine triphosphate
BAT	Brown adipose tissue
BPE	Bovine pituitary extract
BrdU	5-bromo-2-deoxyuridine
bSC	Bulge stem cell
Ca^{2+}	Calcium
CACT	Carnitine acylcarnitine translocase
CD34	Cluster of differentiation 34
CD36	Fatty acid translocase, FAT
ceUCP	C. elegans uncoupling protein
CO_2	Carbon dioxide
CoA	Coenzyme A
CPT1	Carnitine palmitoyl transferase 1
CPT2	Carnitine palmitoyl transferase 2
DHE	Dihydroethidium
DNA	Deoxyribonucleic acid
DMBA	7,12-dimethylbenz[*a*]anthracene
DMEM	Dulbecco's modified Eagle's medium

e^-	Electrons
EDTA	Ethylenediaminetetraacetic acid
EGF	Epidermal growth factor
EGFR	Epidermal growth factor receptor
eIF4G	eukaryotic initiation factor 4G
EMEM	Eagle's minimum essential medium
ETC	Electron transport chain
Eto	Etomoxir ethyl ester
FACS	Fatty acyl CoA synthetase
FACS	Fluorescence activated cell sorting
$FADH_2$	Flavin adenine dinucleotide
FAT	Fatty acid translocase, CD36
FBS	Fetal bovine serum
FFA	Free fatty acids
FH	Fumarate hydratase
FITC	Fluorescein isothiocyanate
FOXO	Forkhead Box protein O
G6P	Glucose-6-phosphate
G6PD	Glucose-6-phosphate dehydrogenase
GC/MS	Gas chromatography mass spectrometry
GLUT	Glucose transporter protein
GSK-3	Glycogen synthase kinase-3
GTP	Guanosine triphosphate
H+	Protons
H2DCF-DA	2',7'-dichlorodihydrofluorescein diacetate
HBSS	Hank's balanced salt solution
hESC	Human embryonic stem cells
HIF	Hypoxia inducible factor
HK	Hexokinase
HRP	Horseradish peroxidase

IDH1	Isocitrate dehydrogenase 1
IDH2	Isocitrate dehydrogenase 2
IFE	Interfollicular epidermis
IGF-1	Insulin-like growth factor 1
Ivl	Involucrin
K15	Keratin 15
K5	Keratin 5
K5-UCP3	Keratin 5 – uncoupling protein 3
KSFM	Keratinocyte serum free medium
LDH	Lactate dehydrogenase
Lor	Loricrin
LRC	Label retaining cell
MAPK	Mitogen activated protein kinase
MPC	Mitochondrial pyruvate carrier
mtDNA	Mitochondrial DNA
mTOR	Mammalian target of rapamycin
mTORC1	mTOR complex 1
mTORC2	mTOR complex 2
NADH	Nicotine adenine dinucleotide
NADPH	Nicotine adenine dinucleotide phosphate
NHK	Neonatal human primary keratinocytes
$O_2^{-\bullet}$	Superoxide free radical
OA	Okadaic acid
PCR	Polymerase chain reaction
PDH	Pyruvate dehydrogenase
PDK1	Phosphoinositide-dependent kinase 1
PE	Phycoerythrin
PFK	Phosphofructokinase
PGC-1α	Peroxisome proliferator-activated receptor-gamma coactivator - 1 alpha

PH	Pleckstrin homology domain
PI3K	Phosphatidylinositol 3-kinase
PIP2	Phosphatidylinositol 4,5-bisphosphate
PIP3	Phosphatidylinositol (3,4,5)-trisphosphate
PKC	Protein kinase C
PKM2	Pyruvate kinase, M2 isoform
PP2A	Protein phosphatase 2A
PP2Ac	Protein phosphatase 2A catalytic subunit
PPP	Pentose phosphate pathway
PTEN	Phosphatase and tensin homolog
Ripa	Radioimmunoprecipitation assay buffer
ROS	Reactive oxygen species
RTK	Receptor tyrosine kinase
RT-PCR	Reverse transcription polymerase chain reaction
SCO2	Synthesis of Cytochrome c Oxidase 2
SDH	Succinate dehydrogenase
SDS-PAGE	Sodium dodecyl sulfate polyacrylamide gel electrophoresis
SLC	Solute carrier
SOD	Superoxide dismutase
Sprr	Small proline rich protein
SREBP	Sterol response element binding protein
TCA	Tricarboxylic Acid
TPA	12-O-tetradecanoylphorbol-13-acetate
TSC2	Tuberous sclerosis 2
UCP	Uncoupling protein
UPLC/MS/MS	ultrahigh performance liquid chromatography/mass spectrometry
VHL	Von hippel lindau protein

Chapter 1: Introduction

1.1 Background: Hallmarks of cancer

Cancer is the general term for a group of over 100 diverse diseases that all stem from the uncontrolled growth of abnormal cells in the body. This uncontrolled growth leads to the formation of tumors, and eventually, the ability to invade other tissues, or metastasize. If left untreated, cancer cells continue to proliferate out of control, crowding out normal cells and causing serious illness and ultimately, death. 40.8% of men and women in the US will be diagnosed with some form of cancer in their lifetime, with 13,397,159 people living with cancer in the US as of 2011, the most recent year for which incidence data is available (NCI, 2014).

The National Cancer Institute estimates that 585,720 patients in the US will die in 2014 from all types of cancer combined. However, with the advent of new therapies and better screening procedures that allow for earlier detection and treatment, mortality rates have been falling on average 1.5% per year from 2001-2010 (NCI, 2014). Even so, many approaches to treat cancers still involve invasive surgeries, and/or therapies that non-selectively target all rapidly growing cells in the body for destruction, and therefore have devastating side effects for patients. Moreover, current therapies are often still not as efficacious as one would hope: only 66.1% of cancer patients survive 5 years after diagnosis, with the survival rates for certain sub-types being much worse (NCI, 2014).

Thus, new strategies to effectively combat cancer with lower patient toxicity are sorely needed.

In 2000, Hanahan and Weinberg released a list detailing the hallmarks of cancer, regardless of the specific disease or tissue of origin, in an effort to describe widespread traits or processes that are functionally central to tumorigenesis, and are therefore attractive therapeutic targets. Their list included six qualities exhibited by most, if not all cancers: sustained proliferative signaling, evasion of growth suppressors, resistance to cell death, replicative immortality, induction of angiogenesis, and the ability to invade and metastasize to distant tissues (Hanahan and Weinberg, 2000). Hanahan and Weinberg postulated that although the order of acquisition may differ in specific cancers, a tumor cell must develop these six abilities in order to become tumorigenic, and ultimately, malignant.

Ten years later, the authors revisited their original list, and added two new processes as additional emerging hallmarks: the ability to evade detection and destruction by the immune system, and the reprogramming of energy metabolism to support the energetic and biosynthetic needs of rampant growth (Hanahan and Weinberg, 2011). Metabolic reprogramming, in particular, has gained attention over the past decade, in part because of the mounting evidence supporting a complex interplay between pervasive oncogenic growth signaling pathways and metabolic control. Herein, we describe a novel strategy to antagonize tumorigenesis by opposing the metabolic phenotype of tumor cells, and uncover a novel mechanism of metabolic regulation of growth signaling.

1.2 Cellular bioenergetics in non-proliferating, differentiated cells

Most cells rely on systemic metabolism to break down food into two major fuel sources: sugars, such as glucose, and fats, which circulate mainly in the form of non-esterified free fatty acids (FFA) bound to albumin. These fuel sources are taken up and further broken down through the pathways of glycolysis (breakdown of sugars) and β-oxidation (breakdown of fatty acids, also called fatty acid oxidation). Ultimately, these pathways feed metabolites into mitochondria, where they are completely oxidized through highly efficient metabolic pathways that maximize energy production in a process known as oxidative phosphorylation, leaving only carbon dioxide (CO_2) and water as byproducts.

1.2.1 Glycolysis

Sugars, such as glucose, are a primary fuel source for cells. Glucose enters the cell through a member of the GLUT family of transporter proteins, and is phosphorylated by the enzyme hexokinase (HK), producing glucose-6-phosphate (G6P). This reaction is the first and rate-limiting step in the pathway of glycolysis, and, because G6P is not transported by GLUTs, this modification functionally "traps" the glucose inside the cell (Berg et al., 2002). G6P can be stored as glycogen in some cell types (mainly muscle and liver), or else is broken down in a series of subsequent glycolytic reactions, resulting in the production of two molecules of pyruvate for each molecule of glucose metabolized (Illustration 1.1). In the process, glycolysis also yields a net of two molecules of

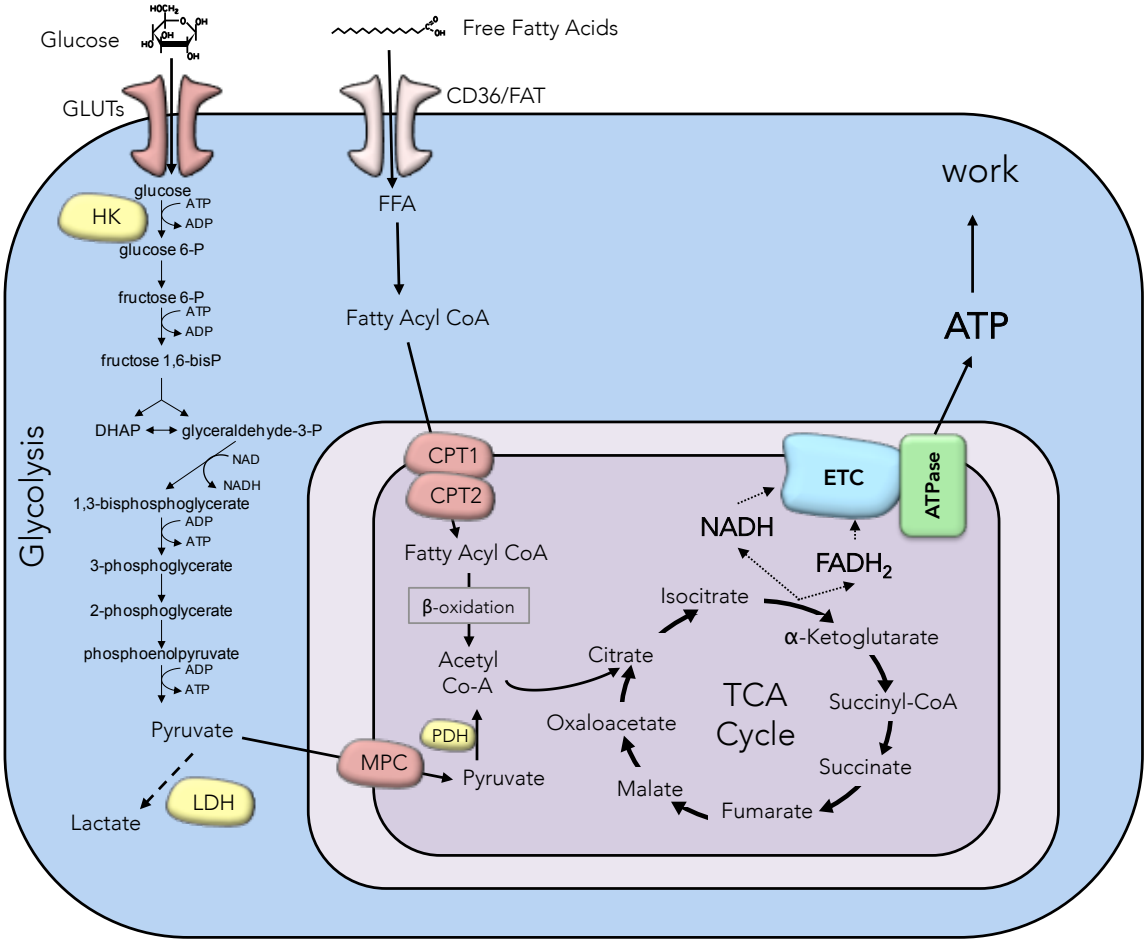

Illustration 1.1 Normal cellular bioenergetics

In non-proliferating, differentiated cells, glycolysis and fatty acid oxidation contribute to the production of acetyl-CoA in the mitochondria. Acetyl Co-A feeds the TCA cycle, which produces the reduced co-factors NADH and $FADH_2$. These serve as substrates for the electron transport chain (ETC), which together with the F_1/F_0-ATPase generates ATP to be used for cellular work. Non-proliferating cells use metabolic pathways that maximize ATP production.

adenosine triphosphate (ATP), the coenzyme used by cells as the molecular energy currency (Berg et al., 2002).

In the absence of oxygen (O_2), pyruvate can be further metabolized to lactate by the enzyme lactate dehydrogenase (LDH) in a process known as lactic acid fermentation. However, in most differentiated cells, lactic acid fermentation is inhibited in the presence of oxygen, a phenomenon commonly referred to as the Pasteur Effect (Warburg, 1926). Very high extracellular glucose concentrations can drive fermentation in the presence of oxygen via the Crabtree Effect, in which the elevated levels of glycolytic intermediates suppress mitochondrial respiration. However, ordinarily, when oxygen is present (and glucose concentrations are not elevated), normal cells further metabolize pyruvate in the mitochondria. Pyruvate is imported into the mitochondria by the mitochondrial pyruvate carrier (MPC) (Bricker et al., 2012), where it is subsequently converted to acetyl-CoA by pyruvate dehydrogenase (PDH) (Illustration 1.1).

1.2.2 Fatty Acid Oxidation

In an analogous process, FFA are imported into cells, often by the fatty acid translocase (FAT/CD36) (Coburn et al., 2000; Febbraio et al., 1999). Although certain FFA are oxidized by peroxisomes, most β-oxidation takes place in mitochondria (Eaton, 2002). Once inside the cell, the fatty acids are modified by one of a number of fatty acyl-Coenzyme A synthetases (FACS), which vary in tissue expression and substrate preference. FACS conjugates the acyl chain to a CoA molecule, and the CoA is then exchanged for a carnitine moiety by carnitine palmitoyl transferase 1 (CPT1), in the rate-

limiting step in β-oxidation (Kopec and Fritz, 1971). Then, the acylcarnitine species is transported into the mitochondria by carnitine acylcarnitine translocase (CACT), and the carnitine is exchanged for CoA again by carnitine palimtoyl transferase 2 (CPT2) (Kopec and Fritz, 1973). The mitochondrial acyl-CoA molecule is then oxidized in a series of subsequent oxidation reactions, resulting in the systematic cleavage of the fatty acid into two-carbon acetyl-CoA units (Illustration 1.1).

1.2.3 Oxidative Phosphorylation

Regardless whether it is formed from glycolysis and pyruvate dehydrogenase, or via β-oxidation of lipids, the acetyl-CoA produced from the breakdown of sugars or lipids becomes a substrate for the Tricarboxylic Acid (TCA) cycle, also referred to as the Citric acid cycle, or Krebs cycle. In the TCA cycle, acetyl-CoA and oxaloacetate are combined to form citrate, which is then further metabolized, ultimately producing two molecules of CO_2, one molecule of guanosine triphosphate (GTP), and regenerating oxaloacetate for the next turn of the cycle (Illustration 1.1) (Berg et al., 2002). The oxidizing reactions of the TCA cycle also produce the reduced cofactors nicotinamide adenine dinucleotide (NADH) and flavin adenine dinucleotide ($FADH_2$) (Illustration 1.1).

Electrons (e^-) are passed from these reduced co-factors through a series of several large protein complexes, known as the electron transport chain (ETC). NADH and $FADH_2$ feed electrons to complex I (NADH dehydrogenase or NADH-Q oxidoreductase) and complex II (succinate dehydrogenase, SDH or succinate-Q reductase) of the ETC, respectively. The electrons are shuttled from complexes I and II to complex III (Q-

cytochrome *c* oxidoreductase) by coenzyme Q, and then cytochrome *c* carries the electrons to complex IV (cytochrome *c* oxidase), where they are used to ultimately reduce molecular oxygen to water (Illustration 1.2). In the process, the flow of electrons through complexes I, III, and IV causes these complexes to pump protons (H^+) from the mitochondrial matrix into the intermembrane space (Saraste, 1999). This establishes an electrochemical proton gradient across the mitochondrial inner membrane that is referred to as the mitochondrial membrane potential (Ψ). The gradient provides the proton motive force that drives the F_1/F_0 ATPase (complex V of the ETC), which allows protons to flow back down their gradient into the matrix, and uses this energy to produce ATP in a process termed oxidative phosphorylation (Boyer, 1993) (Illustration 1.2).

Oxidative phosphorylation produces 17 molecules of ATP from each acetyl-CoA molecule that enters the cycle, or 36 ATP per original glucose molecule, including the 2 ATP formed in glycolysis (Berg et al., 2002). Depending on tissue type, cells maintain a relatively narrow ATP concentration range of about 1-10 mM (Beis and Newsholme, 1975). Cells manage this optimal concentration through a process of "respiratory control," in which high ATP concentrations inhibit the F_1/F_0-ATPase, causing respiration and electron transport to slow. Sometimes, this slowing of respiration can cause e^- to slip from the chain, resulting in the incomplete reduction of oxygen, and the production of reactive oxygen species (ROS), most commonly in the form of superoxide free radical ($O_2^{-\bullet}$) (Turrens et al., 1982), which is readily converted to hydrogen peroxide by superoxide dismutases (SOD). ROS can play diverse roles in cellular physiology depending upon the context, concentration, and spatial microenvironment in which they

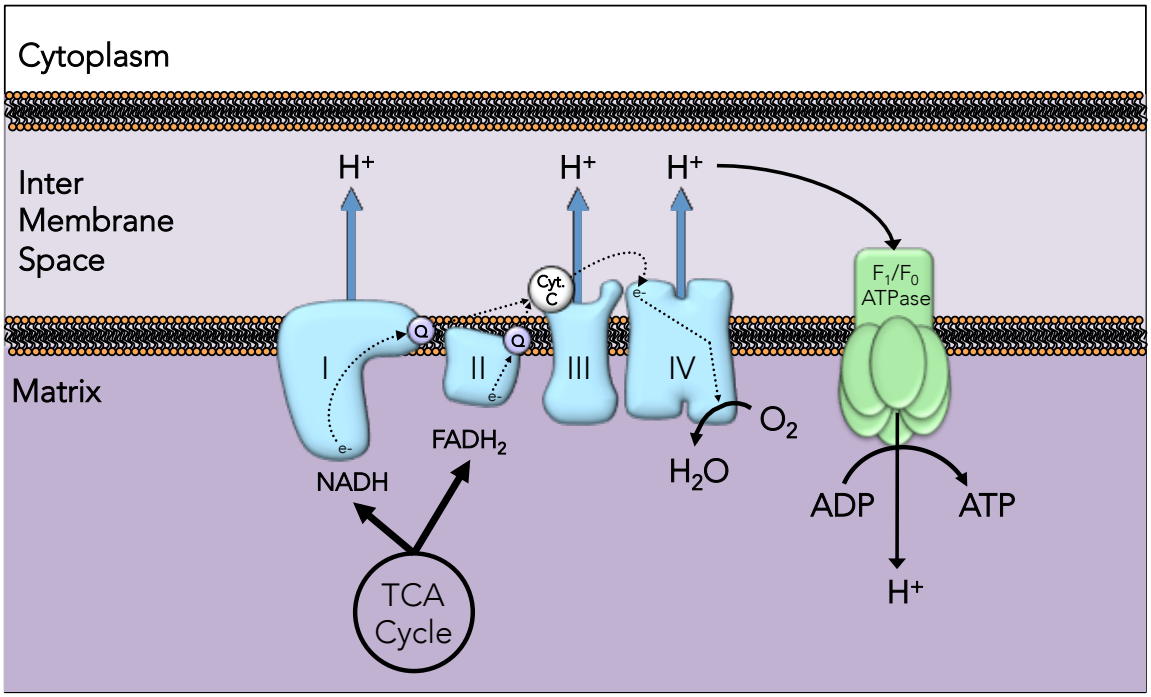

Illustration 1.2 The mitochondrial electron transport chain (ETC) and oxidative phosphorylation

Reactions within the TCA cycle produce the reduced cofactors NADH and $FADH_2$, which feed their electrons (e^-) to complexes I and II of the ETC, respectively. Within the complexes, the electrons are passed to Coenzyme Q, which shuttles them to complex III. Complex III then passes the e^- to Cytochrome c, which passes them to complex IV, where they are ultimately used to reduce molecular oxygen to water. In the process, the movement of e^- through complexes I, III, and IV induces conformational changes in the complexes that cause protons (H^+) to be pumped from the mitochondrial matrix into the intermembrane space. This generates an electrochemical proton gradient that generates the mitochondrial membrane potential (Ψ). The Ψ provides a proton motive force that is used to drive the F1/F0-ATPase (also known as complex V). As H^+ flow back down their gradient, they drive the F1/F0-ATPase in a rotary motion, and catalyze the phosphorylation of ADP, generating the major source of cellular ATP. This process is known as mitochondrial oxidative phosphorylation.

are produced; ROS have been shown to act as pro-growth second messengers (Rhee et al., 2000), but can form deleterious protein and DNA adducts and eventually cause cell death. Thus, mitochondria have evolved antioxidant defense systems to effectively mitigate ROS production while maintaining ideal ATP concentrations (Turrens, 2003).

1.3 Cancer and Metabolism

Most of what we know about cellular bioenergetics comes from early studies performed on whole, intact tissues. As a result, these studies detail the metabolic pathways utilized by normal, differentiated cells. However, the metabolic phenotype exhibited by rapidly dividing cells is actually drastically different from that of post-mitotic, differentiated cells. In the last decade, researchers have renewed efforts to understand Otto Warburg's nearly century-old observation that tumor cells undergo a metabolic switch, implementing aerobic glycolysis (Warburg, 1956b). In addition to up-regulating glycolysis, changes in mitochondrial function appear to suppress mitochondrial oxidative phosphorylation, and re-direct nutrient utilization towards biosynthesis (DeBerardinis et al., 2007; Portais et al., 1996).

This sets up an interesting metabolic dichotomy wherein differentiated cells completely metabolize substrates in favor of maximally efficient energy production, whereas dividing cells favor metabolic pathways that may be less efficient in terms of energy production, but also allow the cells to amass metabolic intermediates (Illustration 1.3). This crucial restructuring of tumor cell metabolism allows cells to balance energy

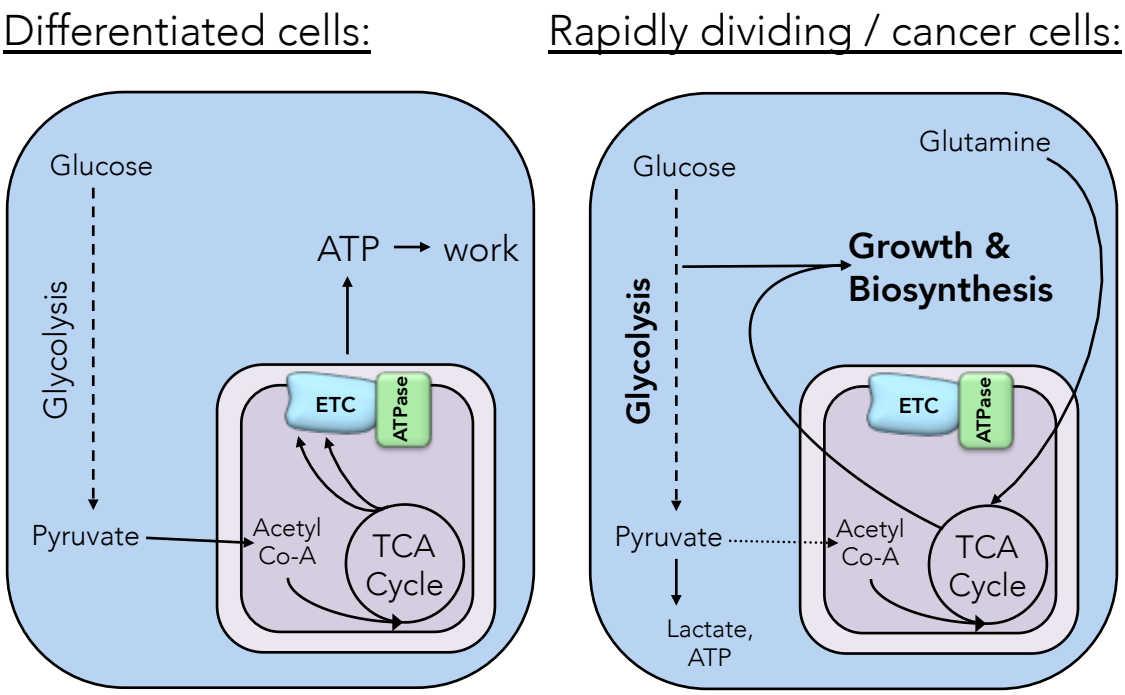

Illustration 1.3 Malignant cells display an altered metabolic phenotype

Differentiated cells utilize metabolic pathways that completely metabolize substrates in favor of maximal energy production. To that end, they rely heavily on mitochondrial oxidative phosphorylation for the production of ATP. In contrast, proliferating cells use metabolic pathways that may be less efficient in terms of energy production, but also provide precursors for macromolecular biosynthesis. Hence, they up-regulate aerobic glycolysis and glutamine anaplerosis.

and biomass production, and is controlled by classical oncoproteins and tumor suppressors, such as *c*-Myc, hypoxia inducible factors (HIFs), p53, mammalian target of rapamycin (mTOR), phosphatidylinositol 3-kinase (PI3K), and Akt (protein kinase B) (Dang and Semenza, 1999; Matoba et al., 2006; Ward and Thompson, 2012).

1.3.1 The Warburg Effect

In the 1920s, Otto Warburg made the seminal observation that, compared to normal cells, cancer cells consume highly elevated quantities of glucose, and metabolize it predominantly through glycolysis and lactic acid fermentation, even in oxygen-replete conditions (Warburg, 1925, 1956a). This process, termed aerobic glycolysis, coincided with drastically lower rates of mitochondrial glucose oxidation in tumor cells (relative to their normal counterparts), an observation that led Warburg to propose that mitochondrial respiratory depression was actually the *cause* of cancer (Warburg, 1956a, b). He suggested that cancer cells arise from a defect in mitochondrial respiration that forces them to rely on aerobic glycolysis in order to compensate for the mitochondrial dysfunction (Warburg, 1956b). Although we now know that Warburg's hypothesis was incorrect, and mitochondrial dysfunction is clearly not the major underlying cause of cancer, a number of studies (detailed below) have identified genetic alterations that do impair mitochondrial respiration in various cancer types. Nonetheless, it appears that in a majority of cancers, the mitochondria are respiration competent, but cells down-regulate mitochondrial oxidative metabolism in favor of aerobic glycolysis (Fantin et al., 2006; Lunt and Vander Heiden, 2011; Moreno-Sanchez et al., 2007).

This phenomenon, now known as "the Warburg effect," seems paradoxical on the surface: Why would cancer cells use aerobic glycolysis, a less efficient means of energy production, rather than oxidative phosphorylation? The phenomenon of aerobic glycolysis is not exclusive to cancer cells – in fact, many normal cell types employ aerobic glycolysis during rapid proliferation. For example, primary lymphocytes up-regulate glucose uptake and lactate production upon proliferative stimulation (Hedeskov, 1968; Wang et al., 1976). Furthermore, chick embryos exhibit the same rate of lactate production whether normal or transformed (Steck et al., 1968). Therefore, it appears that rapidly dividing cells systematically employ aerobic glycolysis, regardless of malignant transformation, likely because it provides some advantage during proliferation.

1.3.2 Balancing energy production & macromolecular biosynthesis

We now appreciate that tumor cells' seemingly paradoxical reliance on the less efficient process of glycolysis for generation of ATP likely confers a growth advantage by permitting cells to balance the need to produce energy with the need to produce biomass. Put simply, dividing cells must adapt their metabolic program to simultaneously generate the biosynthetic precursors necessary for building the lipids, proteins and nucleic acids that will comprise the new daughter cell, along with the energy needed to grow and divide. To accomplish this goal, cancer cells up-regulate pathways that allow them to accumulate metabolic intermediates that can be shunted away from oxidative pathways and into anabolic reactions.

1.3.2.1 Aerobic glycolysis

The glycolytic arm of metabolic reprogramming has become an area of intense research in cancer, in part because it is such a pervasive phenotype. Relative to non-tumorigenic tissue, cancer cells up-regulate GLUTs (Macheda et al., 2005; Medina and Owen, 2002), glycolytic enzymes (Vander Heiden et al., 2009), and LDH (Shim et al., 1997). Malignancies so reliably exhibit increased glucose uptake that this property provides the basis for clinical [F^{18}] fluoro-deoxyglucose positron emission tomography (FDG-PET) imaging. Several studies have shown that glucose is a critical nutrient for dividing cells (Holley and Kiernan, 1974; Pardee, 1974), and glucose deprivation induces apoptosis that is functionally indistinguishable from that seen in response to growth factor withdrawal (Vander Heiden et al., 2001). Extensive work has shown that aerobic glycolysis supports the growth and survival of malignant cells and may be a promising therapeutic target (Dang et al., 1997; Semenza, 2000). However, although the initial phenomenological observations are decades old, and the underlying process is now well described, specifically what benefit the utilization of aerobic glycolysis provides tumor cells was not immediately obvious to researchers.

One possibility to explain why proliferating cells might up-regulate this process is that glycolytic production of ATP can occur more rapidly than oxidative ATP production (Pfeiffer et al., 2001). Be that as it may, the percentage of cellular ATP derived from glycolysis varies dramatically depending on tumor type and experimental context (0.31%-64%), and normal tissues exhibit an overlapping range of glycolytic contribution to total cellular ATP (0.94%-58%) (Zu and Guppy, 2004). Furthermore, it has been

suggested that ATP is likely not limiting in proliferative cells (Lunt and Vander Heiden, 2011). Thus, it appears that aerobic glycolysis likely provides some adaptive value other than enhanced rate of ATP production.

This benefit seems to come in the form of the provision of substrates for biosynthetic pathways that branch off at various steps in glycolysis. As a result, glycolysis provides carbons that are subsequently used for nucleotide, lipid, and amino acid biosynthesis. More specifically, glycolysis contributes to nucleotide biosynthesis through the production of G6P, which can be metabolized by G6P dehydrogenase (G6PD) and subsequent enzymes to produce ribose-5-phosphate and subsequently phosphoribosylpyrophosphate (PRPP), the major precursor for the synthesis of nucleotides (Illustration 1.4) (Berg et al., 2002). This pathway, often termed the pentose phosphate pathway (PPP), also produces the reduced form of the co-factor nicotinamide adenine dinucleotide phosphate (NADPH), which is used to provide reducing equivalents in several anabolic reactions, including fatty acid chain elongation.

Glycolysis also contributes to lipid synthesis through the glycolytic intermediate dihydroxyacetone phosphate, which can be metabolized to glycerol-3-phosphate, the backbone for the synthesis of phospholipids and triglycerides (Illustration 1.4). Furthermore, glucose-derived acetyl-CoA is the major precursor in the synthesis of fatty acids (Bauer et al., 2005). Glycolysis is not a direct source of acetyl-CoA for fatty acid synthesis because pyruvate is imported into the mitochondria before it is converted to acetyl-CoA, and mitochondrial acetyl-CoA is a distinct pool that is not accessible to the cytoplasmic metabolic machinery. However, mitochondrial acetyl-CoA can be used to

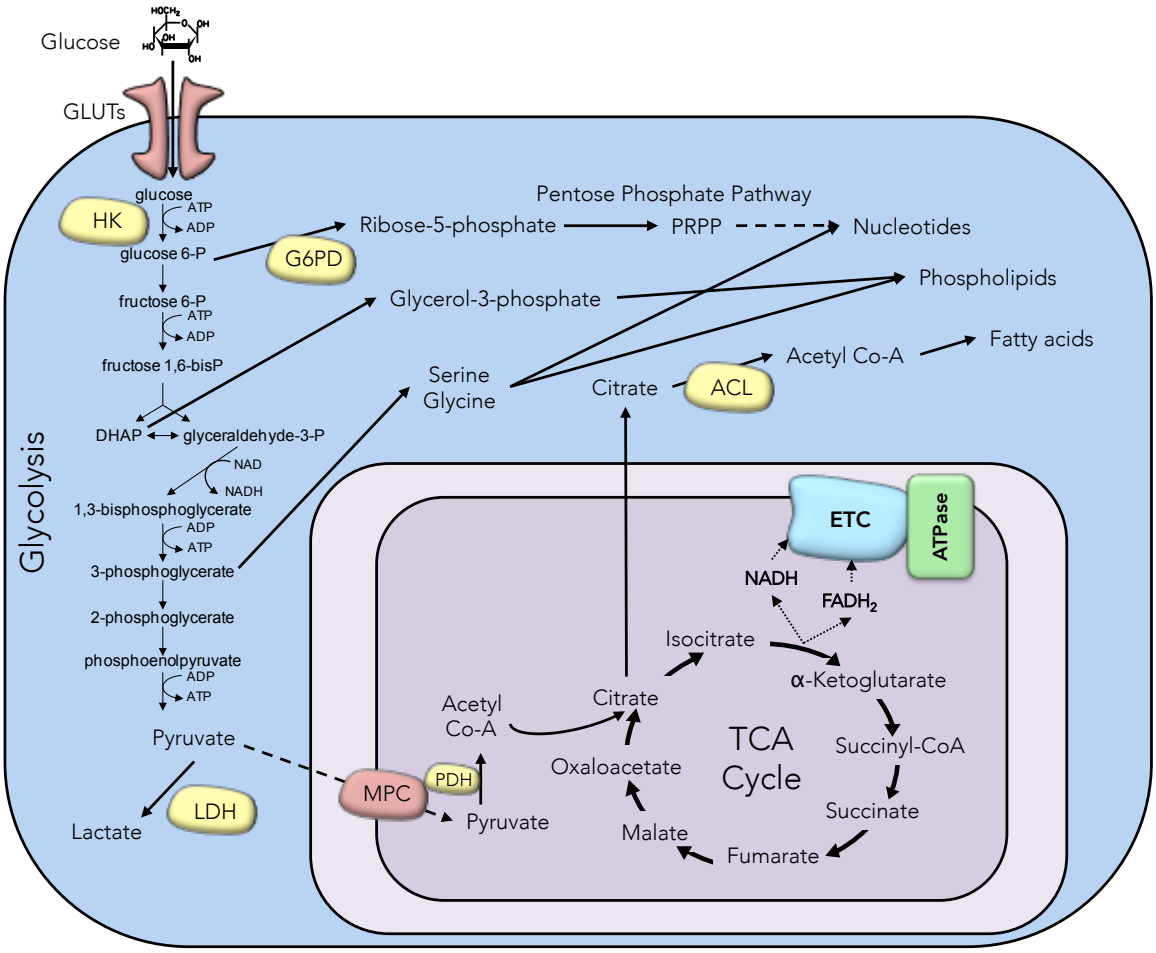

Illustration 1.4 Aerobic glycolysis provides precursors for biosynthetic pathways

Aerobic glycolysis is advantageous for proliferating cells because several glycolytic intermediates are precursors for macromolecular biosynthesis. Glucose-6-phosphate contributes to nucleotide biosynthesis via the pentose phosphate pathway. DHAP can be metabolized to glycerol-3-phosphate, the backbone for phospholipids and triglycerides. 3-phosphoglycerate contributes to both nucleotide and phospholipid head group biosynthesis via its ability to be metabolized to the amino acids serine and glycine. Finally, citrate formed downstream of glycolytically derived acetyl Co-A can be exported to the cytoplasm, where it is metabolized back to acetyl CoA by ATP citrate lyase (ACL). Cytoplasmic acetyl Co-A is the major precursor for the *de novo* synthesis of fatty acid chains.

generate citrate, which can be exported from the mitochondria and subsequently metabolized by ATP citrate lyase (ACL) to regenerate acetyl-CoA in the cytoplasm (Kaplan et al., 1993; Srere, 1972; Sullivan et al., 1974), where it can be used for fatty acid chain elongation (Illustration 1.4). Glycolysis also plays a role in the synthesis of some non-essential amino acids; for example, pyruvate is a precursor for the synthesis of the amino acid alanine.

Finally, the glycolytic intermediate 3-phosphoglycerate (3-PG) has multiple roles in the aforementioned biosynthetic pathways (Vander Heiden et al., 2011). Many of the actions of 3-phosphoglycerate stem from its ability to be metabolized to form the amino acids cysteine, serine, and glycine. Serine and glycine derived from 3-PG are important intermediates in the biosynthesis of purine nucleotides, as well as the production of folates (de Koning et al., 1998; Yoshida et al., 2004), key one-carbon donors in anabolic metabolism. Serine derived from 3-PG is also directly added to glycerol to form the head group of phosphatidylserines, and acts as a precursor for the synthesis of choline and ethanolamine (the other two major phospholipid head groups), along with sphingolipids, a significant class of structural and signaling lipids (Yoshida et al., 2004). Thus, through 3-PG alone, glycolysis plays a central role in all three processes of amino acid, nucleotide, and lipid production by providing carbon metabolites that act as precursors for macromolecular biosynthesis (Illustration 1.4).

1.3.2.2 Glutamine anaplerosis

As well as up-regulating glycolysis, cancer cells use the efflux of TCA cycle intermediates from the mitochondria to supply even more metabolic precursors to the cytoplasm, in a process called cataplerosis. Increased citrate cataplerosis, mentioned above, provides a source of cytoplasmic acetyl-CoA for *de novo* lipid biosynthesis (Bauer et al., 2005; Parlo and Coleman, 1984), and cataplerosis of oxaloacetate and α-ketoglutarate supports the biosynthesis of the amino acids glutamate, aspartate, asparagine, and proline (Owen et al., 2002). In order for this process to be sustainable for any length of time, the TCA cycle intermediates must be replenished through a complementary process, termed anaplerosis.

Glutamine appears to be the major metabolite contributor to anaplerosis in proliferating cells (DeBerardinis et al., 2007; Portais et al., 1996). Although most tissues can synthesize glutamine, and thus it is traditionally thought of as a non-essential amino acid, during periods of rapid growth, it appears that cellular demand for glutamine outpaces its supply. Therefore, glutamine is sometimes designated as a "conditionally essential amino acid" (DeBerardinis and Cheng, 2010). Decades before it was shown to be the most abundant amino acid in plasma (Bergstrom et al., 1974), Harry Eagle first described the unique reliance of *in vitro* cell lines on glutamine in cell culture media (Eagle, 1955). He found that HeLa cervical carcinoma cells required 2-10 times the concentration of glutamine in cell culture media compared with a mouse fibroblast cell line, and that this optimal glutamine concentration was also ten times more than the optimal amount of any other amino acid tested (Eagle, 1955). Later studies revealed that

glutamine could be oxidatively metabolized in the mitochondria (Kovacevic and Morris, 1972). However, only within the last decade have researchers truly begun to appreciate the role of glutamine anaplerosis in cancer cell metabolism.

In order to replenish TCA cycle intermediates, glutamine is converted to glutamate, which is subsequently converted to α-ketogluratate, and enters the TCA cycle. In cancer cells with functional mitochondria, α-ketoglutarate then fluxes through the TCA cycle oxidatively, replenishing pools of TCA cycle intermediates, and providing proliferating cells with another source of energy production, in a process termed glutaminolysis (DeBerardinis et al., 2008; Reitzer et al., 1979). In cases in which oxidative phosphorylation is impaired, tumor mitochondria actually perform reductive carboxylation, fluxing backwards to produce citrate, which is then exported to the cytoplasm where it can participate in fatty acid synthesis (Illustration 1.5) (Mullen et al., 2012). Thus, regardless of the oxidative state or capacity of the mitochondria in a particular tumor, glutamine remains an important nutrient in the support of cell growth and malignant transformation.

Some authors have suggested that the contribution of glutaminolysis to cellular ATP production may be underappreciated (Lunt and Vander Heiden, 2011; Reitzer et al., 1979). In the complete oxidation of glutamine, malate derived from glutamine anaplerosis is exported to the cytoplasm, where malic enzyme converts it to pyruvate, which is then metabolized to lactate and CO_2 by LDH. This process also generates NADPH. In addition to its important role in anaplerosis, glutamine metabolism supports

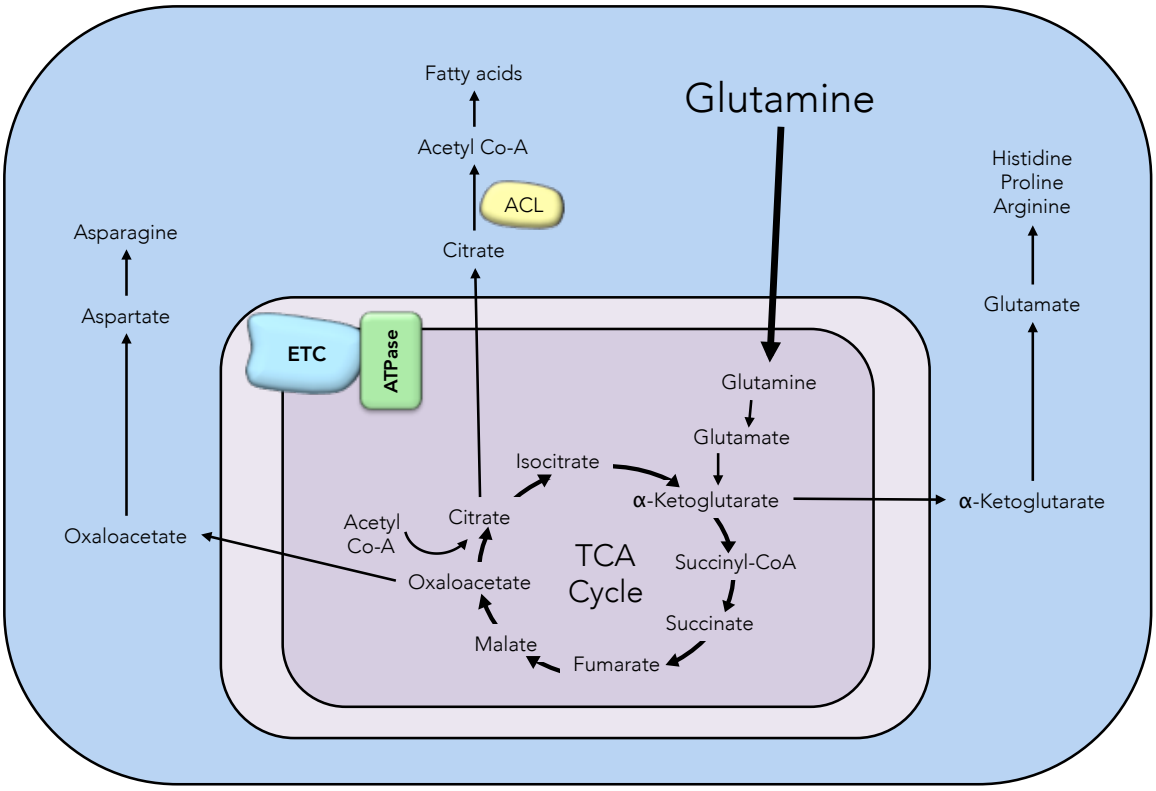

Illustration 1.5 Anaplerosis and cataplerosis

The cataplerosis, or mitochondrial export, of TCA cycle intermediates supports the biosynthesis of several amino acids, along with fatty acid acyl chains. For cataplerosis to be sustainable, TCA cycle intermediates must be replenished through the import of mitochondrial substrates in the complimentary process of anaplerosis. Glutamine is the primary contributor to anaplerosis in proliferating cells. α-ketoglutarate derived from glutamine can either flux forward (oxidatively) through the TCA cycle, or backwards to produce citrate via reductive carboxylation.

other aspects of cellular metabolism and macromolecular biosynthesis as well. Glutamine is also a required nitrogen source for the synthesis of amino acids and both purine and pyrimidine nucleotides (Cory and Cory, 2006). Labeling studies have confirmed that glutamine contributes carbons to CO_2, lactate, amino acids, and fatty acids, showcasing just how many aspects of cellular metabolism depend on glutamine as a nutrient source.

Highlighting the importance of glutamine metabolism in malignancy, a wide variety of cancer cell lines exhibit sensitivity to glutamine deprivation relative to their normal counterparts (Wu et al., 1978; Yuneva et al., 2007). Additionally, decreased expression or pharmacological inhibition of glutaminase (the enzyme responsible for the conversion of glutamine to glutamate) inhibits the growth of cancer cell lines (Cheng et al., 2011; Gao et al., 2009; Wang et al., 2010). However, despite these promising preclinical results, several therapeutic strategies aimed at targeting glutamine metabolism have failed, largely due to their massively toxic effects on normal tissues (Wise and Thompson, 2010).

1.3.2.3 Other mitochondrial changes in cancer

Although mitochondrial dysfunction may not cause the Warburg effect, there is significant evidence that cancer cells do in fact accumulate defective mitochondria. In diverse human malignancies, the extent of mitochondrial respiratory dysfunction positively correlates with tumor growth rates and the aggressiveness of metastasis (Pedersen et al., 1970). Malignant cells typically display several defects in mitochondrial

respiration: 1.) mitochondrial number and O_2 consumption are reduced, 2.) Ψ is elevated, 3.) mitochondria are less abundant, smaller, and have fewer cristae, and 4.) ROS production is increased (Pedersen, 1978; Wallace, 2005). This dysfunction often arises from mutations in the mitochondrial genome (mtDNA). mtDNA mutations appear to accumulate in primary tumors (Polyak et al., 1998), and lead to the generation of flawed ETC complexes and resultant elevated ROS production (Ishikawa et al., 2008; Petros et al., 2005). However, more research is still needed to determine whether mtDNA mutations truly drive tumorigenesis and metastasis, or are merely a marker of dysfunctional tumor mitochondria (Boland et al., 2013).

Mutations in nuclear-encoded mitochondrial genes also play a role in the mitochondrial dysfunction seen in several types of cancer. Chief among these are mutations in TCA cycle enzymes. Mutations in isocitrate dehydrogenase 1 (IDH1) and 2 (IDH2) have been found to play an important role in glioblastoma and acute myeloid leukemia (AML) (Cohen et al., 2013; Mardis et al., 2009). Fumarate hydratase (FH) mutations give rise to hereditary leiomyomas and renal cell carcinomas (Launonen et al., 2001; Tomlinson et al., 2002). Germline mutations in genes encoding subunits B, C, and D of succinate dehydrogenase (SDH) lead to complex II dysfunction and increased susceptibility to hereditary paragangliomas and pheochromocytomas (Neumann et al., 2004). The consequences of TCA enzyme mutations in cancer are still an area of intense research interest. Mutant IDH1/IDH2 convert isocitrate to the oncometabolite 2-hyrdoxyglutarate (Ward et al., 2010), while FH and SDH mutations lead to a buildup of their respective substrates, fumarate and succinate. Increased levels of fumarate,

succinate, or 2-hydroxyglutarate contribute, along with ROS, to the activation of oncogenes (e.g. hypoxia inducible factor -1α, HIF-1α) (Selak et al., 2005; Zhao et al., 2009) and further metabolic changes (Zhang et al., 2007).

1.4 Oncogenes & tumor suppressors in onco-metabolism

Aerobic glycolsis and glutaminolysis are both driven by numerous oncogenic pathways (DeBerardinis and Cheng, 2010; Elstrom et al., 2004; Frauwirth et al., 2002; Rathmell et al., 2003). Similarly, the oncoproteins HIF-1α, Ras, and *c*-Myc each inhibit mitochondrial oxidative metabolism in mice (Zhang et al., 2007), while the tumor suppressor p53 maintains mitochondrial function at several levels (Matoba et al., 2006). The interconnected nature of prominent cell growth signaling pathways and metabolic control lends further support to the notion that metabolic reprogramming is a necessary component of carcinogenesis. This section details our current understanding of some of the most important relationships between oncoproteins and metabolic reprogramming, however, this list is by no means exhaustive. It is likely that new important connections between cell growth signaling and metabolic control will be elucidated as our understanding of these processes continues to improve.

1.4.1 Oncogenes drive the Warburg effect

One critical oncoprotein that exerts significant control of cellular metabolism is HIF-1α. HIF-1α is a transcription factor that is stabilized and promotes anaerobic glycolysis only under low oxygen conditions in normal cells. Through a variety of

mechanisms, cancer cells up-regulate HIF-1α, or increase its stabilization in the presence of normal oxygen levels. Constitutive HIF-1α stabilization in normoxia can occur as the result of mutations in the tumor suppressor von hippel lindau (VHL). As mentioned above, increased levels of fumarate, succinate, or 2-hydroxyglutarate due to mutations in TCA cycle enzymes contribute, along with ROS, to HIF-1α stabilization even under normoxic conditions (Selak et al., 2005; Zhao et al., 2009). HIF-1α activation further impairs mitochondrial function in a feed forward mechanism of respiratory failure (Zhang et al., 2007). Among its many effects on cell growth and cellular metabolism, HIF-1α up-regulates LDH and lactate production, and decreases pyruvate flux into the TCA cycle by up-regulating pyruvate dehydrogenase kinase, which inhibits PDH. HIF-1α also has purported effects on expression of the M2 isoform of pyruvate kinase (Tong et al., 2009).

Although it is not an oncogene *per se*, tumor cells preferentially express the M2 isoform of the glycolytic enzyme pyruvate kinase (PKM2) (Mazurek, 2011; Reinacher and Eigenbrodt, 1981), which catalyzes the conversion of phosphoenolpyruvate (PEP) to pyruvate. PKM2 is a less active isoform relative to the M1 isoform that is predominantly expressed in most normal tissues, and thereby switching to PKM2 down-regulates the amount of pyruvate generated by glycolysis (Christofk et al., 2008a; Christofk et al., 2008b; Dombrauckas et al., 2005). In doing so, PKM2 regulates the flux of carbon into the PPP, effectively functioning as a gatekeeper that directs the flow of carbon into biosynthetic pathways and away from complete catabolism (Christofk et al., 2008a).

Another prominent oncoprotein, *c*-Myc, is particularly important in the control of glutamine uptake and metabolism (DeBerardinis and Cheng, 2010). c-Myc increases expression of glutamine transporter proteins, as well as expression of glutaminase (Gao et al., 2009; Wise et al., 2008). Like other oncoproteins, *c*-Myc also up-regulates genes encoding glycolytic enzymes, along with LDH (Osthus et al., 2000; Shim et al., 1997). Furthermore, *c*-Myc also increases expression of several genes involved in nucleotide biosynthesis (Liu et al., 2008; Mannava et al., 2008). Tumor cells transformed by the *myc* oncogene are also particularly sensitive to glutamine withdrawal (Yuneva et al., 2007).

In contrast, the tumor suppressor p53 promotes oxidative phosphorylation at several levels. The p53 target gene *TIGAR* inhibits glycolysis and lowers cellular ROS (Bensaad et al., 2006). p53 also induces Synthesis of Cytochrome c Oxidase 2 (SCO2), a positive regulator of complex IV of the ETC (Matoba et al., 2006), along with subunit I of complex IV itself (Okamura et al., 1999). Finally, p53 also induces expression of p53R2, a ribonucleotide reductase responsible for the maintenance of mitochondrial DNA (Bourdon et al., 2007). Hence, loss of p53 in cancers removes a significant positive regulator of mitochondrial oxidative metabolism, supporting the idea that mitochondrial oxidative phosphorylation is a tumor suppressive mechanism.

In addition to the ability of many oncoproteins to exert simultaneous control over growth signaling and metabolic pathways, some proteins, like mTOR, also receive regulatory inputs from metabolic second messengers. mTOR is activated in response to growth factors, and plays an important role in the regulation of protein translation and

amino acid synthesis, consequently controlling the expression of genes involved in many facets of growth and metabolism. In the context of low cellular energy status (low ATP/high AMP), AMP-activated protein kinase (AMPK) inhibits mTOR complex 1 (mTORC1) through multiple mechanisms (Corradetti et al., 2004; Gwinn et al., 2008). Conversely, high levels of available branched chain amino acids activate mTORC1 through the Ragulator complex (Sancak et al., 2010; Sancak et al., 2008). When active, mTORC1 promotes protein translation through its actions on S6 kinase and eukaryotic initiation factor 4 binding protein (4EBP). Thus, mTORC1 sits at the interface between growth factor signaling and metabolism, integrating incoming signals from growth factor stimuli with the current metabolic state of the cell, and adjusting energy expenditure, metabolic pathway utilization, and cell growth in response. Although relatively less well understood, mTOR complex 2 also regulates growth signaling and cell metabolism upstream of Akt, and may have important, under-appreciated effects on growth signaling outside of this role (Masui et al., 2014). However, while all of the aforementioned proteins play important and substantial roles, arguably the most important regulator of growth promoting metabolism is the PI3K/Akt pathway.

1.4.2 Akt as "the Warburg kinase"

Akt is a serine/threonine kinase that is one of the most commonly up-regulated oncoproteins in a variety of cancers. Through a series of steps, Akt is activated in response to mitogens such as epidermal growth factor (EGF), insulin-like growth factor 1 (IGF-1), and insulin (Illustration 1.6). Upon activation, it phosphorylates a myriad of

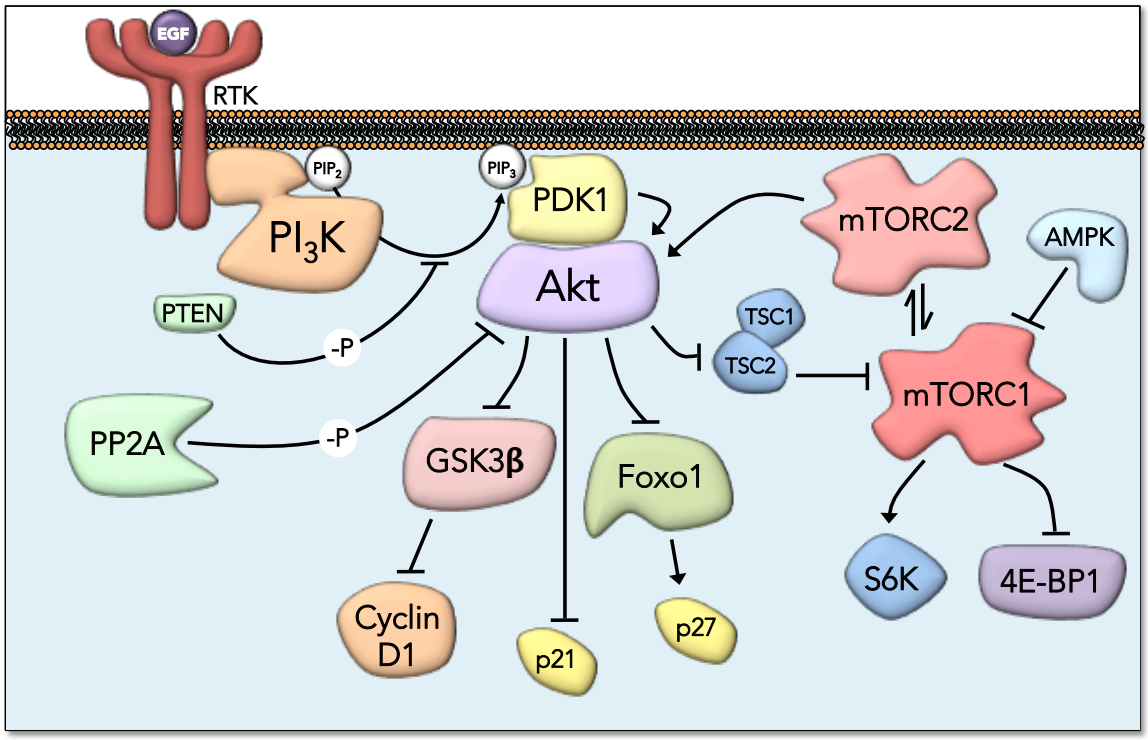

Illustration 1.6 The PI3K/Akt signaling pathway

Upon growth factor stimulation, receptor tyrosine kinases (RTKs) dimerize, and the monomers trans-phosphorylate one another, stimulating the recruitment of scaffolding proteins and ultimately recruiting and activating PI3K. Active PI3K phosphorylates the membrane phospholipid PIP2, converting it to PIP3. This recruits proteins with pleckstrin homology (PH) domains to the plasma membrane, including PDK1 and Akt. At the membrane, Akt is activated by PDK1 and mTORC2 by phosphorylation on T308 and S473, respectively. Once activated, Akt phosphorylates a myriad of substrates, including GSK-3, FOXO1, and TSC2. Phosphorylation of GSK-3 and FOXO leads to the transcriptional up-regulation of cyclins, and the repression of cell cycle inhibitory proteins. Phosphorylation of TSC2 dis-inhibits the mTORC1 complex, which in turn activates a variety of substrates, mainly involved in protein translation. The phosphatases PTEN and PP2A negatively regulate Akt activity. PTEN catalyzes the conversion of PIP3 back to PIP2, while PP2A dephosphorylates Akt directly.

proteins involved in protein translation, metabolism, cell survival/anti-apoptosis, and cell cycle progression, including among others Glycogen Synthase Kinase-3α/β (GSK-3α/β), Forkhead Box protein O (FOXO) transcription factors, tuberin/tuberous sclerosis 2 (TSC2), p21 (Cip1/Waf1) and p27 (Kip1) (Brazil et al., 2004; Manning and Cantley, 2007). Simultaneously, Akt controls proliferation in part by driving metabolic reprogramming (Elstrom et al., 2004; Rathmell et al., 2003).

Akt stimulates glycolysis directly and indirectly on several levels, by increasing glucose uptake (Rathmell et al., 2003), and activating glycolytic enzymes transcriptionally and post-translationally (Illustration 1.7) (Manning and Cantley, 2007). Akt enhances glucose uptake by increasing expression and membrane localization of GLUT1, the major contributor to basal glucose uptake in most cell types, through an mTOR-dependent, post-transcriptional mechanism (Rathmell et al., 2003; Taha et al., 1999). It also boosts glycolytic flux by stimulating the activity of several glycolytic enzymes. Akt phosphorylates hexokinase (Miyamoto et al., 2008), the rate-limiting enzyme in glycolysis, promoting its mitochondrial localization and activity (Gottlob et al., 2001). Phosphofructokinase 2 is another Akt target; its activation by Akt in turn stimulates activity of phosphofructokinase 1 (PFK) (Deprez et al., 1997). Activated Akt also enhances translation of HIF-1α through its actions on mTOR (Hudson et al., 2002; Majumder et al., 2004; Zhong et al., 2000), which in turn activates glycolytic genes as described above (Semenza et al., 1994). Combined, these changes substantially augment glycolytic rate and lactate production (Elstrom et al., 2004).

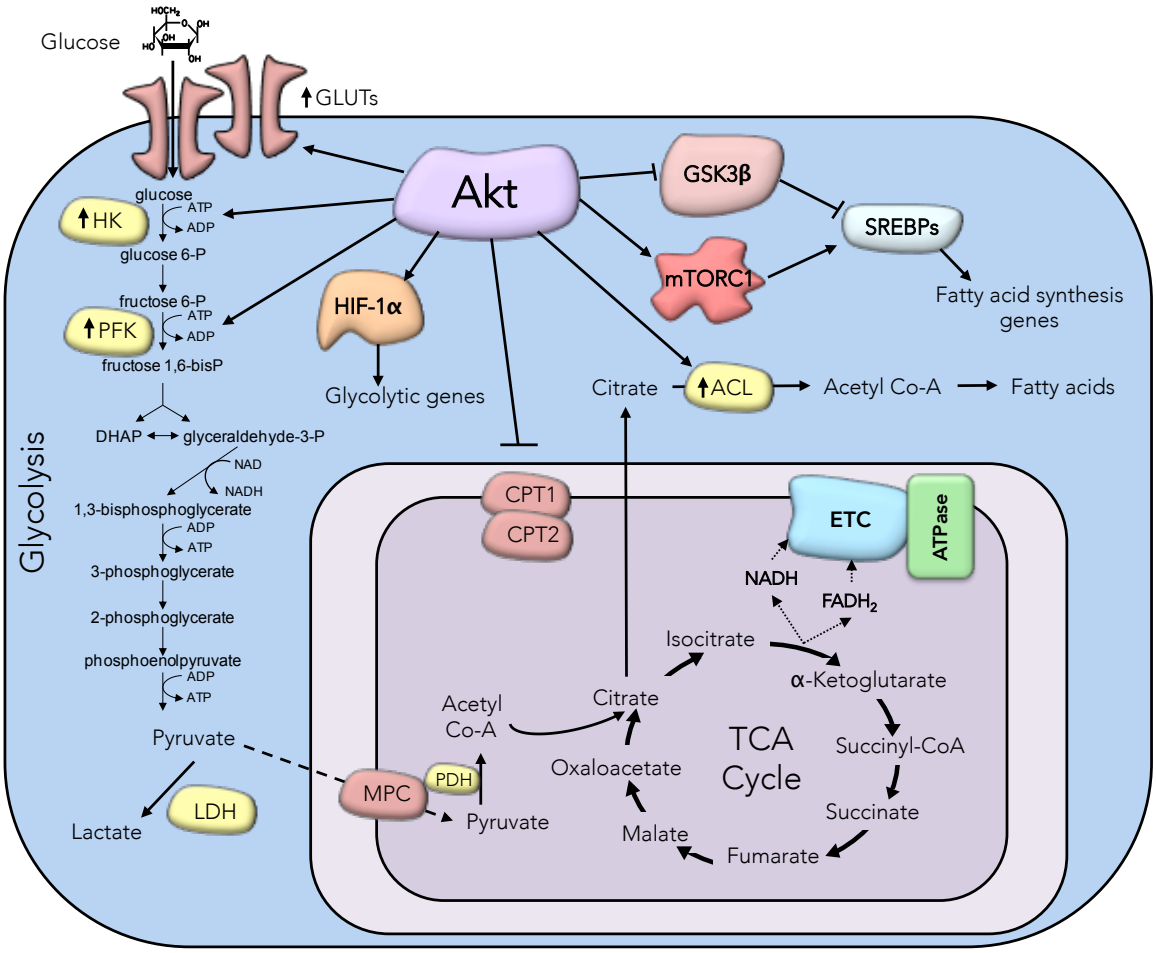

Illustration 1.7 Akt controls many facets of metabolism

Akt activation up-regulates anabolic metabolism through several pathways. Akt stimulates aerobic glycolysis by enhancing the activities of glycolytic enzymes like hexokinase (HK) and phosphofructokinase (PFK), which also increasing GLUT and other glycolytic gene expression through HIF-1α. At the same time, Akt up-regulates *de novo* lipid biosynthesis via the activation of SREBP transcription factors and the activation of ATP citrate lyase (ACL). Finally, Akt also suppresses macromolecular degradation through the inhibition of carnitine palmitoyltransferase and mitochondrial oxidative phosphorylation.

Akt also plays an important role in *de novo* lipid synthesis (Illustration 1.7) (Yecies et al., 2011). One way in which Akt signaling affects lipid metabolism is through the inhibitory phosphorylation of GSK-3α/β. GSK-3 has been shown to promote the degradation of sterol regulatory element binding proteins (SREBPs), a class of transcription factors well known for their ability to induce genes involved in fatty acid biosynthesis (Sundqvist et al., 2005). Thus, Akt induces SREBPs by preventing GSK-3 from marking them for degradation. In addition, Akt indirectly induces SREBPs through its actions on mTOR (Yecies et al., 2011). Akt also controls fatty acid biosynthesis through direct phosphorylation and activation of ACL (Berwick et al., 2002). As mentioned earlier, ACL catabolizes the conversion of cytoplasmic citrate to acetyl Co-A, which is then used as a precursor for the synthesis of new fatty acids. Highlighting its importance in cancer development, knockdown or suppression of ACL opposes Akt-mediated proliferation and tumorigenesis (Bauer et al., 2005; Hatzivassiliou et al., 2005).

Finally, while promoting anabolic pathways, Akt also suppresses macromolecular degradation. Studies have shown that Akt can inhibit fatty acid oxidation, at least in part through modulation of CPT1 expression (Buzzai et al., 2005; Deberardinis et al., 2006). Akt also negatively regulates mitochondrial oxidative phosphorylation through the direct phosphorylation and inhibition of PGC-1α, a transcriptional co-activator that positively regulates mitochondrial biogenesis and oxidative metabolism (Li et al., 2007). Thus, Akt simultaneously controls lipid synthesis and breakdown, via multiple pathways of metabolic regulation.

1.4.3 Metabolic regulation of Akt

In addition to the governance of cellular metabolism by growth signaling, metabolic changes are well known to exert reciprocal control of growth signaling pathways through specific proteins (e.g. AMPK and mTOR) (Ward and Thompson, 2012). However, in contrast to the many well-established roles of Akt in the metabolic regulation of glycolysis, lipogenesis, and mitochondrial oxidative phosphorylation (discussed above), there is a paucity of information regarding whether and how metabolic state modulates Akt signaling.

Some evidence suggests that lipids can exert reciprocal regulation of Akt. The lipids sphingosine 1-phosphate, poly-unsaturated fatty acids, and arachidonic acid have each been implicated to play some role in Akt activation (Gu et al., 2013; Schuppel et al., 2008; Villegas-Comonfort et al., 2014). In one recent study, knockdown of ACL inhibited Akt activation (Hanai et al., 2012). However, these reports are far from conclusive regarding the specific mechanisms underlying Akt regulation by these diverse lipid species. Further studies are necessary to understand the relationships between cellular metabolic status and control of Akt signaling.

1.5 Mitochondrial uncoupling proteins (UCPs)

With the renewed focus on metabolic reprogramming as an essential component of transformation has come intense interest in the development of cancer therapies that target or oppose the metabolic phenotype of tumor cells. One effective strategy to drive

nutrient oxidation and limit energy production is to decrease the efficiency of mitochondrial oxidative phosphorylation through proton leak. Mitochondrial uncoupling proteins (UCPs) are evolutionarily conserved, nuclear-encoded members of the mitochondrial solute carrier (SLC) superfamily that increase proton leak across the inner mitochondrial membrane in a variety of tissues, including brown fat, heart, skeletal muscle, and most recently, skin (Brand et al., 1999; Cannon et al., 1982; Mori et al., 2008a; Lago et al., 2012). Five uncoupling protein homologs have now been described in mammals, with varying tissue distribution and diverse physiological roles.

UCPs are so named because the proton leak that they generate disengages (i.e. "uncouples") fuel oxidation and electron transport from ATP synthesis, and as a result, uncoupled cells increase substrate oxidation and electron transport in an effort to maintain mitochondrial membrane potential (Ψ) (Illustration 1.8) (Esteves and Brand, 2005; Krauss et al., 2005). In effect, UCP expression decreases Ψ, increases ETC activity and O_2 consumption, and decreases ROS generation (Esteves and Brand, 2005). Uncoupled respiration fails to generate ATP, and therefore mitochondrial uncoupling not only drives mitochondrial respiration, but also escapes the "respiratory control" caused by feedback inhibition normally seen at supraphysiological ATP concentrations. Thus, the effects of uncoupling on mitochondrial bioenergetics are in direct opposition to the corresponding bioenergetic respiratory phenotypes observed in malignant cancer cells (Table 1.1).

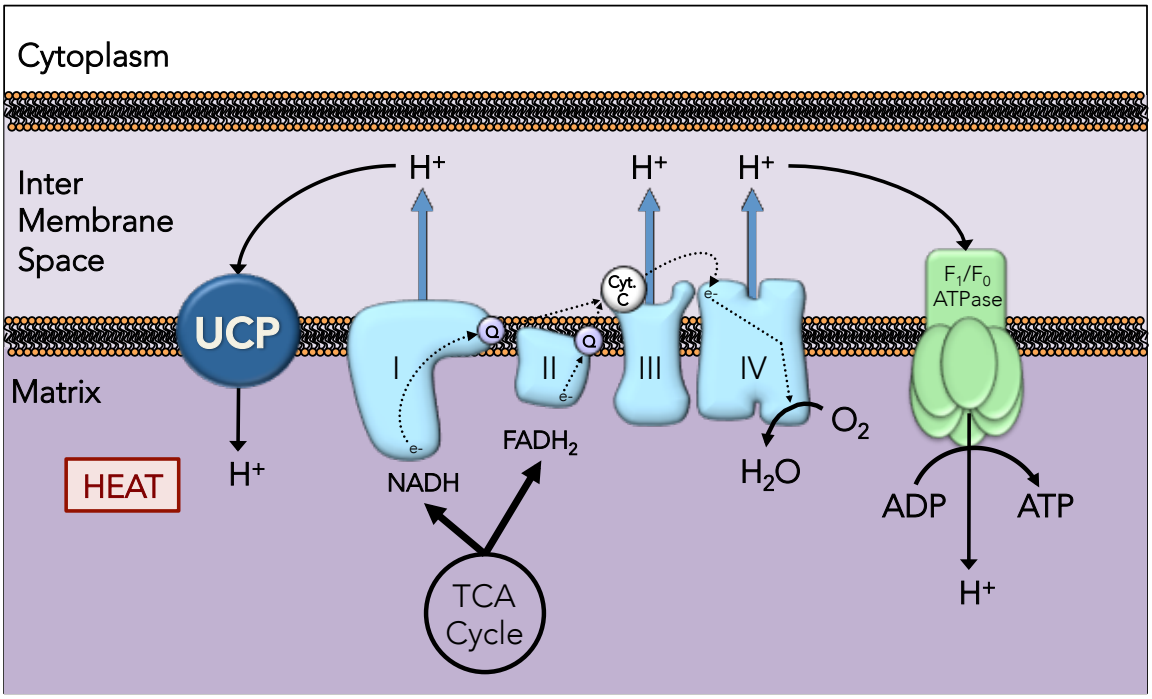

Illustration 1.8 Mitochondrial uncoupling proteins disengage eletron transport from ATP production

Mitochondrial uncoupling proteins (UCPs) are a family of nuclear-encoded solute carriers that are localized to the inner mitochondrial membrane. UCPs allow proton (H+) leak back into the mitochondrial matrix, but without ATP production. Since this reaction is favorable (because the H+ are moving back down the electrochemical gradient), the potential energy is released in the form of heat. Because of the lowered Ψ, ETC activity increases, in an effort to replenish the H+ gradient that is depleted by the UCP. This drives increased oxygen consumption, and lowers levels of reduced NADH, thus cells increase catabolic metabolism and TCA cycle flux to restore NADH levels.

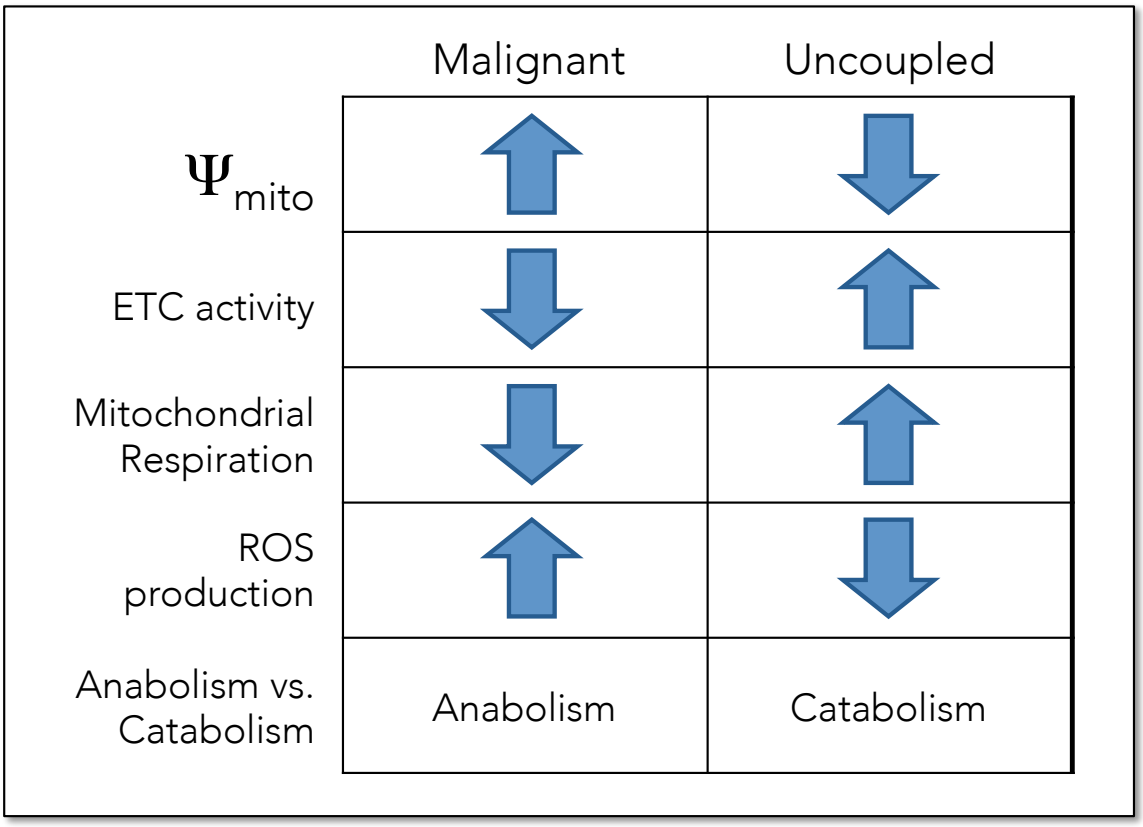

Table 1.1 Mitochondrial uncoupling opposes the metabolic phenotypes of cancer

Many of the effects of mitochondrial uncoupling are in direct juxtaposition to the mitochondrial phenotypes of malignant or rapidly proliferating cells. While cancer cells typically display high mitochondrial membrane potential (Ψ) and ROS production, and decreased eletron transport and oxygen consumption, mitochondrial uncoupling lowers Ψ and ROS production, while increasing ETC activity and respiration. In effect, these changes drive catabolic metabolism in uncoupled cells, in opposition to the immense anabolic needs of rapidly dividing tumor cells.

1.5.1 The uncoupling protein homologs

UCP1, also called thermogenin, was the first uncoupling protein to be discovered, and later cloned, in a series of studies that took place in the late 1970's and early 1980's (Bouillaud et al., 1985; Cannon et al., 1982; Nicholls, 1976). Its expression is restricted to brown adipose tissue (BAT), where it has been shown to be an important mediator of non-shivering (adaptive) thermogenesis, as the energy released by protons traveling down their gradient is discharged in the form of heat (Enerback et al., 1997; Thomas and Palmiter, 1997).

Pursuant to its status as the prototype UCP, UCP1 is the best described of the five mammalian UCP homologs. Although to date there is still no complete, high-resolution crystal structure of any UCP, some evidence suggests that UCP1 may function as a homodimer; however, these findings are not conclusive (Klingenberg and Appel, 1989; Lin et al., 1980). The mechanism of proton transport by UCP1 was recently elucidated in an elegant study by Fedorenko et al. (2012), which showed that a protonated fatty acid enters UCP1 through the central channel and releases a proton into the mitochondrial matrix, but does not enter the matrix itself. UCP1 knockout mice fail to maintain body temperature when exposed to cold ambient temperatures (Enerback et al., 1997), and are prone to obesity if housed in conditions that do not require them to generate body heat (i.e. thermoneutrality) (Feldmann et al., 2009). Along with complimentary studies, these results led researchers to conclude, perhaps prematurely, that UCP1 was the sole mediator of mammalian adaptive thermogenesis.

The first two novel UCP1 homologs, UCP2 and UCP3, were identified in 1997, and presumed to act as uncouplers based on sequence homology to UCP1 (Boss et al., 1997; Fleury et al., 1997). UCP2 and UCP3 share about 73% homology with one another, and roughly 59% and 57% homology with UCP1, respectively. Although they were discovered nearly 20 years ago, the physiological function(s) of UCP2 and UCP3 in diverse contexts continue to be a matter of active investigation.

UCP2 is expressed in a wide variety of diverse tissues, including (but not limited to) immune cells, lung, liver, stomach, and pancreas (Fleury et al., 1997; Pecqueur et al., 2001). Perhaps the most well described function of UCP2 is its role in insulin secretion. Pancreatic β-cells sense glucose concentration and secrete insulin in response to high cellular ATP concentrations. High cellular ATP causes the closure of ATP sensitive potassium channels, triggering plasma membrane depolarization and the subsequent opening of voltage sensitive calcium channels, calcium influx, and stimulation of insulin secretion via exocytosis (Ashcroft and Gribble, 1999). By lowering mitochondrial ATP production, UCP2 inhibits insulin secretion, particularly in circumstances of elevated glucose and/or FFA, both of which induce UCP2 expression (Chan et al., 2004a; Zhang et al., 2001). Accordingly, UCP2 knockout mice exhibit enhanced insulin secretion (Zhang et al., 2001). Interestingly, UCP2 knockout mice have no known thermoregulatory defects, possibly due to the lack of UCP2 protein expression in major thermogenic tissues (Arsenijevic et al., 2000).

UCP3 is expressed in BAT, heart, skeletal muscle, and most recently identified by our lab and others, skin (Boss et al., 1997; Mori et al., 2008a; Vidal-Puig et al., 1997,

Lago et al., 2012). Similar to UCP2, early work with UCP3 seemed to indicate that unlike UCP1, UCP3 did not play a major role in the determination of basal metabolic rate or cold-induced thermogenesis, and therefore researchers concluded that UCP1 was the sole mediator of adaptive thermogenesis (Golozoubova et al., 2001; Gong et al., 2000; Vidal-Puig et al., 2000). However, UCP3 also plays an important, if underappreciated role in non-shivering thermogenesis. Although UCP3 knockout mice survive upon cold exposure, they lack the hyperthermic response that wild type mice exhibit in response to treatment with pharmacological amphetamines (Mills et al., 2003), norepinephrine (Sprague et al., 2007), and bacterial lipopolysaccharide (unpublished data).

In addition to the role of UCP3 in thermogenesis, UCP3 and UCP2 have also both been implicated in the control of mitochondrial ROS production (Arsenijevic et al., 2000). Chemical uncouplers are well known for their ability to lower ROS production by the ETC, and a number of studies have shown that UCP3 expression mitigates mitochondrial ROS production (Anderson et al., 2007; MacLellan et al., 2005; Vidal-Puig et al., 2000), and decreases ROS-induced protein damage in skeletal muscle (Barreiro et al., 2009). Superoxide activates UCP2 and UCP3; thus, the model that has developed is that elevated levels of ROS activate the novel UCPs, causing mild uncoupling, which relieves respiratory inhibition and thereby decreases ROS production (Echtay et al., 2002a; Echtay et al., 2002b).

Finally, UCP3 has been proposed to play an important part in fatty acid oxidation. Fasted UCP3 knockout mice have lower whole-body fat oxidation than wild type mice (Bezaire et al., 2001), and UCP3 overexpression in skeletal muscle increases fatty acid

oxidation (Bezaire et al., 2005; MacLellan et al., 2005). In fact, overexpression of UCP3 favors fatty acid oxidation over glucose oxidation (Garcia-Martinez et al., 2001), and a recent study showed that reduction of UCP3 not only decreased fatty acid oxidation, but also led to insulin resistance (Senese et al., 2011). These studies have led to the proposal that at least one major physiological role for UCP3, and perhaps its molecular mechanism of uncoupling, may be through the export of fatty acid anions from the matrix, regenerating free coenzyme A and thus facilitating rapid β-oxidation and also providing protection from lipotoxicity (Himms-Hagen and Harper, 2001). The role of UCP3 in fatty acid oxidation is of substantial importance given the current obesity epidemic and the rise of related metabolic syndrome spectrum disorders, and therefore is an area of ongoing research focus.

Relative to the other novel uncoupling protein homologs, UCP4 and UCP5 share less sequence homology with UCP1 (~34%) (Sanchis et al., 1998). UCP4 is most closely related to the *c. elegans* uncoupling protein (ceUCP), and therefore may be the "ancestral" uncoupling protein (Sokolova and Sokolov, 2005). Expression of both UCP4 and UCP5 is restricted to nervous tissues, and although they were only discovered a few years after UCP2 and UCP3, their functions are less well described. Because they are so dissimilar from the other UCPs, it has been speculated that UCP4 and UCP5 may not function as classical uncouplers, but may instead play a role in mitochondrial transport of other molecules. In fact, ceUCP and human UCP4 were recently shown to transport succinate across the mitochondrial inner membrane (Pfeiffer et al., 2011)(& unpublished data).

1.5.2 UCPs in cancer

The role of uncoupling proteins in carcinogenesis is controversial: while some studies have reported that up-regulation of UCP2 confers tumors a survival advantage (Derdak et al., 2008; Horimoto et al., 2004), others have shown that UCP2 expression negatively impacts tumorigenesis (Derdak et al., 2006; Su et al., 2012). We have previously shown that expression of UCP2 kills tumor cells but not a non-tumorigenic fibroblast cell line (Mills et al., 2002). Animals that express an epidermal UCP1 transgene are resistant to two-stage chemical skin carcinogenesis (unpublished data), and mice expressing UCP1 specifically in skeletal muscle are protected from the development of lymphomas and other age related diseases (Gates et al., 2007). A recent report correlated UCP3 expression with Akt down-regulation in a high throughput assay for FOXO1 nuclear localization (Senapedis et al., 2011), and analysis of UCP3 expression in the Oncomine database revealed seventeen studies in which UCP3 was among the top 10% of down-regulated genes in cancer tissues compared to normal tissue controls (Table 4.1). These studies, together with the knowledge of how UCP3 opposes the metabolic phenotype of rapidly proliferating tumor cells, provided the basis for a mechanistic investigation of the relationships between mitochondrial uncoupling and carcinogenesis.

1.6 Dissertation objectives: Utilizing UCPs to target carcinogenesis

Given that mitochondrial uncoupling drives catabolic metabolism, contrary to the anabolic needs of cancer cells, we hypothesized that driving this process would oppose

tumorigenesis. Part of the difficulty in targeting tumor cell metabolism lies in the flexibility of metabolic systems and the panoply of nutrients to which tumor cells have access. Mitochondrial uncoupling provides the unique ability to increase substrate oxidation without increasing ATP production (and in fact, can actually lower cellular ATP). Furthermore, mitochondrial uncoupling should in theory drive oxidation of a diverse array of substrates – including fatty acids, glucose, and amino acids – thus it simultaneously depletes biosynthetic precursors across a variety of pathways. At the same time, enforced uncoupling should lower mitochondrial ROS production, another possible tumor suppressive mechanism. Therefore, we set out to examine the relationships between mitochondrial uncoupling and tumorigenesis.

In order to do so, we chose to develop a novel transgenic mouse model, the K5-UCP3 mouse, as a tool to show proof-of-principle whether enforced mitochondrial uncoupling could affect cancer susceptibility and development. K5-UCP3 mice express a murine UCP3 transgene targeted to the basal epidermis by the keratin 5 promoter (K5). Because UCP3 expression has recently been shown in skin (Mori et al., 2008a), and because the process of two-stage skin carcinogenesis (including tissue dynamics, tumor progenitor cell populations, and major mechanistic pathways) is so well described, this model provided an ideal setting in which to test our hypothesis.

1.6.1 The two-stage chemical skin carcinogenesis model

Murine skin consists of an outer layer called the epidermis, and an inner layer, the dermis, which is separated from the epidermis by a basement membrane. The epidermis

includes the sebaceous (oil) glands, hair follicles, and interfollicular epidermis (IFE), which forms the surface of the skin (Alonso and Fuchs, 2006). About 95% of cells within the epidermis are keratinocytes, so named because they express specific filamentous keratin proteins depending on their differentiation status and epidermal skin layer (Fuchs and Green, 1980). Within the IFE, proliferating, undifferentiated keratinocytes form a basal cell layer that anchors the rest of the tissue to the basement membrane. As they proliferate, some of these basal keratinocytes will detach from the basement membrane, migrating out toward the skin surface as they undergo terminal differentiation.

This process is directed at least in part by an endogenous calcium gradient that exists in the epidermis, with calcium concentrations highest in the outermost layers of the skin (Cornelissen et al., 2007; Menon et al., 1985). The mechanisms underlying calcium-induced keratinocyte differentiation are complex, but involve extracellular calcium-induced release of intracellular calcium stores, and the subsequent activation of calcium-sensitive signaling proteins (e.g. protein kinase C)(Tu et al., 2004). As cells migrate outward and undergo differentiation, they display expression of a number of different keratin and other filamentous protein markers that correlate well to the differentiation status of the cell (Illustration 1.9)(Fuchs and Green, 1980). By the time the keratinocytes reach the outermost layer, called the cornified epithelium, they have terminally differentiated, losing their organelles and nucleus, and forming dead, protein filled sacs called squames (Alonso and Fuchs, 2006).

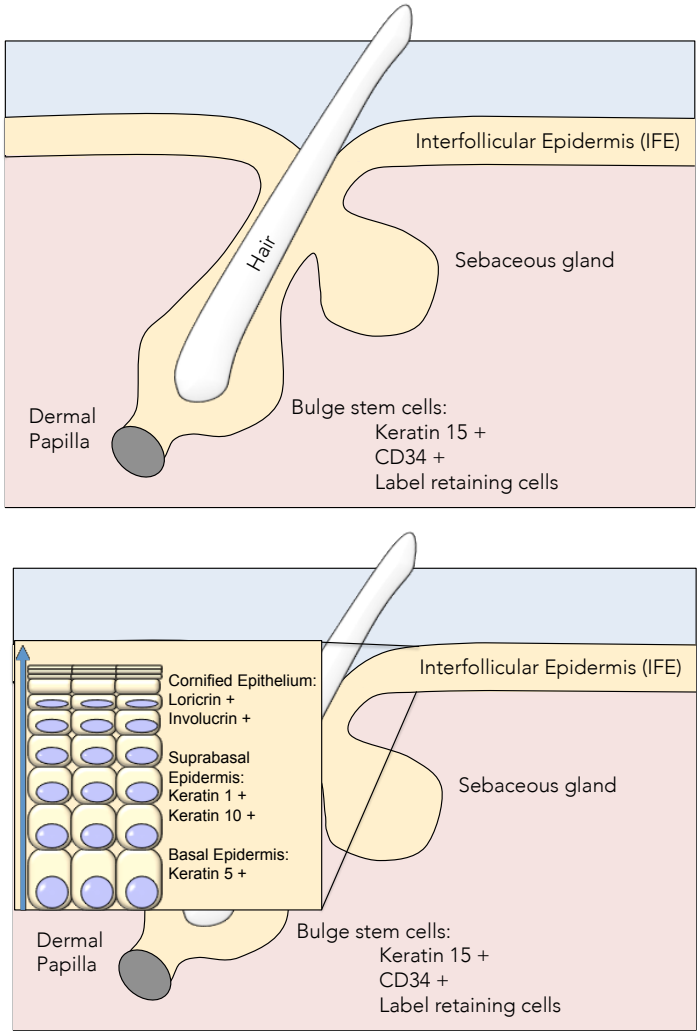

Illustration 1.9 Cell populations in murine epidermis

The epidermis consists of the hair follicles, sebaceous glands, and interfollicular epidermis (IFE). Within the hair follicle, the slow cycling, quiescent bulge stem cell (bSC) population is located below the sebaceous gland, and is responsible for maintenance or regeneration of all three epidermal structures. bSC are marked by expression of keratin 15 and CD34, and the capacity to retain labels (because of their slow cycling nature). Within the IFE, undifferentiated basal keratinocytes form the layer immediately above the basement membrane, and express keratin 5. As the basal keratinocytes proliferate, they move outward and differentiate in response to an in vivo calcium gradient. Differentiating keratinocytes express keratin 1 and 10, and ultimately loricrin and involucrin. Terminally differentiated keratinocytes are called squames, and are basically dead protein filled "sacs" that form the cornified epithelium, the outer barrier between the skin and the environment.

Within the hair follicle lies the most well described adult stem cell population in murine skin, the bulge stem cells (bSC), so named for the shape of the region where they are localized, halfway down the hair follicle (Alonso and Fuchs, 2003; Cotsarelis et al., 1990). The bSC have been shown to play important roles in hair follicle and sebaceous gland development (Claudinot et al., 2005), and contribute to IFE regeneration after wound healing or proliferative stimuli (Ito et al., 2005b). These cells are slow-cycling, and marked by expression of keratin 15, CD34, and high levels of α6-integrin (Liu et al., 2003; Trempus et al., 2003)(Illustration 1.9). As such, they have been shown to be the only cell population in the skin capable of producing carcinomas when targeted by carcinogens (Morris, 2000).

The mouse skin model is one of the best-established models for the study of step-wise tumorigenesis *in vivo*. In a typical two-stage chemical carcinogenesis regimen, mice receive an initial, sub-carcinogenic dose of an initiating agent that makes an irreversible change (DNA mutation), however is not enough to drive tumor formation alone (Abel et al., 2009). This is followed by repeated application of a tumor promoting agent, which is typically an inflammatory or other pro-growth stimulus, resulting in the formation of small, pre-malignant outgrowths of cells called papillomas. With repeated promoter application, these papillomas progress to carcinoma *in situ*, and ultimately, invasive carcinomas (Abel et al., 2009). The two-stage skin carcinogenesis model is advantageous over other rodent cancer models because it more closely approximates the "multi-hit" nature of the origin of most human cancers than complete carcinogenesis approaches (Lawley, 1994). It also allows for the separation of effects on each stage (initiation vs.

promotion), and tumor development can be monitored visually throughout the experiment. Furthermore, the age and the wide usage of various two-stage skin carcinogenesis protocols has resulted in a plethora of knowledge about the system, making it one of the most well-described tumor models available today (Abel et al., 2009).

1.6.2 The K5-UCP3 mouse

The keratin 5 promoter has been extensively used to target transgenes to the basal epidermis and other stratified epithelia (DiGiovanni et al., 2000; Liang et al., 2009; Segrelles et al., 2007). Thus, creation of the K5-UCP3 mouse provided the opportunity to drive UCP3 overexpression in the proliferative compartment of the epidermis, along with the putative tumor progenitor stem cell population. This allowed us to perform experiments to test whether and how mitochondrial uncoupling affected keratinocyte proliferation and tumorigenesis. The experiments herein describe the initial characterization of this novel mouse model, its strikingly tumor resistant phenotype, and the molecular mechanisms underlying UCP3-induced chemoresistance.

In large part, we believe that mitochondrial uncoupling opposes malignancy by driving catabolic mitochondrial metabolism, forcing cells to degrade metabolites in order to sustain mitochondrial membrane potential rather than use them for macromolecular biosynthesis. Herein, we show that K5-UCP3 mice are strikingly protected from tumor promotion through blockade of PI3K/Akt signaling. Blunted Akt activation corresponded to increased activity of protein phosphatase 2A (PP2A), along with reduced

membrane recruitment of Akt, and overexpression of wild type Akt rescued phorbol ester induced proliferation and two-stage chemical carcinogenesis. Finally, blockade of Akt membrane recruitment was accompanied by markers of membrane phospholipid breakdown that suggest alterations in membrane composition and dynamics, as a result of UCP3-driven lipid catabolism. In support of this idea, inhibition of mitochondrial β-oxidation activated Akt. These results establish a mechanism for UCP3-induced chemoresistance, and identify a novel relationship between mitochondrial metabolism and Akt signaling.

Chapter 2: Materials and Methods

2.1 Chemicals

12-O-tetradecanoylphorbol-13-acetate (TPA) and okadaic acid (OA) were purchased from LC Laboratories (Woburn, MA). Etomoxir ethyl ester (Eto) was purchased from US Biological (Salem, MA). Acetone, 7,12-dimethylbenz[*a*]anthracene (DMBA), and all other reagents (unless otherwise noted) were purchased from Sigma (St. Louis, MO).

2.2 Animals

The mouse strains used in these studies were wild type FVB/N, K5-UCP3 (FVB/N background), K5-UCP1 (FVB/N background), C57Bl6/j, UCP3-/- (C57Bl6/j background), UCP3-/- (FVB/N background), Tg.AC (FVB/N background), bitransgenic K5-UCP3/Tg.AC (FVB/N background), K5-Akt (FVB/N background), and bitransgenic K5-UCP3/K5-Akt (FVB/N background). K5-UCP3 and K5-UCP1 animals were generated using a bovine keratin-5 promoter (K5) targeting construct as previously described (DiGiovanni et al., 2000; Lago et al., 2012). Multiple founders of K5-UCP3 and K5-UCP1 mice were identified by PCR and Southern blot analysis and maintained as hemizygous breeder colonies. K5-Akt FVB/N mice were previously generated using a bovine keratin 5 (K5) targeting construct as described (DiGiovanni et al., 2000; Segrelles et al., 2007), maintained as hemizygous breeder colonies, and crossed K5-UCP3 x K5-Akt to produce bitransgenic K5-UCP3/K5-Akt mice and littermate controls.

FVB/N mice were purchased from Harlan (Indianapolis, IN) for the studies described in Chapter 3, and from Jackson Laboratories (Bar Harbor, ME) for the studies described in Chapter 4. C57Bl6/j animals were purchased from Jackson Labs (Bar Harbor, ME). Tg.AC mice were purchased from Taconic (Hudson, NY). Unless otherwise indicated, all experiments were performed using adult, 6-8 week old mice. All animal husbandry and experiments were carried out in strict accordance to guidelines defined by the Association for Assessment and Accreditation of Laboratory Animal Care (AAALAC) and approved by the institutional animal research committees at The University of Texas at Austin and UT-MD Anderson, Science Park Research Division.

2.3 Immunoblotting

Epidermal tissue or whole cell lysates were prepared by lysis in RIPA buffer (50 mM Tris-HCl, 1% NP-40, 0.5% Na Deoxycholate, 0.1% SDS, 150 mM NaCl, 2 mM EDTA) supplemented with protease and phosphatase inhibitor cocktails (Roche, Nutley, NJ). For analysis of mitochondrial protein expression, mitochondria were isolated using differential centrifugation and lysed in RIPA buffer as described in (Brand et al., 2005). For membrane localization experiment, tissue fractionation was performed using differential centrifugation and density gradients as described (Cox and Emili, 2006). Protein lysates were separated by SDS-PAGE and transferred to nitrocellulose.

Blots were probed with the following primary antibodies: α-mUCP3, α-hUCP3, α-cytokeratin 10 (Abcam, Cambridge, MA), α-phospho Akt S473, α-phospho Akt T308, α-Akt, α-phospho FOXO1 S256, α-phospho FOXO1 S319, α-phospho GSK-3β S9, α-

GSK-3β, α-phospho TSC2 S939, α-phospho mTOR S2448, α-phospho mTOR S2481, α-mTOR, α-phospho 4EBP1 T36/47, α-4EBP1, α-phospho rs6 T240/244, α-rS6, α-phospho eIF4G S1108, α-phospho EGFR Y1086, α-EGFR, α-phospho p38 MAPK T180/Y182, α-p38 MAPK, α-PTEN, α-PP2Ac, α-PP2Aa, α-phospho ERK T202/Y204, α-ERK, α-phospho p90 RSK T359/S363, α-p90 RSK, α-β-Actin, (Cell Signaling Technology, Danvers, MA), α-Cyclin D1, α-Cyclin A, α-p21, α-p27, α-α tubulin (Santa Cruz Biotechnology, Dallas, TX), α-α3 Integrin (Chemicon, Billerica, MA), α-cytochrome C (BD Pharm, San Jose, CA), α-DNA polymerase γ (Neomarkers, Fremont, CA), and α-UCP3 (Washington Biotechnology, Simpsonville, MD).

Following primary antibody, blots were incubated with α-rabbit-HRP or α-mouse-HRP (GE Healthcare, Piscataway, NJ), and developed using chemiluminescent substrate (Thermo Scientific, Rockford, IL). Results are representative of three separate experiments.

2.4 Cell cultures

All cell lines were cultured under standard conditions of 5% CO_2, 37°C. The human keratinocyte cell line (HaCaT) was kindly provided by Dr. Van Wilson, College of Medicine, Texas A&M. MCA3D and CH72 cell lines have been widely used by our lab and others for skin carcinogenesis studies (Navarro et al., 1991; Rundhaug et al., 1997c).

2.4.1 Mouse primary keratinocyte isolation

Primary mouse keratinocytes were harvested from the dorsal skin of adult mice and cultured as previously described (Morris et al., 1990). For a detailed isolation protocol, please refer to Appendix 1. Briefly, mice were sacrificed by CO_2 asphyxiation or isofluorane overdose, and a depilatory agent was applied to the skin. Dorsal skins were excised and sub-cutis material was removed, then skins were floated on trypsin to separate the epidermis from the dermis. The epidermis was then scraped into growth medium, minced with scissors, and further separated on a percoll gradient to exclude fibroblasts. Isolated primary mouse keratinocytes were used directly for experiments or plated on collagen-coated dishes and grown in EMEM-2 with 1% FBS and 0.05 mM Ca^{2+} unless otherwise indicated.

2.4.2 Human neonatal primary keratinocyte isolation

Primary neonatal human keratinocytes (NHK) were isolated as previously described (Welter et al., 1995) and cultured in Keratinocyte Serum Free Media (KSFM, Life Technologies, Grand Island, NY) for no more than 5 passages. For a detailed isolation protocol, please see Appendix 2. Briefly, foreskin tissue was trimmed to lay flat and floated on 10 mg/mL Dispase in Hank's Balanced Salt Solution (HBSS) with sodium bicarbonate, HEPES, 5 μg/mL gentamycin, and 10 ng/mL fungizone, overnight at 4°C. The next day, epidermis was removed and incubated in 0.25% trypsin with 1 mM EDTA at 37°C for 5-7 minutes. The reaction was quenched with DMEM + 10% FBS media, and cells were collected by centrifugation, resuspended, and plated in KSFM in normal

cell culture dishes (no feeder layer or special coating procedure is necessary with this protocol).

2.5 UCP3 immunohistochemistry and mitochondrial localization

2.5.1 UCP3 immunohistochemistry in cells

Primary mouse keratinocytes were fixed in 4% paraformaldehyde and immunostained using primary rabbit anti-hUCP3 (Chemicon, Billerica, MA), followed by secondary α-rabbit Alexa 568 (Invitrogen, Carlsbad, CA). Nuclei were stained with Hoescht 33342 (Invitrogen, Carlsbad, CA). All fluorescent images were acquired with a Nikon Eclipse Ti-S microscope, using a 60x Nikon Plan Apo VC Oil objective with NA=1.40. Images were taken with a Photometrics Coolsnap EZ camera and processed using NIS Elements BR 3.0 software. Results are representative of three separate experiments.

2.5.2 UCP3 immunohistochemistry in tissues

Dorsal skin sections were fixed overnight in 10% formalin, moved to 70% ethanol, and embedded in paraffin. Samples were rehydrated and antigens were retrieved by boiling in 0.01 M sodium citrate buffer. Slides were blocked in 10% goat serum for 1 hour at room temperature, then incubated with primary rabbit α-mUCP3 (Abcam, Cambridge, MA) for 1 hour at room temperature, followed by secondary α-rabbit Alexa 568 (Invitrogen, Carlsbad, CA) for 1 hour at room temperature. Nuclei were stained with Hoescht 33342 (Invitrogen, Carlsbad, CA). Fluorescent images were acquired on the

DiGiovanni lab confocal microscope. Results are representative of n=3 animals per genotype.

2.5.3 UCP3-dependent oxygen consumption in mouse epidermis

Isolated epidermis was placed into the respiration chamber in 900μl of 37°C Krebs Ringer supplemented with 10 mM glucose. Oxygen consumption was measured using a polaragraphic Clark-type electrode (Instech, Plymouth Meeting, PA). Respiratory rates were measured from n=3 animals per genotype at linear regions on the curve under conditions of no treatment, 1 μg/ml oligomycin, and 250μM 2,4-dinitrophenol (DNP) to determine state 3, state 4, and maximal respiration, respectively.

2.6 Flow cytometry

2.6.1 MitoTracker Green

Primary keratinocytes were stained with 200nM MitoTracker Green (Invitrogen, Carlsbad, CA) in growth medium for 45 minutes at 37°C. Flow cytometric analysis was performed using a BD Biosciences FACS Calibur. Analyses were performed in triplicate for n=2 animals per genotype.

2.6.2 Bulge stem cell marker labeling

Primary keratinocytes were isolated as described above and incubated with fluorescently conjugated α-CD34-FITC and α-α6-Integrin-PE primary antibodies in Dulbecco's modified PBS (DPBS, lacking calcium and magnesium) + 3% FBS + 0.09% sodium azide for 30 minutes in the dark on ice. Cells were washed to remove residual

antibody and resuspended in DPBS, then analyzed using a BD Biosciences FACS Calibur. Staining with 7AAD was used to gate for cell viability. For each experiment, cells from n=2-3 mice were pooled during the isolation to collect a sufficient number of cells for all samples, single stained, and unstained controls. Results are representative of n=3 separate experiments.

2.7 Electron microscopy

Primary keratinocytes were grown on ACLAR® film in 0.05mM Ca^{2+} normal growth medium for 24hrs then switched to KGM-2 media supplemented with either 0.03mM or 1.2mM Ca^{2+} as indicated and grown until confluent. Cultures were fixed in 2.5% glutaraldehyde / 2% paraformaldehyde in 0.1M cacodylate buffer, pH 7.4 for 1.5hrs at room temperature. Cells were post-fixed in 2% osmium tetroxide / 2% potassium ferrocyanide in cacodylate buffer, then rinsed, dehydrated in graded ethanols, and transferred to acetone for infiltration with epoxy resin (1:1 mixture of Spurr and EMbed 812, Electron Microscopy Sciences, Hatfield, PA). Ultrathin sections (60-70nm) were collected on copper grids, counterstained with uranyl acetate and lead citrate, and visualized with a Philips EM208, FEI, Oregon operated at 80kV.

2.8 RT-PCR and microarray analyses

Total RNA was extracted using TRIzol® Reagent (Invitrogen, Carlsbad, CA) followed by the QIAGEN RNeasy mini kit (QIAGEN, Inc.) and was reverse transcribed using SuperScript II Reverse Transcriptase (Invitrogen, Carlsbad, CA). For mUCP3 expression in keratinocytes, primers were as follows: sense 5'-

ACTATGGATGCCTACAGAACC and antisense 5'-GACCCGATACATGAACGCT. RNA integrity was assessed using expression of mouse β2 microglobulin with the following primers: sense 5'-GACTGGTCTTTCTATATCCTGG and antisense 5'-CAATTTATGCACGCAGAAAG. For global gene expression analysis, RNA was isolated from untreated dorsal skin from n=3 mice per genotype. RNA was labeled with biotin-16-UTP (Perkin Elmer Life and Analytical Sciences, Boston, MA) and hybridized to the Illumina MouseRef-6 BeadChip (Illumina, Inc., San Diego, CA). Arrays were scanned with an Illumina Bead array Reader, and data processing and analysis was performed using Illumina BeadStudio software.

2.9 Keratinocyte differentiation and stem cell markers

Dorsal skin sections were fixed and embedded as described above. Sections were stained with haematoxylin and eosin (H&E) for light microscopy. Bulge stem cells were identified with primary α-CD34 (eBioscience, San Diego, CA) and α-K15 (Lab Vision, Freemont, CA). K15 data represent N≥250 hair follicles / n=2 animals per genotype. Markers of early and late stage keratinocyte differentiation were assessed using primary α-K1 (Covance, Austin, TX), α-loricrin, and α-involucrin (BabCo, Austin, TX).

2.10 5-bromo-2-deoxyuridine (BrdU) labeling & histology

2.10.1 Label Retaining Cell Assay

Slow-cycling bulge stem cells were identified by pulse/chase with 5-bromo-2-deoxyuridine (BrdU) as described (Taylor et al., 2000). Briefly, n=3 neonatal mice per genotype were injected subcutaneously with BrdU (Sigma, St. Louis, MO; 50μg/g body

weight) twice daily for 3 days. Cells retaining the label after 8 weeks were identified as label-retaining cells (LRCs).

2.10.2 Epidermal Turnover Assay

The epidermal turnover assay was performed similarly to the LRC assay, with the following changes: Mice received a single *i.p.* injection of 100μg/g body weight BrdU at 6 weeks of age. Following injection, mice were sacrificed and dorsal skin biopsies were collected at 2 hours, 5 days, 7 days, 9 days, and 18 days post injection. Labeled cells in the basal interfollicular epidermis were quantified for >100 cells from 5 randomly selected skin sections (total >500 cells) from each of n = 3 mice per genotype at each time point. Labeled cells that had detached from the basement membrane and migrated outward were not counted in either group.

2.10.3 Epidermal proliferation in response to promoter treatment

24 hours after acetone or single TPA treatment, mice were injected i.p. with 10 mg/kg BrdU in sterile saline, then sacrificed 30 minutes after injection. For 4x TPA treatment, mice received biweekly treatments for 2 weeks (total of 4 treatments), and were injected with BrdU and sacrificed 48 hours after the final TPA treatment. Dorsal skin biopsies were collected and fixed overnight in 10% neutral buffered formalin, moved to 70% ethanol, and embedded in paraffin. Sections were stained as previously described (Naito et al., 1987). Labeling index was calculated as the percentage of basal epidermal cells positive for BrdU. >100 cells from 5 randomly selected skin sections

(total >500 cells) were counted from each of n = 3 mice per genotype in each treatment group.

2.11 Topical treatments

For all experiments involving topical application of chemicals, mice were shaved on dorsal skin 48 hours prior to treatment. Two to four animals per group were used for each experiment. Mice were treated topically with 200μL acetone (vehicle control), 12.5 μg/mL TPA (2.5 μg dose), 25 mM OA (5 nmol dose), or 5 mg/mL Eto (1 mg dose) and sacrificed at the indicated time points. Nair depilatory cream was applied to remove remaining hair, and epidermal biopsies were collected and placed on ice. Subcutaneous fat and muscle was removed from each sample by scraping the ventral side of each piece of tissue. Samples were then flipped dorsal side up and epidermal tissue was collected by scraping with scalpel. Following collection, samples were either lysed in Ripa buffer for immunoblotting as described above, flash frozen for storage, or used for other analyses as indicated.

2.12 EGF signaling experiments

2.12.1 Signaling in mouse primary keratinocytes

For signaling experiments, isolated mouse primary keratinocytes were grown in EMEM-2 with 1% FBS for 48-72 hours following isolation, then starved overnight (~18 hours) before treatment. Cells were treated with 40 ng/mL EGF (Gemini Bioproducts, West Sacramento, CA) or 0.0001% BSA (vehicle control, Fisher Scientific, Pittsburgh,

PA), incubated at 37°C, 5% CO_2 until the indicated time point, then harvested and used for immunoblotting as described above.

2.12.2 Signaling in human neonatal primary keratinocytes

For transfection, cells were split using 0.5% Trypsin-EDTA as usual, counted, plated, and transfected while still in suspension. Transfections were performed using Lipofectamine 2000 reagent (Life Technologies, Grand Island, NY). DNA and Lipofectamine 2000 were complexed for 30 minutes at room temperature prior to addition to the cells, according to the manufacturer's instructions. For experiments in 6-well plates, 2 μg total DNA per well was used, with a 1:3 ratio of DNA:Lipofectamine 2000 (6 μL Lipofectamine 2000 per well). Media was changed 6-8 hours after transfection. To allow for future experiments with titrated expression of UCP3, the repressible pTetOff system was used with a pTRE2hyg-UCP3 construct cloned in our lab (Clontech, Mountain View, CA). Signaling experiments were performed 72 hours after transfection. NHK were moved to KSFM without epidermal growth factor (EGF) and bovine pituitary extract (BPE) supplements 18 hours prior to treatment. Cells were treated with 40 ng/mL EGF (Gemini Bioproducts, West Sacramento, CA) or 0.0001% BSA (vehicle control, Fisher Scientific, Pittsburgh, PA), incubated at 37°C, 5% CO_2 until the indicated time point, then harvested and used for immunoblotting as described above.

2.13 Epidermal wounding

Epidermal wound healing was measured on 5 week old WT FVB/N and K5-UCP3 mice (n=10). Epidermal wounds were generated with ~1 cm diameter felt wheel

and wound diameters were measured with calipers every other day until all wounds completely healed. Experiments were performed in duplicate with n ≥4 animals per genotype.

2.14 PP2A activity assay

PP2A was immuno-precipitated using primary α-PP2Ac (Millipore, Billerica, MA), incubated with a target phospho-peptide, and free phosphate release was measured via Malachite Green assay per the manufacturer's instructions (Millipore, Billerica, MA). n=2-3 animals per genotype were pooled for each experiment. Results are representative of 5 separate experiments.

2.15 ROS measurement

ROS production by isolated mitochondria was measured using Amplex Red as previously described (Hirasaka et al., 2011). Mitochondria from wild type and K5-UCP3 epidermis were suspended in a buffer containing 5 mM MOPS (pH 7.4), 70 mM sucrose and 220 mM mannitol, and mitochondrial protein concentration was determined using a BCA protein assay (Pierce Biotechnology, Rockford, IL). 5 mg mitochondrial protein/well were incubated in a reaction mixture containing 50 mM Amplex Red, 0.2 U/ml horseradish peroxidase (HRP), and 30U/ml superoxide dismutase (SOD) at room temperature for 30 min, protected from light. SOD was added to convert all superoxide into H_2O_2. Fluorescence was recorded using a microplate reader (VICTOR™ 3V; Pelkin Elmer, Waltham, MA) with 531 nm excitation and 595 nm emission wavelengths.

2',7'-dichlorodihydrofluorescein diacetate (H2DCF-DA, Life Technologies, Grand Island, NY) and dihydroehidium (DHE, Life Technologies, Grand Island, NY) were used to detect cellular hydrogen peroxide and superoxide, respectively. Isolated primary keratinocytes were incubated with HBSS containing 5 μM H_2DCF-DA or DHE. Fluorescence was analyzed by flow cytometric analysis using a BD Biosciences FACS Calibur. Treatment with 10 mM succinate,10 μM antimycin A, or their combination was used to stimulate ROS production.

The redox state of Akt and PP2A was determined by analysis of cell extracts pre-incubated with AMS (4-acetamido-4′-maleimidylstilbene-2,2′-disulfonic acid) as previously described (Hirasaka et al., 2011). Briefly, cells were precipitated with 10% ice-cold trichloroacetic acid for 30 min at 4°C and centrifuged at 12,000 g for 30 min to collect precipitated protein. Protein pellets were re-suspended in 100% acetone and incubated at 4°C for 30 min. Following centrifugation at 12,000 g for 10 min, the acetone was removed and protein pellets were dissolved by sonicating in 20 mM Tris/HCl, pH 8.0, containing 15 mM AMS and incubated at room temperature (25°C) for 3 hours. Akt and PP2A redox forms were separated by SDS-PAGE in the presence of non-reducing loading buffer. Treatments with dithiothreitol or hydrogen peroxide were used to demonstrate reduced vs oxidized state of each protein.

2.16 Metabolomic Analysis

For metabolic profiling, mice were fasted for 5 hours prior to sample collection to control for metabolic variation due to feeding, and then sacrificed via cervical

dislocation. Dorsal skin biopsies were taken and epidermal tissue was harvested as described above. Samples were flash frozen in liquid N_2 and stored at -80°C until processed.

Unbiased metabolomic profiling analysis was performed by Metabolon (Durham, NC) as described elsewhere (Theriot et al., 2014). Briefly, samples were prepared with the automated MicroLab STAR system from Hamilton Company using an aqueous methanol extraction process to remove proteins while allowing maximum recovery of small molecules. Aliquots of the resulting extract were analyzed by ultrahigh performance liquid chromatography/mass spectrometry (UPLC/MS/MS; positive mode), UPLC/MS/MS (negative mode), or GC/MS. Raw data were extracted, peak identified, processed against quality control standards, and normalized to total protein content by Metabolon. Compounds were identified by comparison with a library of >2,400 purified standards' analytical characteristics on Metabolon's LC and GC platforms. Compounds with a p-value <0.05 in a Welch's two-sample t-test were considered to be significantly different between genotypes.

2.17 Tumor experiments

For Tg.AC tumor experiment, 16 week-old mice (Tg.AC n=20, K5-UCP3/Tg.AC n=20) were shaved dorsally and treated with biweekly applications of TPA (2.5 μg) for two weeks for a total of 4 treatments, as described (Battalora et al., 2001). For K5-UCP3/K5-Akt rescue experiment, adult (6-8-week) WT FVB/N (n=28) and hemizygous K5-UCP3 (n=27), K5-Akt (n=29), and K5-UCP3/K5-Akt (n=18) littermates were

initiated topically on shaved dorsal skin with a single application of DMBA (100 μg) followed two weeks later with biweekly applications of TPA (2.5 μg) for 26 weeks, as described (Rundhaug et al., 1997b). In both experiments, mice were scored weekly for tumor incidence (percentage of mice with skin tumors) and tumor multiplicity (number of skin tumors per mouse). Mice were sacrificed if moribund, if any individual tumor reached a diameter of >1 cm, or at the termination of the experiment.

2.18 Statistics

Analysis of variance comparisons between genotypes were analyzed by student's t-test or single factor ANOVA followed by Dunnett's post hoc test, with a $p < 0.05$ set *a priori* as statistically significant.

Chapter 3: Mitochondrial uncoupling protein 3 drives keratinocyte differentiation and blocks skin carcinogenesis.[1]

3.1 Introduction

As described in Chapter 1, in order to study relationships between mitochondrial metabolism and tumorigenesis, we developed a novel mouse model that overexpresses a UCP3 transgene targeted to the basal epidermis and other stratified epithelia by the keratin 5 promoter (K5, K5-UCP3 mice). The keratin 5 promoter has been extensively utilized to regulate gene expression in dividing basal keratinocytes, including the tumorigenic stem cell populations in both the interfollicular epidermis and follicular bulge region (Rundhaug et al., 2007). UCP3 expression was recently reported in human skin and keratinocytes (Mori et al., 2008b). Similarly, we observed that UCP3 is expressed in wild type murine skin and keratinocytes and is closely associated with the degree of cellular differentiation. Thus, generation of the K5-UCP3 mouse model provided a strategy with which to test the notion that enforced mitochondrial uncoupling would oppose tumorigenesis in a well-developed assay for skin cancer.

---

[1] Portions of this chapter are adapted from:

Cory U. Lago*, **Sara M. Nowinski***, Joyce E. Rundhaug*, Matthew E. Pfeiffer, Kaoru Kiguchi, Katsuya Hirasaka, Xianmei Yang, Ellen M. Abramson, Shawn B. Bratton, Okkyung Rho, Renata Colavitti, M. Alexander Kenaston, Takeshi Nikawa, Carol Trempus, John DiGiovanni, Susan M. Fischer, and Edward M. Mills. Mitochondrial respiratory uncoupling promotes keratinocyte differentiation and blocks skin carcinogenesis. *Oncogene,* (2012); 31(44): 4725-31. * denotes equal contribution.

Author Contributions:
E.M.M., S.M.F., and C.U.L. conceived the project. C.U.L., S.M.N., and J.E.R., designed and performed all experiments. M.E.P., K.K., X.Y., E.M.A. helped with development of animals or experiments. K.H., M.A.K., S.B.B., R.C., O.R., C.T., T.N., S.M.F. and J.D. aided with experimental design and interpretation of results. C.U.L., S.M.N. and E.M.M. interpreted results and wrote the manuscript.

Both *in vivo* and *in vitro*, differentiation of keratinocytes is calcium (Ca^{2+})-dependent and is typified by dramatically increased cell size and fusion (Watt, 1984). At low [Ca^{2+}] (≤0.05 mM), isolated cells typically remain small and proliferative, but when cultured in 0.1–1.2mM Ca^{2+}, keratinocytes undergo terminal differentiation and are marked by the presence of large cytoplasmic keratin filaments. Remarkably, K5-UCP3 mice exhibited increased keratinocyte differentiation *in vivo* and *in vitro*, along with the loss of quiescent hair follicle bulge stem cell markers, and increased epidermal keratinocyte turnover. Consequently, K5-UCP3 animals exhibit extraordinary resistance to chemically-mediated multistage skin carcinogenesis. Together, the results herein indicate provide proof-of-principle evidence that targeting mitochondrial respiratory uncoupling is a powerful novel strategy in cancer prevention and treatment, and warrants further investigation.

3.2 Results

3.2.1 Endogenous UCP3 expression in mouse and human keratinocytes

Consistent with a recent report showing UCP3 expression in human skin keratinocytes (Mori et al., 2008b), we found that UCP3 was expressed in isolated mitochondria from cultured HaCaT human keratinocytes and increased in response to Ca^{2+}-induced differentiation *in vitro* (Figure 3.1 a). Similarly, UCP3 mRNA expression was increased during the differentiation of wild type mouse primary keratinocytes (Figure 3.1b). In contrast, UCP3 protein was absent in isolated mitochondria from malignant cervical epithelial cells (Figure 3.1 a, HeLa, lane 3), malignant squamous

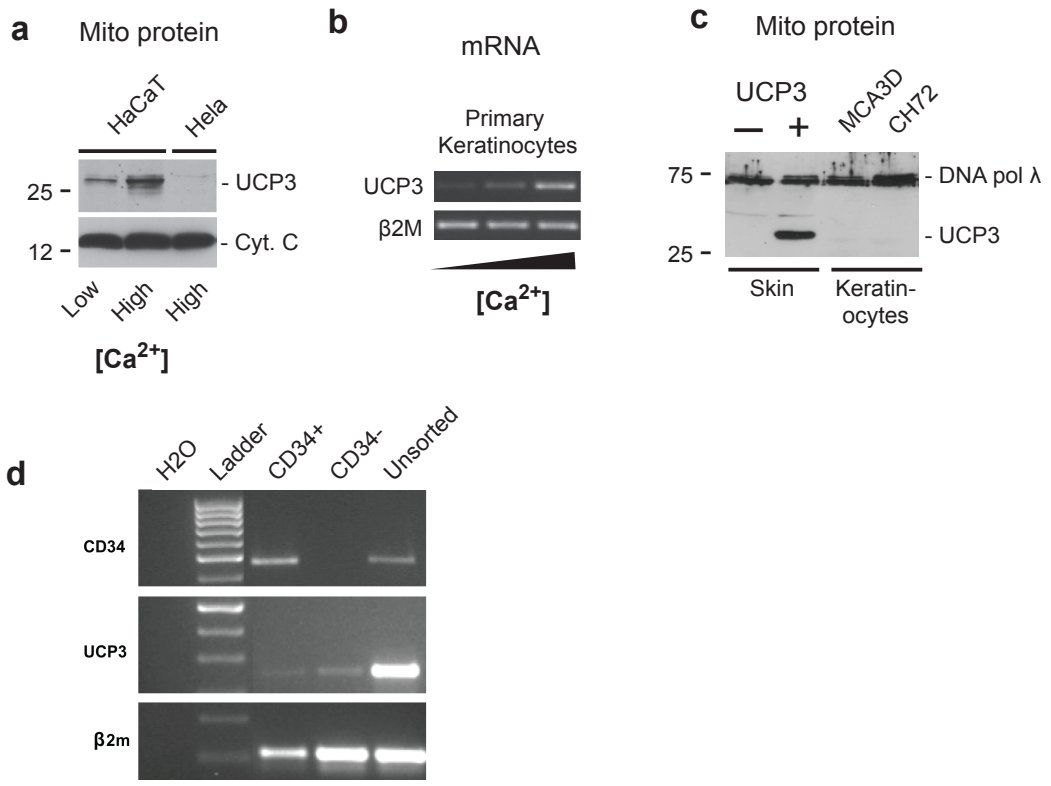

Figure 3.1 UCP3 expression positively correlates with differentiation.

(**a**) Immunoblot for hUCP3 and cytochrome C expression in isolated mitochondria from HaCaT and HeLa cell lines in response to increased Ca^{2+}-stimulated differentiation for 48 hours at 1.2 mM Ca^{2+}. (**b**) Immunoblot for mUCP3 and DNA polymerase γ in isolated mitochondria from wild type C57Bl6/j and UCP3(-/-) whole skin and MCA3D and CH72 keratinocyte cell-lines grown under high calcium conditions. (**c**) RT-PCR for UCP3 and β2 microglobulin (β2M) mRNA expression in WT FVB/N primary keratinocytes in response to Ca^{2+}-stimulated differentiation for 48 hours at 0.05 mM, 0.1 mM, and 1.2 mM Ca^{2+}. (**d**) RT-PCR for UCP3 and β2 microglobulin (β2M) mRNA expression in WT FVB/N primary bSC and daughter keratinocytes.

carcinoma cells (Figure 3.1 c, CH72, lane 4), and initiated, non-malignant immortal keratinocytes (Figure 3.1 c, MCA3D, lane 3). None of these cell lines lacking UCP3 is differentiation competent, i.e. they fail to differentiate in response to extracellular Ca^{2+}, regardless of their tumorigenic capacity.

3.2.2 Characterization of the K5-UCP3 model

To better understand relationships between changes in mitochondrial respiration and epidermal biology, we generated hemizygous FVB/N mice expressing a respiration-inducing bovine keratin-5 promoter UCP3 transgene in epidermal and follicular keratinocytes (Figure 3.2 a, K5-UCP3). K5-UCP3 mice exhibited increased UCP3 protein expression in mitochondria isolated from dorsal skin biopsies compared to wild type (FVB/N) skin and skeletal muscle (Figure 3.2 b). Immunofluorescent staining indicated that UCP3 was properly localized in a punctate, perinuclear mitochondrial pattern in cultured K5-UCP3 primary keratinocytes (Figure 3.2 c). Moreover, UCP3 expression in K5-UCP3 skin was found in the basal and suprabasal epidermal skin layers and the hair follicle (Figure 3.2 d).

To confirm functional UCP3 activity, we measured rates of maximal (state 3) and uncoupled (state 4) oxygen consumption in isolated epidermis *ex vivo*. Both state 3 and uncoupled state 4 epidermal respiration rates were increased in K5-UCP3 compared to wild type mice by approximately 31% and 113%, respectively (Figure 3.2 e). Based on Mitotracker green staining, we observed that mitochondrial mass was increased by approximately 28% in K5-UCP3 keratinocytes compared to wild type (Figure 3.2 f). To

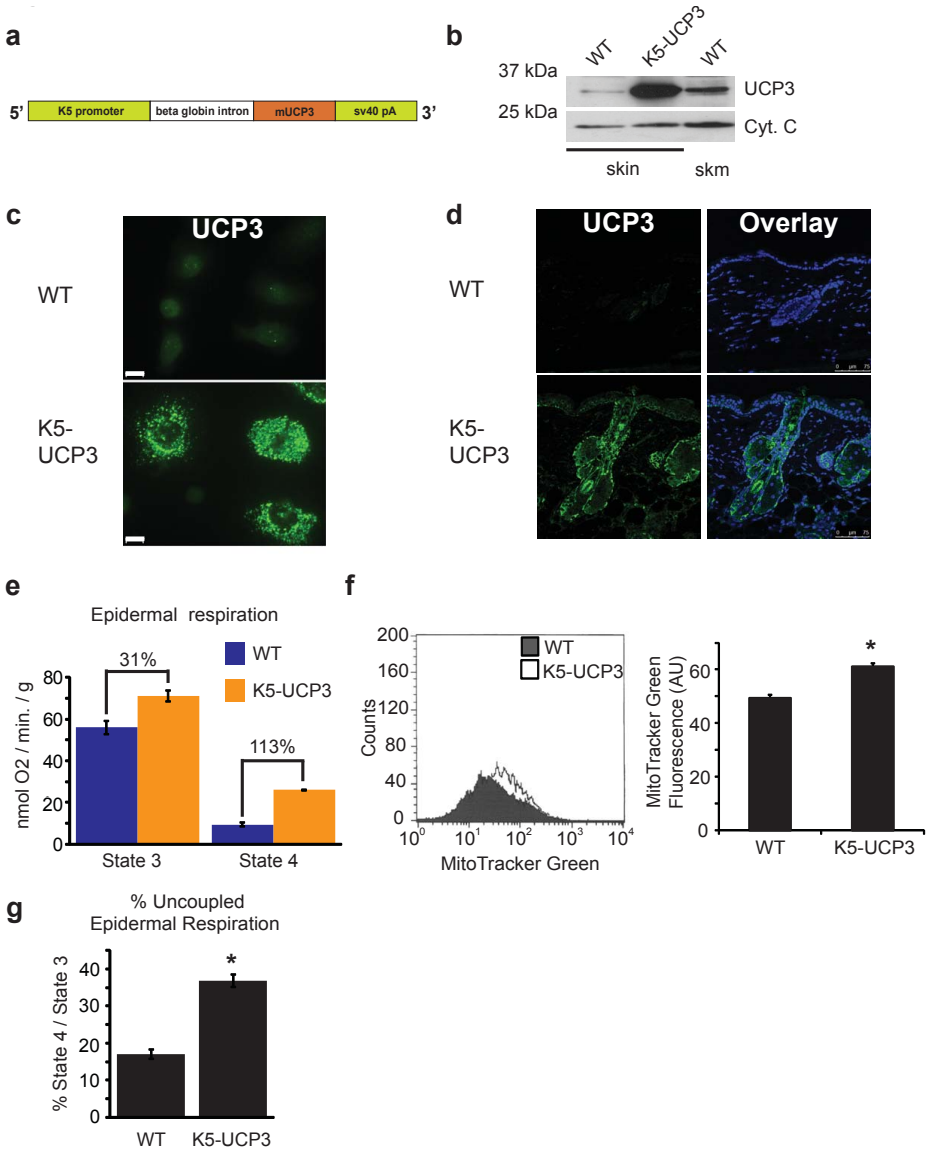

Figure 3.2 UCP3 overexpression increases cutaneous uncoupling.

(**a**) The construct used to generate K5-UCP3 FVB/N mice. (**b**) UCP3 and cytochrome C expression in isolated mitochondria from whole skin & skeletal muscle (skm). (**c**) UCP3 immunohistochemistry in primary keratinocytes. Scale bars = 10 μm. (**d**) Immunohistochemistry for UCP3 in whole skin. (**e**) State 3 (no treatment) and state 4 (with addition of 1μg/mL oligomycin) O_2 consumption per gram of epidermis. (**f**) FACS analysis of MitoTracker Green staining in wild type (WT) and K5-UCP3 primary keratinocytes (* $p < 0.001$). (**g**) % uncoupled respiration out of total respiration, determined by (state 4) / (state 3) x 100% (* $p = 0.019$). Error bars = means +/- SEM.

correct for changes in mitochondrial number, we compared the percentage of uncoupled per total epidermal respiration (state 4 / state 3 X 100%). K5-UCP3 epidermis exhibited an approximately two-fold increase in uncoupled per total respiration, consistent with functional expression of UCP3 (Figure 3.2 g).

3.2.3 UCP3 induces keratinocyte differentiation

During the initial characterizations of the transgenic mice, we observed that isolated K5-UCP3 keratinocytes were significantly larger than wild type cells, and displayed altered morphology, suggesting that enforced UCP3 expression may induce cellular differentiation. Light microscopy revealed that K5-UCP3 cells grown in low (0.05 mM) Ca^{2+} exhibited clear differentiation phenotypes that were absent in wild type keratinocytes (Figure 3.3 a). Similarly, transmission electron micrographs confirmed the UCP3-induced differentiation by revealing that the large filamentous keratin strands induced by high Ca^{2+} in wild type cells were similarly present in K5-UCP3 cells (but not wild type cells) cultured in low Ca^{2+} conditions (Figure 3.3 b).

To better understand the impact of mitochondrial uncoupling on epidermal tissue homeostasis, we performed mRNA expression analysis in adult skin from wild type FVB and K5-UCP3 mice. A large cohort of keratinocyte differentiation markers were significantly ($p < 0.01$) induced in response to UCP3 overexpression (Figure 3.3 c). Among these, increased expression of the early differentiation marker keratin 10 was confirmed by immunoblot in wild type and K5-UCP3 epidermal lysates (Figure 3.3 d), along with immunofluorescent staining of isolated primary keratinocytes (Figure 3.3 e).

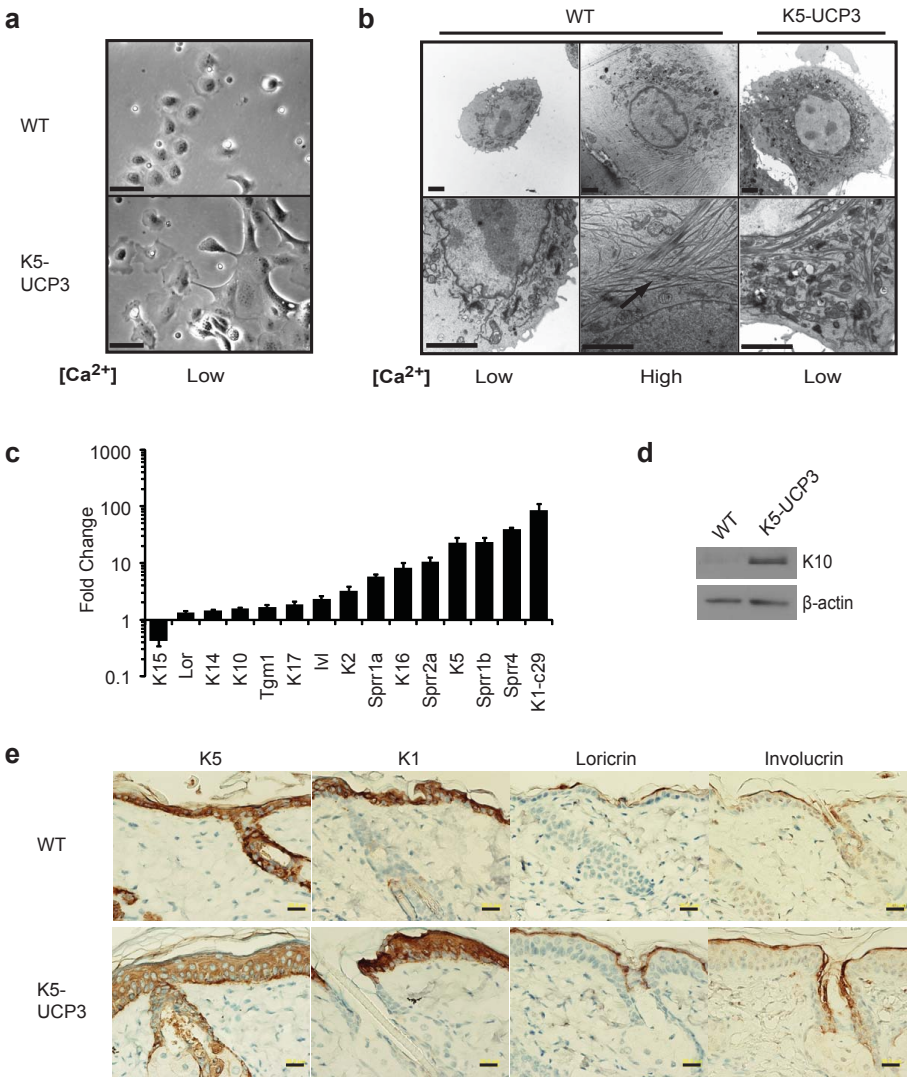

Figure 3.3 UCP3 overexpression induces epidermal differentiation.

(**a**) Wild type (WT) and K5-UCP3 primary keratinocyte morphology (light microscopy) and (**b**) transmission electron microscopy (TEM) in low (0.05 mM Ca^{2+}) and high (1.2 mM Ca^{2+}) calcium medium. Arrows indicate cytoplasmic keratinization (**b**). Scale bars = 20 and 2 μm (**a** and **b**) (**c**) Microarray analysis of K5-UCP3 skin, expressed as fold change compared to wild type. Genes shown significantly differ from wild type ($p < 0.01$). K# = keratin #, Lor = loricrin, Tgm1 = transglutaminase 1, Ivl = involucrin, Sprr# = small proline rich protein #. Error bars are means +/- SEM. (**d**) Immunoblot for keratin 10 and β-actin in epidermal lysates. (**e**) Immunohistochemistry for basal keratinocyte differentiation markers in adult (7 week old) mouse epidermis. Scale bars = 20 μm.

Also increased in K5-UCP3 epidermis were expression of the basal keratinocyte marker K5, along with the early and late keratinocyte differentiation markers K1, loricrin, and involucrin (Figure 3.3 f). Notably, the epidermis in K5-UCP3 is thicker than wild type and has an expanded layer of cells that stain positive for both K5 and K1 above the basal epidermal layer, but had decreased intensity of K5 staining. These changes appeared by three weeks of age (Figure 3.4 a).

3.2.4 K5-UCP3 epidermis lacks bulge stem cell markers

Although hotly debated, increasing evidence supports that the slowly cycling (quiescent), long-lived, multipotent follicular bulge stem cells (bSC) are candidate progenitors of squamous carcinomas (Faurschou et al., 2007; Morris et al., 2000). Quiescent bSC are marked biochemically by the presence of intracellular keratin 15, and the cell surface marker CD34, and by the capacity to retain labels (e.g. bromodeoxyuridine, BrdU) (Cotsarelis et al., 1990). Interestingly, CD34 is both lost during differentiation and required for skin carcinogenesis (Trempus et al., 2007). Remarkably, hair follicle bulge regions in adult K5-UCP3 mice exhibited dramatically decreased (~85%) immunostaining for both K15 and CD34 (Figure 3.5 a-b). Similarly, loss of these bSC markers was developmentally evident by three weeks of age (Figure 3.4 b). To quantify these changes, isolated primary keratinocytes were labeled for CD34 and α-6 integrin and analyzed by fluorescence activated cell sorting (FACS, Figure 3.5 c, Q2) to identify the bSC population (Wu and Morris, 2005). In strong concordance with the histological data, K5-UCP3 mice exhibited an 84% decrease (0.3% vs. 1.8% in wild type)

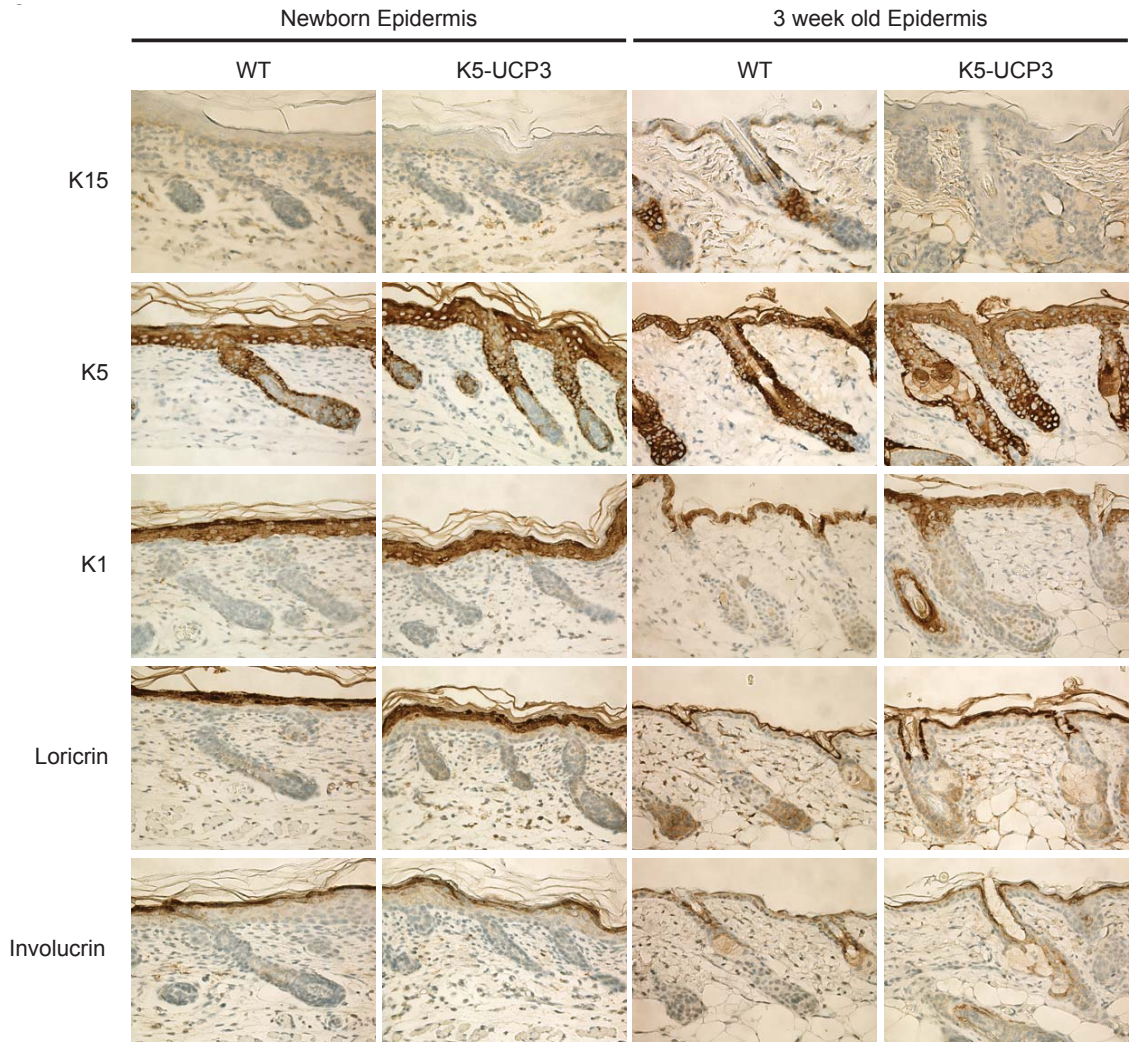

Figure 3.4 UCP3 increases expression of differentiation markers across developmental stages.

Immunohistochemistry for bSC marker keratin 15 (K15), basal keratinocyte marker keratin 5 (K5), and early and late keratinocyte differentiation markers keratin 1 (K1), loricrin, and involucrin across developmental stages in newborn and 3 week old mouse epidermis.

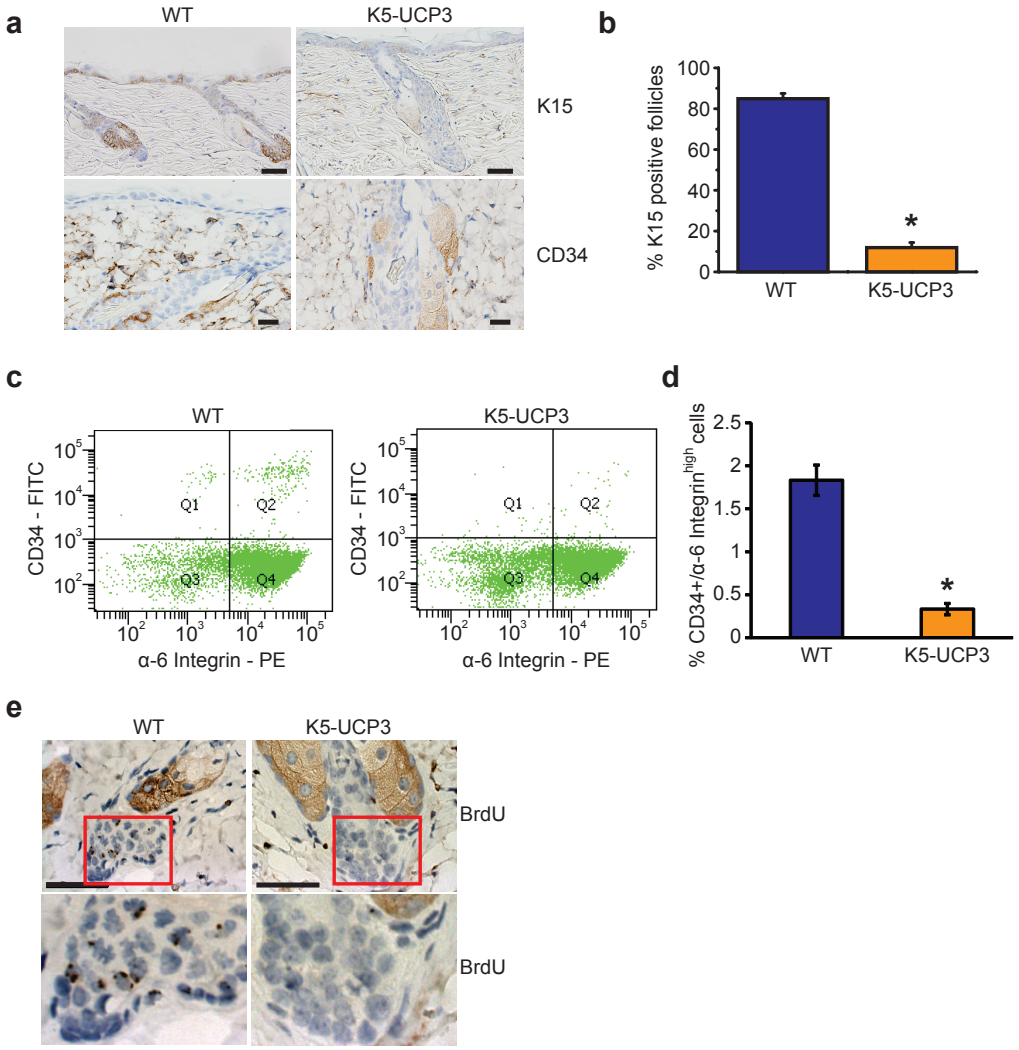

Figure 3.5 UCP3 overexpression decreases markers of quiescent stem cells.

(**a**) Immunohistochemistry for keratin 15 (K15) and CD34 in wild type (WT) and K5-UCP3 skin. Scale bars = 50 microns (K15) and 20 microns (CD34). (**b**) Quantification of K15 positive follicles (N>250 per genotype). Error bars are means +/- SEM; (* $p < 0.001$). (**c**) FACS analysis of WT and K5-UCP3 primary keratinocytes labeled with fluorescent conjugated antibodies for CD34 and α-6 integrin. Q2 shows the CD34 positive, α-6 integrin high bulge stem cell population. (**d**) Quantification of FACS analysis shown as average percentage of cells in Q2 from three separate experiments. Error bars are means +/- SEM; (* $p = 0.0014$). (**e**) BrdU label retention (8-week pulse chase) in WT and K5-UCP3 skin. Bottom panels are magnified follicle bulge regions showing BrdU label retaining cells (arrowheads). Scale bars = 50 microns.

in bSC *ex vivo* (Figure 3.5 d). Additionally, almost no cells in the hair follicle bulge region of K5-UCP3 skin retained BrdU after an eight week pulse-chase labeling regimen (Figure 3.5 e), unlike wild type bulge regions.

The decrease in three biochemical markers of the bSC pool in K5-UCP3 hair follicles can be interpreted as either a loss of the stem cells from death or alternatively, the results may indicate that the bSC have differentiated into a less quiescent, but still functional state. Ruling out that these changes were due to bulge cell death, no evidence of increased apoptosis (Figure 3.6 a) was observed in skin sections from K5-UCP3 mice compared with those from wild type mice. Furthermore, no lack of functionality typically ascribed to bulge stem cells was observed in K5-UCP3 skin. Bulge stem cell depletion or ablation leads to hair follicle and sebaceous gland degeneration (Benitah et al., 2005) and decreased wound healing (Ito et al., 2005a). K5-UCP3 mice not only had normal hair follicle number and overall morphology, they also exhibited enlarged sebaceous glands (Figure 3.6 b) and healed abrasion wounds at comparable rates to wild type mice (Figure 3.6 c).

3.2.5 UCP3 overexpression drives accelerated epidermal turnover

Taken together, the increase in expression of both basal and differentiated keratinocyte markers combined with the loss of bulge stem cell markers, but not bulge stem cell functionality, suggested the possibility that epidermal turnover was accelerated in K5-UCP3 mice. To examine this possibility, we performed a washout experiment, by pulse-labeling basal inter-follicular epidermal (IFE) keratinocytes with BrdU and

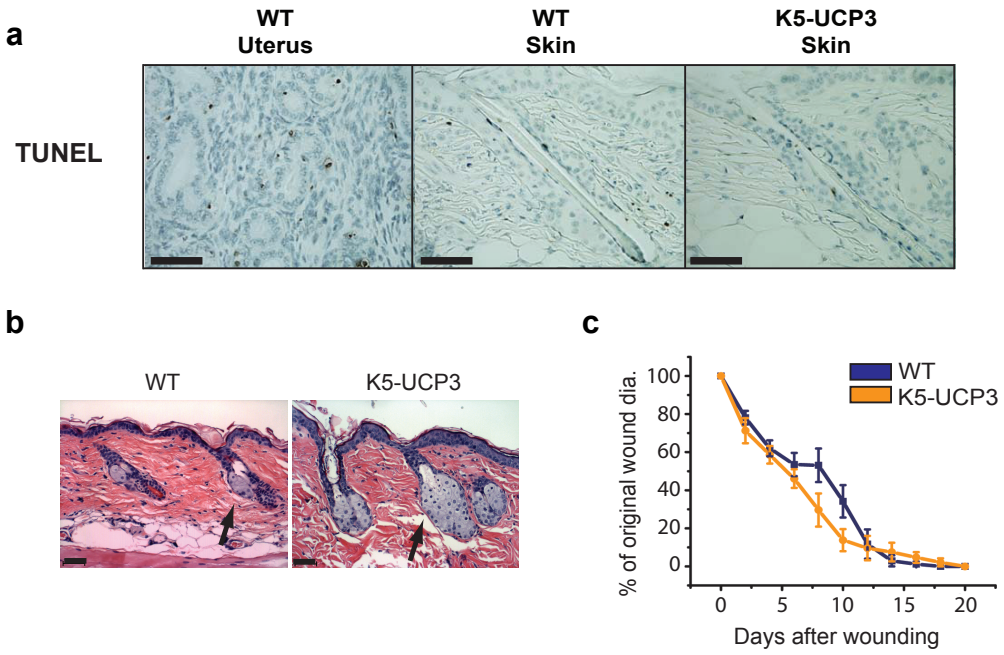

Figure 3.6 bSC functions are maintained in K5-UCP3 epidermis.

(**a**) TUNEL staining for apoptotic cells in skin sections from wild type (WT) and K5-UCP3 epidermis 36 hours after application of TPA (2.5μg/200μL acetone – vehicle). Wild type FVB/N uterus was used as a positive assay control. Scale bars = 50 μm. (**b**) Hematoxylin & eosin staining showing sebaceous gland morphology in wild type (WT) and K5-UCP3 epidermis. Scale bars = 50 μm. (**c**) Rates of wound healing after epidermal abrasion (days). Error bars are means +/- SEM.

quantifying the labeled cells that remaining in the basal layer of the IFE at successive time points. This technique allowed us to essentially monitor the transit of labeled basal keratinocytes as they migrated outward from the basal epidermis. While a slightly increased percentage of K5-UCP3 basal IFE cells stained positive for BrdU compared with wild type at the initial 2 hour time point ($p = 0.052$), there was no quantitative difference between the genotypes 5 days after labeling (Figure 3.7). By 9 days after BrdU treatment the trend had reversed, and at 18 days post-BrdU labeling, wild type basal epidermis retained approximately 1.8% labeled cells while almost no label remained in the K5-UCP3 basal IFE (~0.4%, Figure 3.7). This data indicates an increased rate of epidermal turnover and loss of labeled cells in K5-UCP3 epidermis.

3.2.6 UCP3 overexpression blocks skin carcinogenesis

Given the profound effects of UCP3 expression on mitochondrial respiration, epidermal turnover, and the quiescent bulge stem cell niche, we reasoned that K5-UCP3 mice may be resistant to cancer development. Using a well-established two-stage chemically-induced skin carcinogenesis model (Rundhaug et al., 1997a), adult wild type and K5-UCP3 mice ($n \geq 17$ per genotype) were topically administered a single dose of dimethylbenzanthracene (DMBA) (100 μg) followed two weeks later with biweekly applications of the tumor promoter 12-O-tetradecanoylphorbol-13-acetate (TPA) (2.5 μg) for 26 weeks. After 15 weeks of treatment, wild type mice developed an average of 9 tumors per mouse, with 100% of the animals bearing tumors (Figure 3.8 a-b). In stark contrast, none of the K5-UCP3 mice developed any tumors by 15 weeks (Figure 3.8 a).

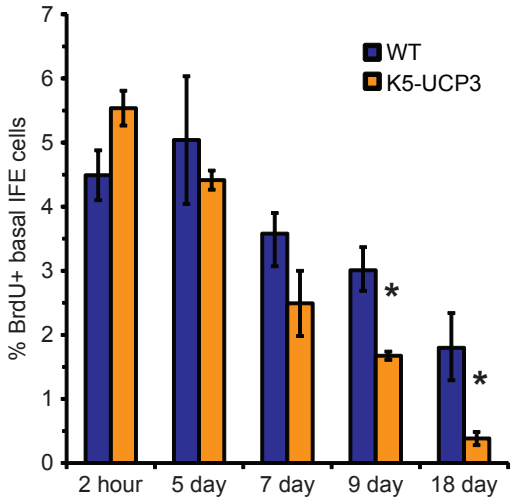

Figure 3.7 K5-UCP3 epidermis displays accelerated epidermal turnover

Epidermal turnover in wild type and K5-UCP3 skin, measured as retention of BrdU in basal interfollicular epidermal (IFE) cells 2 hours, 5 days, and 18 days following intraperitoneal BrdU injection. 500 basal IFE cells from each of three mice per genotype were counted at each time point. Error bars are means +/- SEM. * indicates significantly different from WT at the same time point ($p < 0.05$).

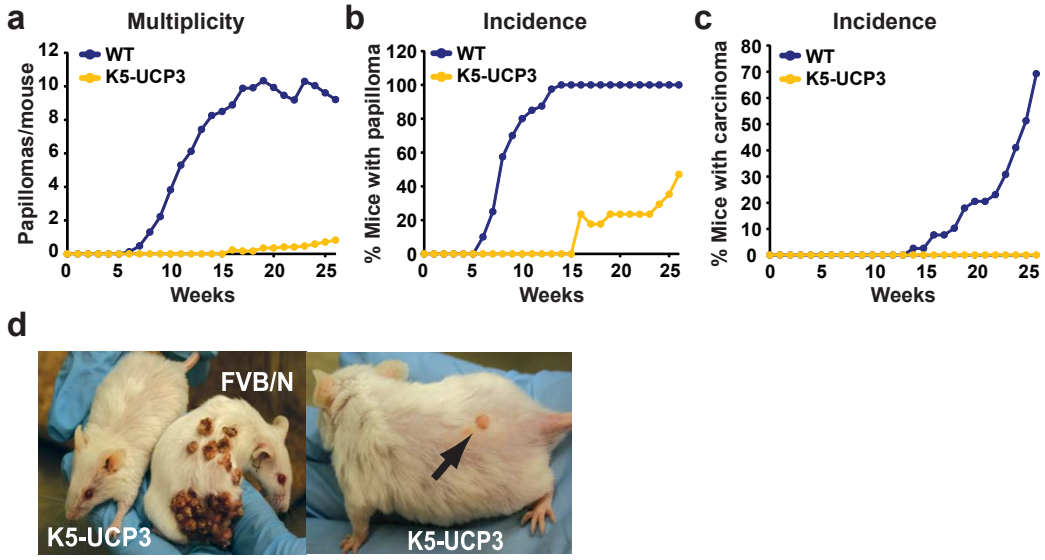

Figure 3.8 Mitochondrial uncoupling strongly inhibits two-stage chemically-induced skin carcinogenesis.

(**a**) Tumor development in wild type FVB/N (WT) and K5-UCP3 mice indicating total papillomas / mouse, (**b**) % mice bearing papillomas and (**c**) % mice bearing carcinomas. (**d**) Representative tumors in K5-UCP3 and WT mice. Arrow indicates a typical K5-UCP3 papilloma.

At 26 weeks, approximately half of the K5-UCP3 mice remained tumor-free, and those that developed tumors typically bore only one small papilloma (Figure 3.8 b and d). Moreover, 70% of wild type animals developed at least one carcinoma by 26 weeks, but remarkably, none of the K5-UCP3 mice developed a malignancy (Figure 3.8 c). Confirming that the cancer resistant phenotype of K5-UCP3 mice was a result of mitochondrial uncoupling, animals expressing a keratin 5 UCP1 transgene (K5-UCP1) were similarly protected from carcinogenesis (data not shown).

3.3 Discussion

Our results provide evidence of a novel role for UCP3 in the regulation of keratinocyte biology and cancer prevention. These observations support Warburg's original idea and a revival of scientific interest in cancer bioenergetics implicating mitochondrial metabolic reprogramming in the development and maintenance of malignancy. As discussed in Chapter 1, to date, only a few studies in the literature deal with relationships between mitochondrial uncoupling proteins and carcinogenesis. The exact molecular mechanisms by which UCP3 expression affects cellular differentiation and thereby prevents skin carcinogenesis in the K5-UCP3 mouse model remain to be defined and are a matter of intense research interest.

We demonstrate for the first time the capacity for any uncoupling protein to promote cellular differentiation, and show that UCP3 is induced physiologically during wild type keratinocyte differentiation. This data is consistent with previous observations

showing that UCP3 expression increases during skeletal myocyte differentiation during metabolic induction in developing muscle (Guigal et al., 2002). Ca^{2+} is the major driver of keratinocyte differentiation in mammalian skin and keratinocyte cultures (Rice and Green, 1979). The prevailing evidence indicates that extracellular Ca^{2+}-induced release of endoplasmic reticulum Ca^{2+} is a pivotal event that leads to the expression of a vast array of differentiation regulatory genes (transglutaminases, involucrin, etc.). Surprisingly, we could find no literature dealing with relationships between mitochondrial bioenergetics and cellular Ca^{2+} levels in keratinocytes. However, in a variety of other contexts including neuronal synapses and contracting muscle fibers, mitochondria sequester large amounts of Ca^{2+} and are pivotal for Ca^{2+}-signaling (Biswas et al., 1999). Additionally, the mitochondrial membrane potential drives mitochondrial Ca^{2+} sequestration, and mitochondrial uncoupling-induced membrane depolarization decreases sequestration (Rial and Nicholls, 1984). Thus, mitochondrial regulation of intracellular Ca^{2+} leading to terminal differentiation of keratinocytes may be another important bioenergetic mechanism underlying UCP3-induced cancer resistance. Consistent with this idea, though Ca^{2+} *per se* was not examined, recent preliminary reports have implicated decreased mitochondrial membrane potential and mitochondrial dysfunction as mediators of keratinocyte differentiation (Tamiji et al., 2005).

The profound cancer resistance of K5-UCP3 mice corresponds with a sharp decrease in three biochemical markers of quiescent bulge stem cells (bSC), the putative progenitors of multistage skin carcinomas. Loss of bulge stem cells leads not only to skin cancer resistance, but also to dramatically decreased folliculogenesis, sebaceous gland

development, and wound healing (Benitah et al., 2005). However, the cancer resistance observed in K5-UCP3 mice did not correspond to any apparent defect in these bSC-mediated functions. Thus, it is likely that the bSC of K5-UCP3 mice are present, but exist in a more differentiated, less quiescent state. This idea is supported by recent observations indicating that common adult stem cell niches, including the hair follicle, contain both quiescent and active cycling populations that cooperatively function (Li and Clevers). It is tempting to speculate that mitochondrial metabolism may functionally participate in the specification of stem cell fate.

Finally, we observed that UCP3 expression was lowest in undifferentiated compared to differentiated keratinocytes, and was absent from isolated mitochondria from malignant cells *in vitro*. Thus, expression of uncoupling proteins may be incompatible with carcinogenesis by driving the initiated stem cells to differentiate, thereby blocking promotion. Future work is needed to understand the complex mechanistic relationships between mitochondrial function and carcinogenesis, especially in relation to the biology of cancer stem cells. Nonetheless, this work supports a growing body of literature indicating that important functional links exist between mitochondrial bioenergetics and carcinogenesis.

Chapter 4: Mechanisms of UCP3-induced cancer resistance: lipid catabolism and PI3K/Akt pathway inhibition.

4.1 Introduction

The discovery of the striking cancer protective phenotype of K5-UCP3 mice generated the immediate question of how UCP3 was able to confer such strong chemoresistance. Because uncoupling proteins alter so many aspects of mitochondrial function and physiology, the possible mechanisms by which UCP3 might antagonize tumorigenesis were numerous. For example, the effects of UCP3 expression on ROS, heat production, and substrate oxidation each could easily exert effects on various tumorigenic processes.

Herein, we show that the mechanism of chemo-prevention in K5-UCP3 mice is via the inhibition of tumor promotion through blockade of PI3K/Akt signaling. Blunted Akt activation resulted from a combination of increased activity of protein phosphatase 2A (PP2A), along with reduced membrane recruitment of Akt. We demonstrate that enforced mitochondrial uncoupling enhances lipid catabolism and membrane phospholipid breakdown, likely changing membrane composition and dynamics, and resulting in restriction of Akt membrane recruitment and activity. Overexpression of wild type Akt rescued phorbol ester induced proliferation and two-stage chemical carcinogenesis. These results establish a mechanism for UCP3-induced chemoresistance, and identify a novel pathway of metabolic regulation of Akt.

4.2 Results

4.2.1 UCP3 expression blocks tumor promotion.

As discussed in Chapter 3, we previously generated K5-UCP3 mice that over-express murine uncoupling protein 3, targeted to the basal epidermis by the bovine keratin 5 promoter (K5) (Lago et al., 2012). K5-UCP3 basal keratinocytes exhibit proper localization of UCP3 in the mitochondria, and K5-UCP3 epidermis exhibits an approximately two-fold increase in uncoupled per total respiration, indicating that the transgene is functional (Lago et al., 2012). Using a two-stage chemical carcinogenesis regimen, we showed that K5-UCP3 mice were extremely resistant to skin tumor formation (Lago et al., 2012).

In order to determine whether UCP3 confers tumor resistance mainly through effects on tumor initiation or tumor promotion, and to test the efficacy of UCP3 over-expression on cancer resistance in a genetic model, we crossed K5-UCP3 animals with Tg.AC mice, which express an oncogenic *v*-Ha-Ras transgene, thereby bypassing effects on tumor initiation (Leder et al., 1990). In response to topical application of the tumor promoter 12-O-tetradecanoylphorbol-13-acetate (TPA), Tg.AC mice rapidly formed tumors; however, bi-transgenic K5-UCP3/Tg.AC mice maintained the potent chemoresistance observed in the K5-UCP3 background alone (Figure 4.1 a-d), indicating that UCP3 over-expression likely interferes with tumor promotion. Consistent with this phenotype, 5-bromo-2-deoxyuridine (BrdU) labeling revealed that UCP3 over-expression dramatically reduced the proliferative response to both single (1x) and multiple (4x) TPA treatments by approximately 80% (Figure 4.1 e). Whereas both 1x and 4x TPA treatment

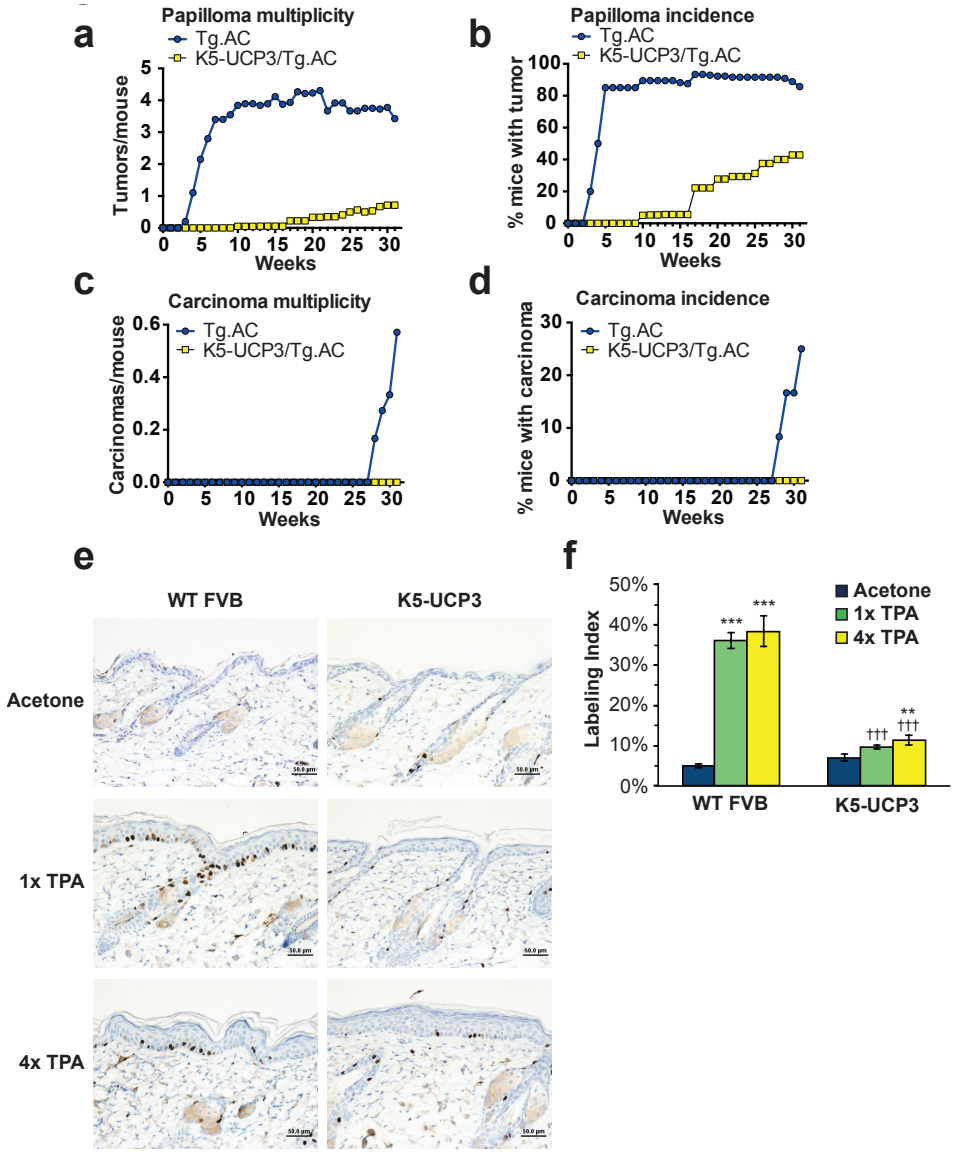

Figure 4.1 UCP3 overexpression impedes tumor promotion.

(**a**) Tumor development in "pre-initiated" Tg.AC and bigenic K5-UCP3/Tg.AC mice indicating total papillomas/mouse, (**b**) % mice bearing papillomas, (**c**) total carcinomas/mouse, and **(d)** % mice bearing carcinomas. (**e**) Immunohistochemistry for BrdU labeled cells following topical treatment with Acetone, single (1x) or multiple (4x) treatments with 2.5 µg TPA. Scale bars = 50 microns. (**f**) Quantification of percent BrdU-positive labeled basal interfollicular cells. Error bars are means +/- SEM. * = significantly differs from Acetone, same genotype (** $p<0.01$, *** $p<0.0001$), † = significantly differs from wild type FVB, same treatment (††† $p<0.0001$).

induced a 7.3-7.8 fold increase in labeling index in wild type FVB/N epidermis compared to acetone (vehicle control), labeling index in K5-UCP3 epidermis only increased by 1.37 and 1.62-fold in response to 1x and 4x TPA treatment, respectively (Figure 4.1 f).

4.2.2 UCP3 expression inhibits Akt activation

The activation of Akt and subsequent induction of cyclins and suppression of cell cycle inhibitory proteins controls proliferation following TPA treatment (Brazil et al., 2004; Rodriguez-Puebla et al., 1998). Consistent with the observed lack of TPA-induced proliferation, 18 hours after TPA treatment, K5-UCP3 epidermis showed blunted cyclin D1 and cyclin A induction, and maintenance of p21 and p27 levels (Figure 4.2 a). In wild type epidermis, Akt was activated 4 hours after TPA treatment, indicated by phosphorylation at both S473 (mTORC2 site) and T308 (PDK1 site). However, K5-UCP3 epidermis showed reduced basal Akt phosphorylation, along with very little activation of Akt after TPA treatment (Figure 4.2 a-b), which corresponded to decreased phosphorylation of direct Akt targets, including GSK-3β and FOXO1 (Figure 4.2 b), as well as TSC2 (Figure 4.2 c).

Given the well-established relationships between metabolic state and mTOR activation, along with the observed lack of Akt activation, we predicted that UCP3 overexpression should correspond to decreased activation of mTOR. Indeed, mTOR phosphorylation at S2448 was diminished, however, auto-phosphorylation at S2481 was unaffected. Furthermore, phosphorylation of targets downstream of mTORC1, including ribosomal protein S6 (rS6), eukaryotic translation initiation factor 4E-binding protein 1

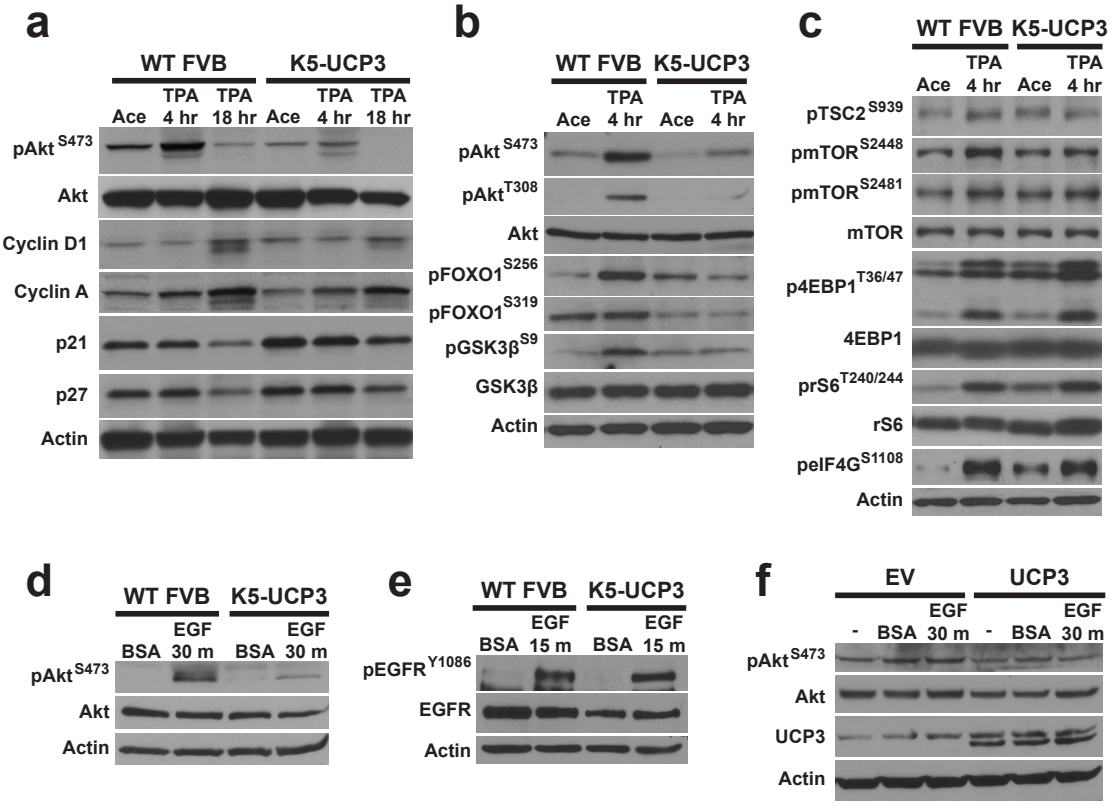

Figure 4.2 UCP3 overexpression inhibits Akt activation.

(**a**) Akt activation and cell cycle protein expression following treatment with Acetone (vehicle control) or 2.5 µg TPA (4 hours & 18 hours post-treatment) in wild type FVB and K5-UCP3 epidermal lysates. (**b**) Akt activation and phosphorylation of Akt targets FOXO1 and GSK3β. (**c**) Phosphorylation of mTORC1 pathway members. (**d**) Activation of Akt in mouse primary keratinocytes 30 minutes after treatment with 40 ng/mL EGF or 0.001% BSA (vehicle control). (**e**) Phosphorylation of EGF receptor (EGFR) in mouse primary keratinocytes 15 minutes after treatment with EGF. (**f**) Akt activation in NHK transiently transfected with UCP3 or empty vector control (EV). Immunoblotting for β-Actin was used to confirm equal loading (**a-f**).

(4EBP1), and eukaryotic initiation factor 4G (eIF4G) was not markedly decreased, implying that UCP3 induces complex metabolic regulation of mTOR (Figure 4.2 c). Although interesting, and perhaps somewhat paradoxical, these effects on mTOR signaling point toward an mTOR-independent mechanism of tumor resistance.

TPA acts as a diacylglycerol mimetic, binding Protein Kinase C (PKC) isoforms and activating subsequent downstream signaling, which, among numerous other effects, increases epidermal growth factor (EGF) ligand expression and ectodomain cleavage, resulting in paracrine/autocrine signaling (Herrlich et al., 2008; Kiguchi et al., 1998). Studies using both chemical inhibitors and dominant negative mutants have shown that EGF receptor (EGFR) activation is necessary for TPA-induced activation of Akt and other pathways (Chan et al., 2004b; Chen et al., 2001; Xian et al., 1995). To rule out the possibilities that UCP3 over-expression prevented TPA-induced Akt activation via inhibition of PKC and/or impaired EGF ligand shedding, we evaluated Akt activation in serum starved, isolated primary keratinocytes treated with EGF. As expected, K5-UCP3 cells showed blunted Akt activation after EGF treatment (Figure 4.2 d). In contrast, EGFR activation was unaffected by UCP3, despite slightly lower total receptor expression (Figure 4.2 e). Importantly, UCP3 expression also blocked activation of Akt by EGF in primary neonatal human keratinocytes (Figure 4.2 f). Together, these observations demonstrate that the UCP3-dependent regulation of Akt activity occurs downstream of EGFR activation in a cell autonomous, species-independent manner.

Subsequent to EGFR activation, PI3K converts phosphatidylinositol 4,5-bisphosphate (PIP2) to phosphatidylinositol (3,4,5)-trisphosphate (PIP3), resulting in the

recruitment of Akt to the plasma membrane. To define the mechanisms by which UCP3 blunts Akt signaling downstream of EGFR activation, we initially focused on phosphatase and tensin homolog (PTEN), a tumor suppressor lipid phosphatase that converts PIP3 back to PIP2, thereby inhibiting Akt. PTEN activity can be regulated by changes in expression, or in the stabilizing phosphorylation of its C-terminal tail, which increases its activity. Levels of both phosphorylated and total PTEN protein were unchanged in K5-UCP3 compared to wild type epidermis, ruling out the likelihood that changes in PTEN function account for UCP3-induced blockade of Akt activation (data not shown).

We then examined another negative regulator of Akt activation, protein phosphatase 2a (PP2A), a serine/threonine phosphatase that dephosphorylates Akt at both S473 and T308 (Li et al., 2003). Although the expression of PP2A A (scaffolding) and C (catalytic) subunits was unchanged from wild type to K5-UCP3 epidermis (Figure 4.3 a), several additional prominent PP2A targets, including p38 mitogen activated protein kinase (p38 MAPK), showed a pattern of reduced phosphorylation in K5-UCP3 epidermal lysates (Figure 4.3 b), implying that PP2A was hyper-active in K5-UCP3 epidermis. Indeed, using an *in vitro* activity assay, K5-UCP3 samples showed a significant but modest increase in PP2A catalytic activity (39%) compared to wild type controls (Figure 4.3 c). Topical treatment with the PP2A inhibitor okadaic acid (OA) was able to completely recover phosphorylation of p38 MAPK, however OA only partially rescued Akt phosphorylation in K5-UCP3 epidermis (Figure 4.3 d). Thus, PP2A hyperactivity likely contributes to, but is not solely responsible for the UCP3-induced

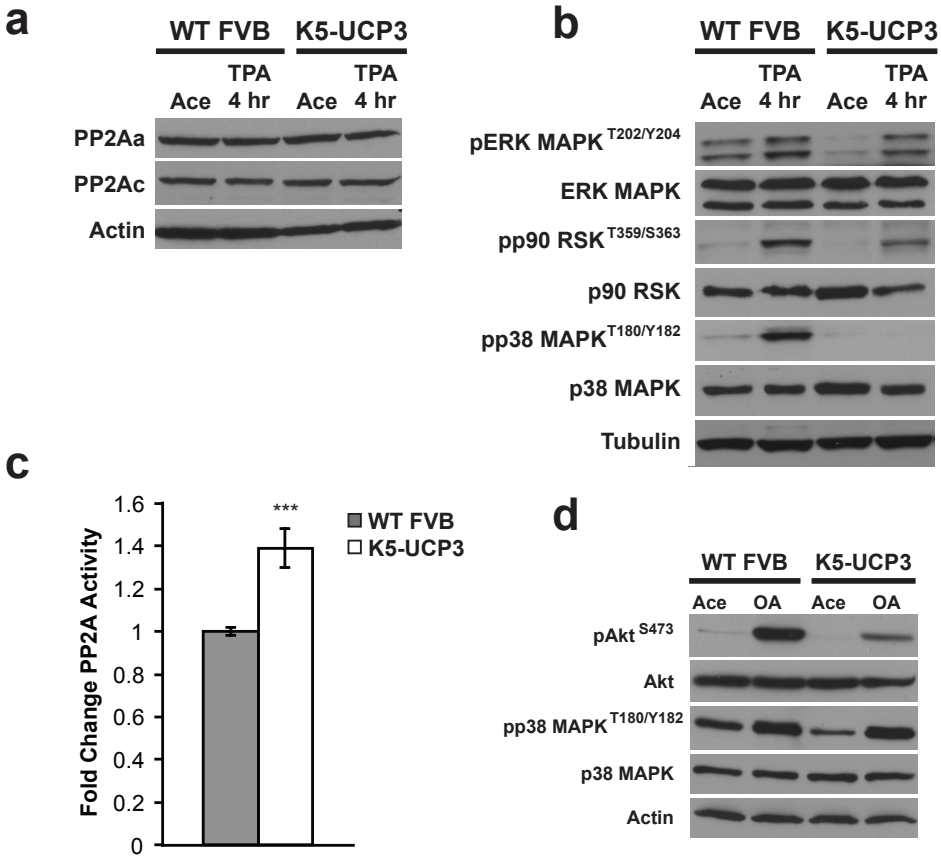

Figure 4.3 PP2A is hyperactive in K5-UCP3 epidermis.

(**a**) Immunoblot for expression of the A (scaffolding) and C (catalytic) subunits of PP2A. Immunoblotting for β-Actin was used to confirm equal loading. (**b**) Immunoblot for phosphorylation of additional PP2A targets, including ERK, p90 RSK, p38 MAPK. (**c**) *In vitro* PP2A catalytic activity. Error bars are means +/- SEM. *** indicates significantly different from wild type ($p<0.001$). (**d**) Akt and p38 MAPK activation 1 hour after treatment with 5 nmol okadaic acid (OA). Immunoblotting for β-Actin was used to confirm equal loading (**a-b,d**).

blockade of PI3K/Akt signaling. However, the striking effects on other PP2A targets, including p38 MAPK, may inform future studies detailing additional Akt-independent pleiotropic mechanisms of UCP3-induced tumor resistance

4.2.3 UCP3 expression alters lipid homeostasis

Because PP2A hyperactivity could not fully explain the UCP3-dependent inhibition of Akt, we focused on two main functions of UCP3: its ability to modulate reactive oxygen species (ROS) generation (Esteves and Brand, 2005), and lipid metabolism (Bezaire et al., 2005). Some evidence suggests that ROS regulate both PP2A and Akt (Murata et al., 2003; Pelicano et al., 2006), therefore, we hypothesized that UCP3 over-expression may inhibit Akt through redox regulation. However, we neither detected a significant difference in either cellular ROS or ROS released from isolated mitochondria, nor did we observe a change in the oxidation state of either PP2A or Akt thiols in response to uncoupling (Figure 4.4).

Studies have indicated that changes in β-oxidation can reshape plasma membrane lipid composition (Kretschmer et al., 2012; Lockshon et al., 2007), and UCP3 is well known for its ability to increase β-oxidation of lipids (Bezaire et al., 2005). Therefore, we reasoned that UCP3 over-expression might affect Akt activation by promoting the oxidation of fatty acids and modifying membrane composition. To examine this possibility, we used an unbiased metabolomic approach and found that UCP3 overexpression drove large scale lipid catabolism in K5-UCP3 epidermis, characterized by decreased steady-state levels of free fatty acids (FFA) (Figure 4.5 a), and long chain

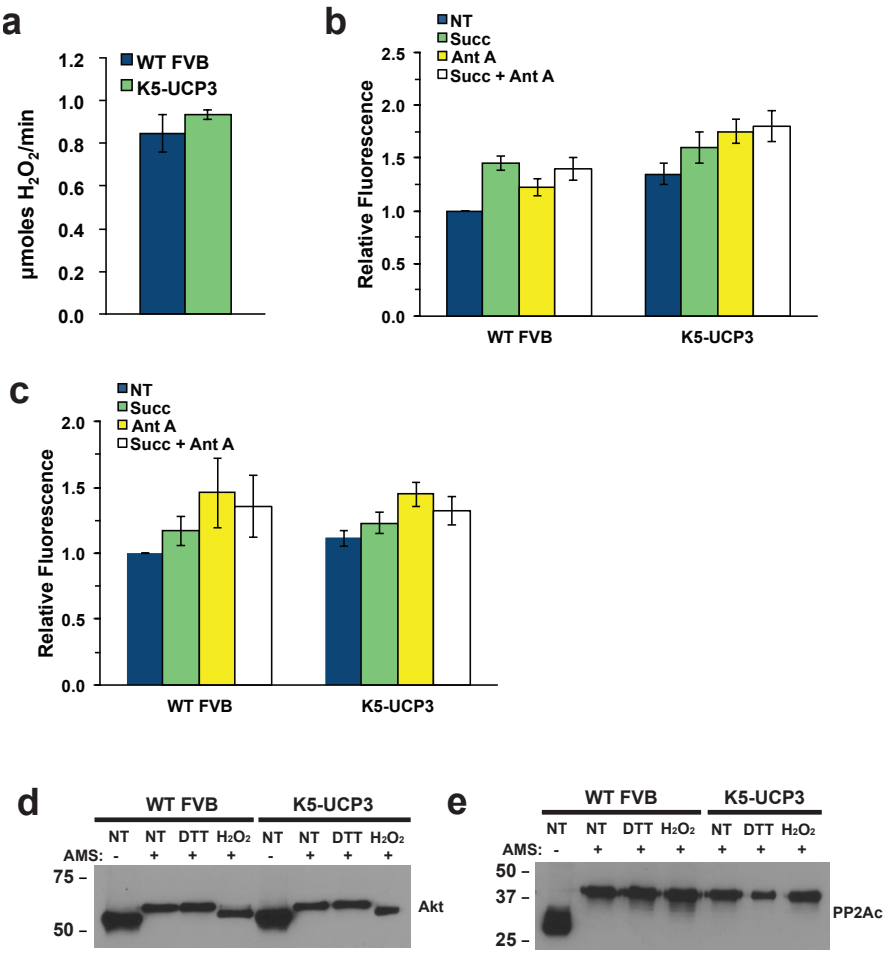

Figure 4.4 Uncoupling has no significant effect on ROS in the K5-UCP3 model.

(**a**) Amplex Red assay for rate of H_2O_2 production by mitochondria isolated from wild type FVB and K5-UCP3 epidermis. (**b**) Dihydroxydichlorofluorescein and (**c**) dihydroethidium staining for cellular hydrogen peroxide and superoxide levels (respectively) in isolated primary mouse keratinocytes unstimulated, or treated with 10 mM succinate (Succ), 10 µM Antimycin A (Ant A), or their combination (Succ + Ant A). Data shown are fold change from mean wild type, unstimulated fluorescence. Error bars are means +/- SEM. (**d & e**) Immunoblots for thiol oxidation status of Akt (**d**) and PP2A (**e**). 4-acetamido-4′-maleimidylstilbene-2,2′-disulfonic acid (AMS) labels reduced cysteines, causing an increase in molecular weight and a resultant upward shift in mobility on the SDS-PAGE gel. Oxidation blocks AMS labeling, thereby blocking this upward shift. Treatment with dithiothreitol (DTT) and hydrogen peroxide (H_2O_2) were used as controls.

acyl-carnitine species (Figure 4.5 b). Concurrently, K5-UCP3 epidermis displayed increased levels of lysophospholipids, which are formed by cleavage of one acyl chain during phospholipid breakdown, suggesting that uncoupled cells scavenge fatty acid tails from membrane lipids as substrates for β-oxidation (Figure 4.5 c). Consistent with the idea that UCP3 induced global, unbiased lipid breakdown rather than oxidation of a specific lipid species or activation of a specific phospholipase, neither the decreases in FFA, nor the increases in lysophospholipid levels followed any discernible pattern in terms of chain length, saturation, or head group (Figure 4.6).

To test whether these changes in lipid homeostasis corresponded to functional differences in membrane recruitment of Akt, we isolated epidermal membranes from acetone and TPA treated mice. As predicted, less Akt was present in the membrane fraction from TPA treated K5-UCP3 epidermis compared with wild type (Figure 4.7 a). Of note, in the same assay we observed similar levels of PTEN membrane localization in wild type and K5-UCP3 epidermis, another indication that PTEN activity is unchanged (Figure 4.7 a). Combined, these results led us to hypothesize that UCP3-induced lipid catabolism may be associated with changes in PIP3, the signal for Akt membrane recruitment.

Membrane phospholipids, including phosphatidylinositides, were not identified in the metabolomic screen due to the extraction and detection methods utilized. Therefore, we utilized a specialized technique that couples phosphate methylation to high-performance liquid chromatography–mass spectrometry to accurately assess PIP levels (Clark et al., 2011). To our surprise, we found that PIP3 levels in K5-UCP3 epidermis

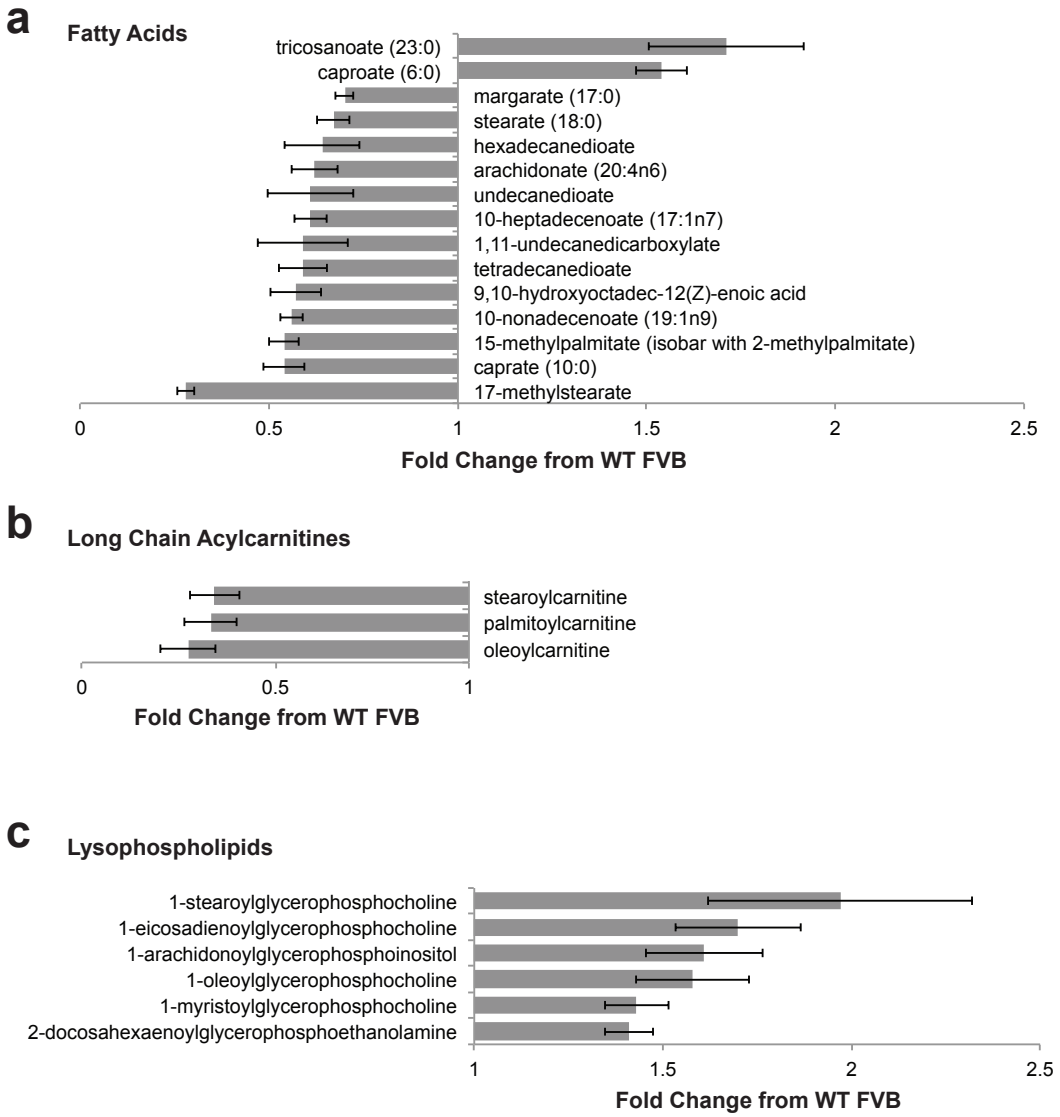

Figure 4.5 Unbiased metabolomic analysis of K5-UCP3 epidermis reveals enhanced lipid catabolism.

(**a-c**) Analysis of (**a**) fatty acid, (**b**) acylcarnitine, and (**c**) lysophospholipid metabolite levels in K5-UCP3 dorsal epidermis identified by gas chromatography mass spectrometry (GC-MS) or liquid chromatography mass spectrometry (LC-MS), and expressed as fold change compared to wild type FVB. Metabolites shown significantly differ from wild type with a p-value <0.05. Error bars are means +/- SEM. All identified lipids are shown in Extended Data Figure 3.

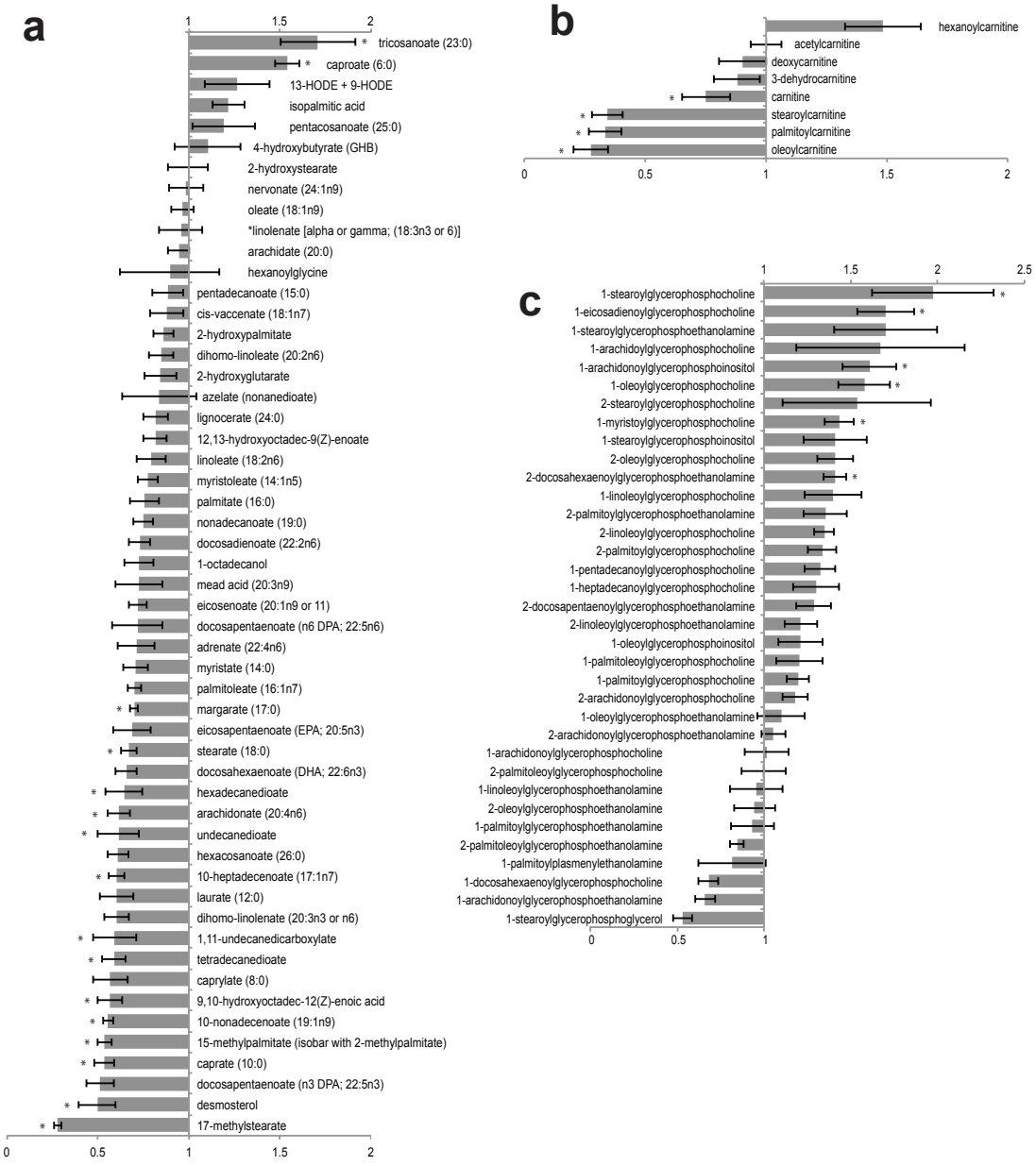

Figure 4.6 All lipid species identified in unbiased metabolomic analysis of K5-UCP3 epidermis.

(**a-c**) Analysis of (**a**) fatty acid, (**b**) acylcarnitine, and (**c**) lysophospholipid metabolite levels in K5-UCP3 dorsal epidermis identified by gas chromatography mass spectrometry (GC-MS) or liquid chromatography mass spectrometry (LC-MS), and expressed as fold change compared to wild type FVB. * indicates significantly different from wild type with a p-value <0.05. Error bars are means +/- SEM.

were comparable to wild type epidermis (Figure 4.7 b). Therefore, it appears that, at least under basal conditions, inhibition of Akt phosphorylation occurs despite normal levels of PIP3 in the membrane, perhaps as a result of changes in membrane dynamics. However, further studies are necessary to detail the mechanisms underlying inhibition of Akt plasma membrane recruitment by mitochondrial uncoupling.

In order to establish the capacity of mitochondrial β-oxidation to affect Akt signaling, we treated mice with the carnitine-palmitoyl transferase (CPT-1) inhibitor etomoxir (Eto) at a dose previously shown to inhibit mitochondrial fatty acid uptake by roughly 50% when applied topically (Caspary et al., 2005). Not only did Eto treatment augment basal Akt activation in K5-UCP3 epidermis, it also did so in wild type epidermis (Figure 4.7 c). These results demonstrate that mitochondrial fatty acid oxidation is a novel regulator of Akt signaling in wild type epidermis, and warrant further investigation.

4.2.4 Akt over-expression rescues tumorigenesis

To establish the functional importance of UCP3-mediated changes in lipid homeostasis and Akt activation in UCP3-induced cancer resistance, we inter-bred K5-UCP3 animals with mice that over-express an epidermally targeted, wild type Akt transgene (K5-Akt) (Segrelles et al., 2007). As previously published, K5-Akt mice exhibited heightened Akt expression and activation compared with wild type controls. Bi-transgenic K5-UCP3/K5-Akt mice restored Akt activation in response to TPA treatment (Figure 4.8 a). In every treatment group, Akt over-expression increased epidermal proliferation measured by BrdU incorporation, and rescued TPA-induced proliferation in

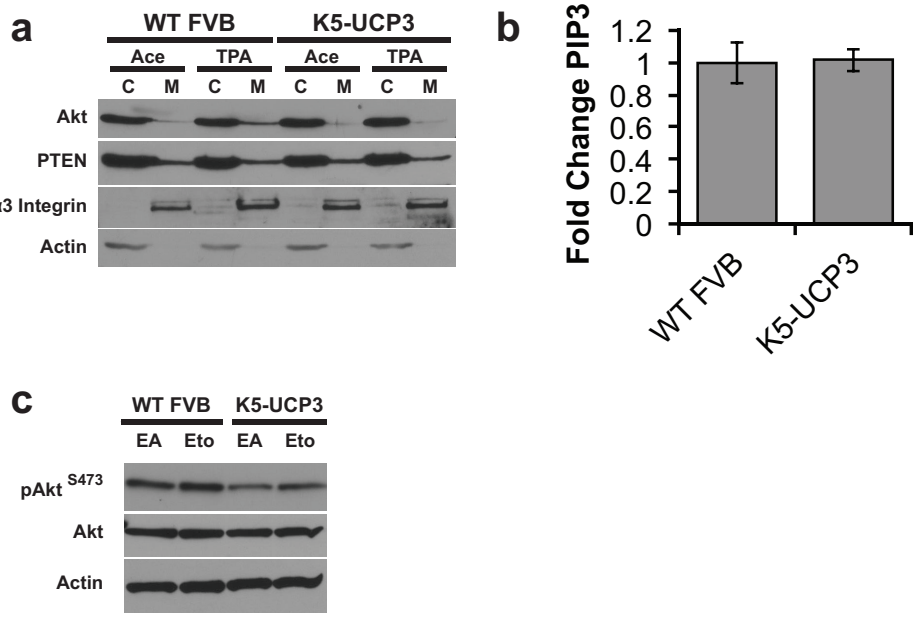

Figure 4.7 Mitochondrial β-oxidation alters plasma membrane lipids & signaling.

(**a**) Immunoblot for sub-cellular localization of Akt and PTEN in membrane and cytoplasmic fractions from wild type FVB and K5-UCP3 epidermis topically treated with 2.5 μg TPA or Acetone. Immunoblots α-6 Integrin and β-Actin were used as controls to verify membrane and cytoplasmic fractions, respectively. (**b**) Relative quantification of phosphatidylinositide(3,4,5)trisphosphate (PIP3) in wild type and K5-UCP3 epidermal lipid extracts. (**c**) Immunoblot for Akt Ser 473 phosphorylation in wild type FVB and K5-UCP3 epidermal lysates 6 hours following topical treatment with 1 mg etomoxir ethyl ester (Eto) or ethyl acetate (EA, vehicle control). Immunoblotting for β-Actin was used to confirm equal loading.

K5-UCP3/K5-Akt animals (Figure 4.8 b-c). When subjected to a two-stage chemical carcinogenesis regimen, Akt over-expression overcame metabolic regulation and rescued skin tumorigenesis in K5-UCP3/K5-Akt mice. Bi-transgenic K5-UCP3/K5-Akt mice and K5-Akt single transgenics both formed more papillomas than wild type mice, and displayed nearly overlapping papilloma incidence curves (Figure 4.9 a). Papilloma multiplicity revealed a slightly increased latency before papilloma development in K5-UCP3/K5-Akt animals; however, bi-transgenic mice still formed papillomas more rapidly and abundantly than wild type littermates (Figure 4.9 b). K5-UCP3/K5-Akt mice also formed more carcinomas than wild type mice, however they still showed a significant reduction in carcinoma formation compared with K5-Akt mice (Figure 4.9 c-d), suggesting that UCP3 may also inhibit tumor progression, even in the context of Akt over-expression. However, this difference may be explained by the fact that the transgene can still be regulated by the same changes that reduce endogenous Akt activation in K5-UCP3 mice. Notably, no K5-UCP3 single transgenic animal developed a carcinoma (Figure 4.9 c-d), in accordance with our previous findings (Lago et al., 2012). Taken together, these findings establish a new mitochondrial pathway of metabolic Akt regulation that results in the profound blockade of tumorigenesis via changes in fatty acid metabolism and membrane homeostasis.

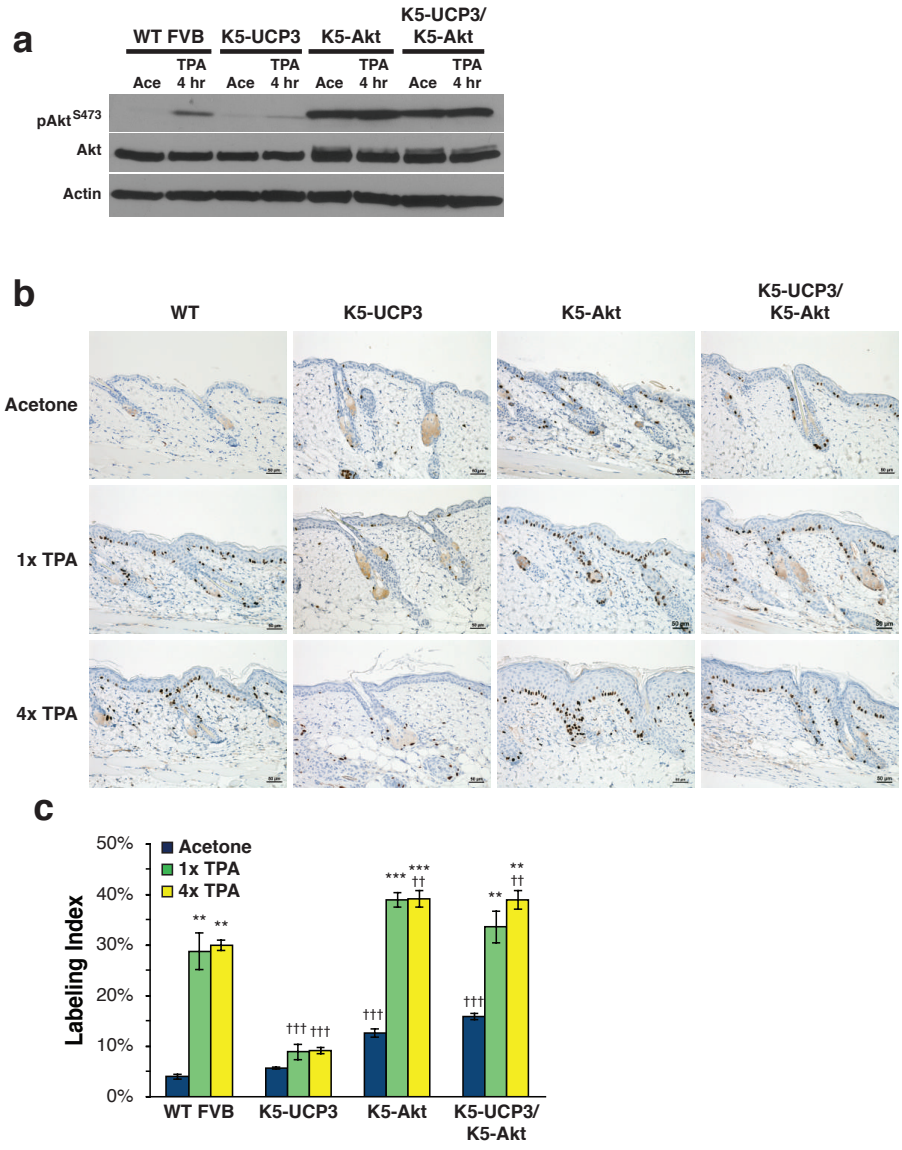

Figure 4.8 Overexpression of Akt rescues proliferation in K5-UCP3 epidermis.

(**a**) Akt phosphorylation at Ser 473 in wild type FVB, K5-UCP3, K5-Akt, and bitransgenic K5-UCP3/K5-Akt epidermal lysates, 4 hours following topical treatment with 2.5 µg TPA or Acetone. (**b**) Immunohistochemistry for BrdU labeled cells following treatment with single (1x) or multiple (4x) treatments with 2.5 µg TPA or Acetone. Scale bars = 50 microns. (**c**) Quantification of BrdU labeled cells. >500 cells were counted from n = 3 mice per genotype in each treatment group. Error bars are means +/- SEM.
* = significantly differs from Acetone, same genotype (** $p<0.01$, *** $p<0.0001$).
† = significantly differs from wild type FVB/N, same treatment (††† $p<0.0001$).

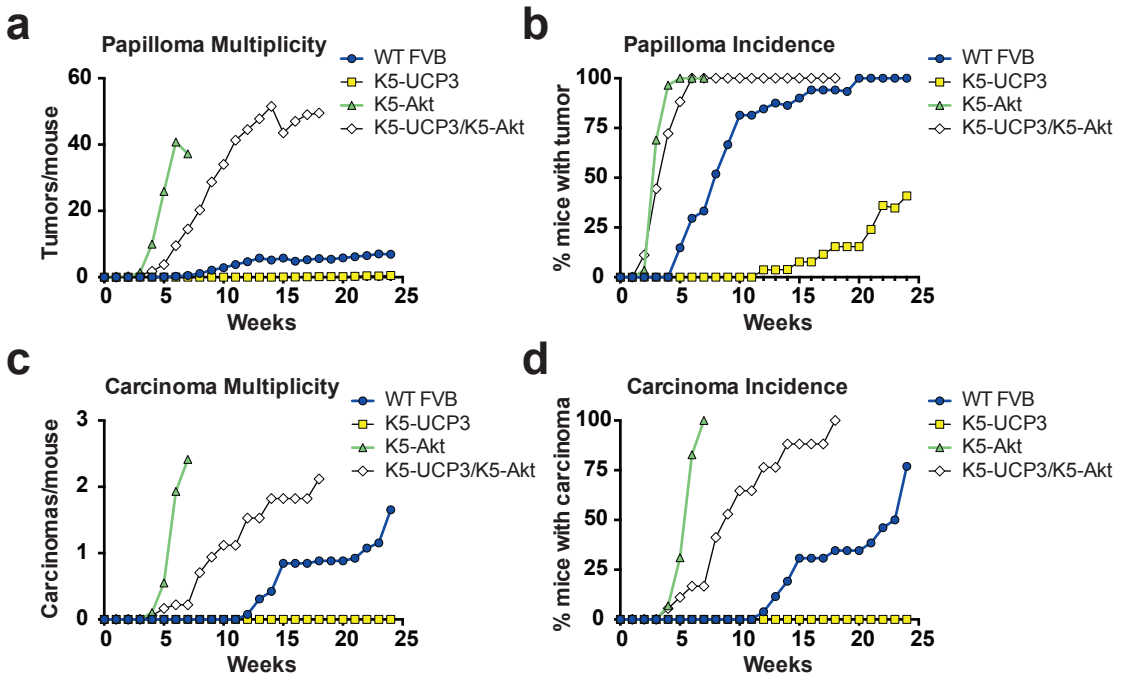

Figure 4.9 Overexpression of Akt rescues tumorigenesis.

(**a**) Tumor development in wild type FVB, K5-UCP3, K5-Akt, and bitransgenic K5-UCP3/K5-Akt mice indicating total papillomas/mouse, (**b**) % mice bearing papillomas, (**c**) total carcinomas/mouse, and **(d)** % mice bearing carcinomas.

4.3 Discussion

As discussed earlier, several lines of evidence suggest that mitochondrial oxidative metabolism is tumor suppressive. Our observations strongly support a chemopreventive action of mitochondrial respiration using a novel mouse model that expresses a skin-targeted, mitochondrial respiration-inducing UCP3 transgene. In contrast to the more well-described pathways through which mitochondria can regulate cellular proliferation through modulation of ATP, ROS, and amino acid metabolism, the lipid-dependent regulation of cell growth signaling is relatively less well understood. Here we show that mitochondrial uncoupling drove β-oxidation of lipids, which corresponded to failed Akt membrane recruitment and blockade of tumor promotion (Illustration 4.1). Inhibition of mitochondrial β-oxidation resulted in Akt activation. Our data imply that strategies that promote lipid oxidation over lipogenesis may be a novel and effective therapeutic approach that circumvents many of the toxic manifestations of traditional chemotherapeutics.

As stated previously, the role of uncoupling proteins in carcinogenesis is controversial, with some studies outlining a pro-carcinogenic role for UCPs. Our data clearly show that UCP expression has chemopreventative actions. Analysis of UCP3 expression in the Oncomine database revealed seventeen studies in which UCP3 was among the top 10% of down-regulated genes in cancer tissues compared to normal tissue controls (Table 4.1). The present study is the first to establish a molecular mechanism for UCP3-induced cancer protection, and is also the first report to show that enforced UCP3 expression can block Akt activation in mouse and human keratinocytes. As interest in

Cancer type	Fold change	p-value	Reference
Pancreatic adenocarcinoma	-3.075	5.07E-07	Logsdon, C. D. *et al.* Molecular profiling of pancreatic adenocarcinoma and chronic pancreatitis identifies multiple genes differentially regulated in pancreatic cancer. *Cancer research* **63**, 2649-2657 (2003).
Tounge squamous cell carcinoma	-4.231	1.07E-05	Estilo, C. L. *et al.* Oral tongue cancer gene expression profiling: Identification of novel potential prognosticators by oligonucleotide microarray analysis. *BMC cancer* **9**, 11, doi:10.1186/1471-2407-9-11 (2009).
Glioblastoma	-1.441	5.67E-05	The Cancer Genome Atlas - Glioblastoma Multiforme Gene Expression Data (No associated paper, 2013/06/03)
Astrocytoma	-1.649	6.39E-04	Shai, R. et al. Gene expression profiling identifies molecular subtypes of gliomas. Oncogene 22, 4918-4923, doi:10.1038/sj.onc.1206753 (2003).
Oligodendroglioma	-1.679	1.54E-04	
Pleomorphic liposarcoma	-3.334	1.00E-03	Detwiller, K. Y. et al. Analysis of hypoxia-related gene expression in sarcomas and effect of hypoxia on RNA interference of vascular endothelial cell growth factor A. Cancer research 65, 5881-5889, doi:10.1158/0008-5472.can-04-4078 (2005).
Leiomyosarcoma	-3.673	2.91E-04	
Tounge carcinoma	-1.188	4.38E-05	Pyeon, D. et al. Fundamental differences in cell cycle deregulation in human papillomavirus-positive and human papillomavirus-negative head/neck and cervical cancers. Cancer research 67, 4605-4619, doi:10.1158/0008-5472.can-06-3619 (2007).
Oral cavity carcinoma	-1.34	3.53E-04	
Germinal Center B-Cell-Like Diffuse Large B-Cell Lymph	-1.428	2.69E-07	Compagno, M. et al. Mutations of multiple genes cause deregulation of NF-kappaB in diffuse large B-cell lymphoma. Nature 459, 717-721, doi:10.1038/nature07968 (2009).
Diffuse Large B-cell Lymphoma	-1.33	5.25E-11	
Activated B-Cell-Like Diffuse Large B-Cell Lymphoma	-1.3	3.04E-08	
Familial Parathyroid Hyperplasia	-1.288	3.00E-02	Morrison, C. et al. Molecular classification of parathyroid neoplasia by gene expression profiling. The American journal of pathology 165, 565-576, doi:10.1016/s0002-9440(10)63321-4 (2004).
Parathyroid Gland Adenoma	-1.354	7.00E-03	
Dedifferentiated Liposarcoma	-1.182	6.00E-03	The Cancer Genome Atlas - Sarcoma DNA Copy Number Data (No associated paper, 2013/05/23)
Angioimmunoblastic T-Cell Lymphoma	-1.245	3.75E-05	Piccaluga, P. P. et al. Gene expression analysis of peripheral T cell lymphoma, unspecified, reveals distinct profiles and new potential therapeutic targets. The Journal of clinical investigation 117, 823-834, doi:10.1172/jci26833 (2007).
Follicular Lymphoma	-1.224	4.00E-03	Brune, V. et al. Origin and pathogenesis of nodular lymphocyte-predominant Hodgkin lymphoma as revealed by global gene expression analysis. The Journal of experimental medicine 205, 2251-2268, doi:10.1084/jem.20080809 (2008).

Table 4.1 Cancers in which UCP3 is among the top 10% of down-regulated genes.

tumor metabolism continues to intensify, it is likely that Akt will be found to have even more inputs into control of cellular metabolism, so it makes sense that it would also receive feedback control from metabolic state. Our data imply that simultaneously targeting the PI3K/Akt pathway may sensitize tumors to metabolically targeted therapies, and future studies aimed at understanding the complex mechanistic relationships between mitochondrial function, Akt signaling, and tumorigenesis will be incredibly informative as we continue to develop metabolically targeted therapeutic approaches.

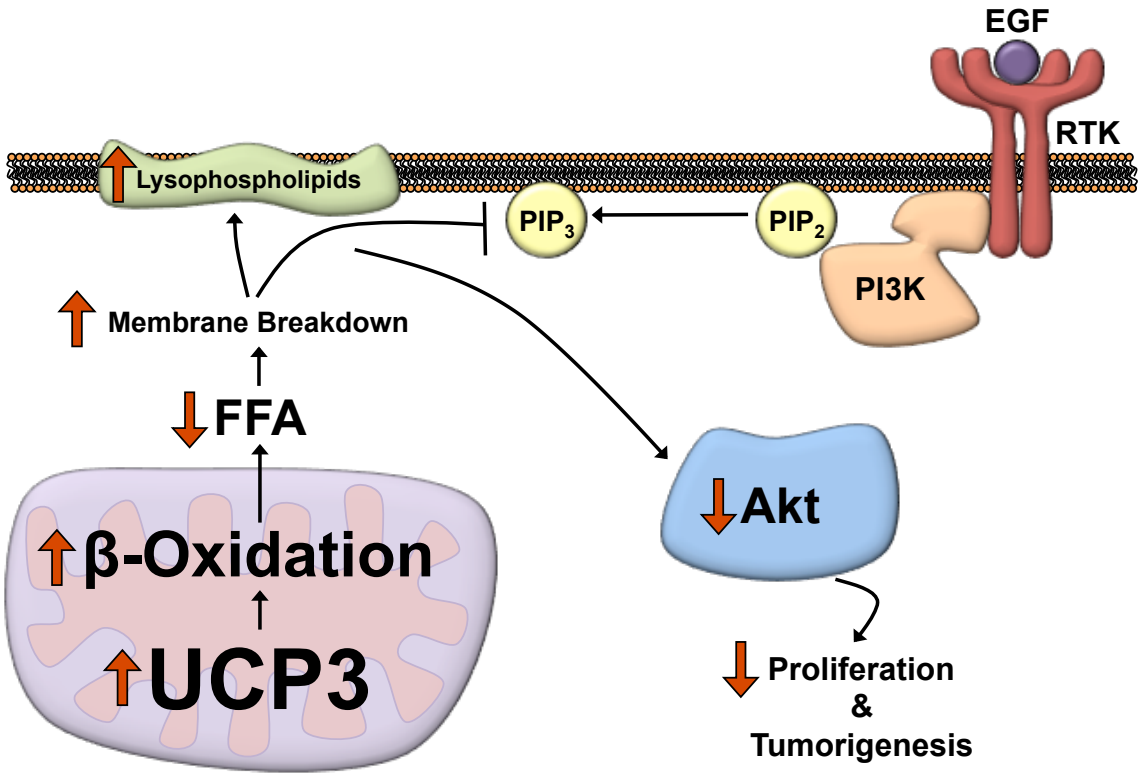

Illustration 4.1 UCP3 overexpression drives lipid catabolism and blockade of Akt signaling.

Herein, we show that overexpression of UCP3 drives enhanced fatty acid oxidation, resulting in the depletion of free fatty acids (FFA). The data suggest that the depletion of FFA causes cells to scavenge fatty acid tails from membrane phospholipids, resulting in increased markers of membrane phospholipid breakdown (lysophospholipids). These data corresponded to failure to recruit Akt to the plasma membrane, along with decreased Akt activation, despite normal levels of PIP3. We hypothesize that the failed membrane recruitment of Akt may result from changes in membrane composition and dynamics due to the increased levels of lysophospholipids.

Chapter 5: Concluding Remarks

While Otto Warburg originally proposed that mitochondrial defects caused cancer, we now understand that metabolic reprogramming likely confers tumor cells a growth advantage by simultaneously supplying the energy and biomass necessary to rapidly build new daughter cells. Here we show that enforced mitochondrial uncoupling leads to cancer resistance, likely as a result of pleiotropic changes in metabolism that converge at least in part on Akt signaling. These results add to a growing number of reports that suggest that manipulation of mitochondrial metabolism and cellular energy balance has profound effects on growth signaling. However, there are still many mechanistic details yet to be elucidated. Future studies to further examine the molecular mechanisms by which UCP3 overexpression drives keratinocyte and bulge stem cell differentiation will provide useful knowledge with relevance not only to cancer, but also to other diseases such as psoriasis. Furthermore, the work herein has identified a novel pathway of metabolic regulation of the PI3K/Akt pathway, one of the most commonly up-regulated oncogenic pathways in cancer. A more detailed mechanistic understanding of exactly how mitochondrial β-oxidation controls Akt plasma membrane recruitment could provide a new therapeutic window for novel cancer therapies. Although there are still many questions to be answered, these studies provide the foundation for future experiments to explore mechanisms of UCP3-induced cancer resistance in greater detail.

One of the least studied aspects of stem cell biology deals with the relationships between stem cell phenotypes and mitochondrial function. This is particularly true for

skin stem cell populations; we could find no study that addresses their mitochondrial bioenergetics in the literature. Nonetheless, our data argue that mitochondrial uncoupling in bulge stem cells promotes their differentiation and thereby impacts tumor resistance. Related studies in human embryonic stem cells (hESC) support this view. Morphologically, undifferentiated hESC have few mitochondria each with few cristae (St John et al., 2005), which indicates that they have low oxidative respiratory capacity and increased requirements for glycolytic ATP production. Interestingly, mitochondrial proliferation is thought to be required for hESC differentiation (Ezashi et al., 2005). In colonies of undifferentiated hESC, the more differentiated cells on the periphery exhibit increased mitochondrial number (Cho et al., 2006). Other studies show that glycolysis not only promotes hESC "stem" phenotypes, but it is repressed in favor of mitochondrial energy production during hESC differentiation (Chung et al., 2010). Additionally, both low membrane potential (Schieke et al., 2008) and calcium (Spitkovsky et al., 2004) are reported to be associated with cellular differentiation.

Though to our knowledge no publications confront the topic of mitochondrial calcium in keratinocyte differentiation, in other systems mitochondrial calcium sequestration is a major determinant of cellular calcium signaling (Bowser et al., 1998; Cheranov and Jaggar, 2004; Zenisek and Matthews, 2000). The mitochondrial membrane potential (Ψ) is a critical determinant of mitochondrial calcium sequestration, with high Ψ favoring calcium uptake, while low Ψ favors release into the cytoplasm (Nicholls and Ward, 2000). Given its effects on Ψ, pharmacologic mitochondrial uncoupling has been implicated in the protection from mitochondrial calcium overloading (Stout et al., 1998)

and numerous reports indicate that uncoupling increases intracellular calcium levels (Bernardi et al., 1984; Biswas et al., 1999; Kessler et al., 1976; Luo et al., 1997; Pozzan et al., 1977; Sandoval, 1980). Both UCP2 and UCP4 have been shown to restrict mitochondrial calcium influx through effects on Ψ (Chan et al., 2006; Teshima et al., 2003). In contrast, a controversial manuscript by Trenker et al. posited that in certain immortalized cells, UCP3 failed to regulate Ψ, but rather mediated calcium import into mitochondria (Trenker et al., 2007). Our data agree with the conclusions drawn in a published critique of this paper which suggests that UCP3 may decrease mitochondrial calcium storage and increase cytoplasmic levels (Brookes et al., 2008). Unlike Trenker et al., we have always observed an effect of UCP3 over-expression on Ψ, as has been extensively reported. Thus, we believe that UCP3 overexpression may cause mitochondrial calcium export, raising cytoplasmic calcium concentrations and thereby driving keratinocyte differentiation.

Another possibility that has yet to be explored is the relationship between the differentiating effects of UCP3 expression and the UCP3-induced blockade of Akt signaling. One likely link between these phenotypes may be protein kinase C (PKC) signaling, as PKC is the main target of TPA activation, and the classical PKC isoforms are calcium sensitive as well. Furthermore, PKCs must also be recruited to the plasma membrane in order to signal efficiently (Pinton et al., 2002), thus modulation of mitochondrial β-oxidation and lipid catabolism may have similar effects on PKC activation as those observed with Akt. Active PKC can drive proliferation or differentiation, depending on the active isoform(s) and cellular context (Bollag, 2009;

Jerome-Morais et al., 2009). Nevertheless, the UCP3-induced suppression of Akt signaling in response to EGF treatment implies that at least some of the inhibitory actions of UCP3 overexpression occur downstream of PKC activation/inactivation.

In contrast to the more well-described pathways through which mitochondria can regulate cellular proliferation through modulation of ATP, ROS, and amino acid metabolism, the lipid-dependent regulation of cell growth signaling is relatively less well understood. Several indirect lines of evidence support our observation that changes in cellular lipid homeostasis can control proliferation. For example, studies have shown that inhibiting mitochondrial citrate export can block the cell cycle (Rao and Coleman, 1989), and knockdown or inhibition of ACL results in inhibition of PI3K/Akt signaling and tumorigenesis (Buzzai et al., 2005; Hanai et al., 2012). As discussed in Chapter 1, a few other reports in the literature have suggested that lipids can affect Akt signaling through bioactive lipid signaling mediators, such as sphingosine-1-phosphate, or through changes in membrane composition and structure (Gu et al., 2013; Schuppel et al., 2008). Additionally, lysophospholipids have been shown to affect membrane recruitment and cellular signaling in an array of diverse contexts (Chowdhury et al., 2008; Grzelczyk and Gendaszewska-Darmach, 2013), however the exact mechanisms are not well understood. Future mechanistic studies are needed to further detail how UCP3-induced lipid catabolism affects signaling events and plasma membrane recruitment of Akt. Nonetheless, along with the few reports cited above, our observations lay the foundation, and support an urgent need for greater exploration of how lipid metabolism may control cell growth in general.

In the past decade, metabolic intermediates have emerged as novel players linking mitochondrial dysfunction to carcinogenesis (Ward et al., 2010; Zhao et al., 2009). The suppression of mitochondrial substrate oxidation may lead to caterplerotic reactions that provide mitochondrial substrates to the cytoplasm necessary for the biosynthetic needs of rampant cell division. Thus, UCP3-driven uncoupling could limit the flux of Kreb's cycle intermediates to the cytoplasm and thereby limit the biosynthetic supplies necessary for tumor development. Although not discussed in the current work, metabolomic analysis revealed that in addition to changes in lipid homeostasis, UCP3 overexpression likely drives elevated rates of glycolysis and enhanced catabolism of branched chain amino acids, along with possible changes in several other metabolic pathways (unpublished data). In particular, the up-regulation of glycolysis in K5-UCP3 epidermis is exceptionally interesting, given their tumor resistant phenotype and the large body of literature suggesting that up-regulation of aerobic glycolysis is paramount to tumor formation. More detailed, targeted metabolic studies to describe the flux of metabolites through specific pathways will add to our knowledge of how mitochondrial uncoupling affects nutrient utilization in this model, and may further inform not only our understanding of how UCP3-driven metabolic changes antagonize tumorigenesis, but also what exactly comprise the metabolic requirements for malignant transformation.

The data herein support the argument that mitochondrial uncoupling may be a uniquely powerful metabolic intervention because it simultaneously targets a broad repertoire of interconnected metabolic and signaling changes essential for tumorigenesis. Moreover, tumor cells often exhibit profound metabolic flexibility, utilizing a variety of

nutrient sources for both energy production and biosynthetic reactions, and as a result, many cancers are refractory to singly targeted metabolic therapies. Mitochondrial uncoupling likely restricts this flexibility by enforcing the constitutive oxidation of substrates, without concurrent ATP production. As our data indicate, uncoupled cells scavenge non-traditional nutrient sources, simultaneously limiting both the intermediates available for biomass production, along with growth signaling. Ultimately, the pleotropic effects of mitochondrial uncoupling provide a strategy to target both cancer cell metabolism and signaling, and may be a novel and effective therapeutic approach that circumvents many of the toxic manifestations of traditional chemotherapeutics.

Appendices

Appendix 1: Mouse Epidermal Keratinocyte Primary Culture Protocol

Mediums and Buffers:

Collagen Coating: no filtration, make up and store at 4°C, can be used repeatedly until gone.

MCDB 151-100mL: *Irvine Sci* (cat# 9061 or M6645)
Fibronectin-1mg (1 ampule): *Sigma* (cat# F-4759)
PureCol– 1mL: *Inamed Biomaterials* (cat# 5409)
BSA-10mg: *Sigma* (cat# A-3156)
HEPES-1mL of 2M HEPES: *Sigma* (cat# H-9135)

2.5% Trypsin (10X): *Gibco* (cat# 15090-046); 100mL/bottle, dilute 1:10 in sterile PBS for use.

22.5% Percoll:
100% Percoll: *Pharmacia* (cat# 17-0891-01, sterile); Invert the bottle to suspend particles before usage

For 400mL of 22.5% Percoll: 90mL Percoll + 10mL 1N NaCl (filtered) + 300mL PBS

*Store at 4°C. Invert several times before usage

Preparation: do this set up the day before the cell culture

1. Medium and Buffers
    a. Collagen Coating (4°C)
    b. 22.5% Percoll (4°C)
    c. 10X or 2.5% Trypsin (-20°C)
    d. Penn-Strep (-20°C)
    e. EMEM#2 medium (4°C)
    f. FBS (4°C)
    g. PBS (4°C)
2. Autoclave the following:
    a. Glassware: Numbers are for 2 genotype prep:
        a. 400 mL large beakers (2)
        b. 50 mL small beakers (4)
        c. 15 cm glass plate (1)
        d. 10 cm glass plates (# mice/3 for each genotype + 2)
        e. Glass funnels (2)

f. 100 mL bottle or Erlenmeyer flask (for preparing dilute trypsin)

3. Turn on UV light in the hood O/N

Preparation: <u>do this set up on the day of the cell culture</u>

1. Soak the following in a 400mL beaker filled with 70% EtOH & place in cell culture hood; Make sure to rinse tools in 1X PBS once they are taken out of this 70% EtOH beaker and before they are used on the animals
    a. Scissors (1)
    b. Forceps (2)
    c. #22/23 Scalpel (1)
    d. Polypropylene monofilament mesh: *Small Parts, Inc*. (cat# CMP149-C) (1 per genotype)
    e. Small stir bars (1 per genotype)

2. Fill the second 400 mL beaker with sterile PBS in cell culture hood.

3. Wipe down hood with 70% EtOH
4. Put out in the cell culture hood: 1 large glass petri dish (150mm); plastic petri dishes (100mm) for scraping (1dish/mouse); glass petri dishes for floating (1dish/3mice).

5. Dilute Pen-Strep 1:50 in PBS in 50mL beakers (1 per each genotype).
   Dilute 2.5% (10X) Trypsin 1:10 in PBS – 5mL Trypsin/45mL PBS (~15mL needed to cover bottom of each glass petri dish).

6. Set out large plastic beaker near sink with betadine and 70% ethanol for sterilizing mice, set up a bench pad with clippers and Nair for hair removal.

<u>Procedure:</u>

7. Sacrifice mice using cervical dislocation or CO_2.

8. Shave mice (if not done 2 days prior) and apply Nair for ~1min. Rinse off Nair with tap water & gentle massaging, then place mouse in betadine beaker so that it is completely covered.

9. Once all mice are in betadine, rinse out container with tap water until solution is clear (some of the betadine will stick to the hair that is left on the mouse, but try and get rid of most of it).

10. Rinse 2X with 70% EtOH (don't rinse with water between these rinses). Dry animals with absorbent bench pad & place in hood.

11. Placing animals in 150mm dish one at a time (and dabbing off excess EtOH), remove dorsal skins with scissors and place in small beaker w/PBS + Pen-Strep.
    *Rinse tools in 1xPBS after being soaked in 70% EtOH and before using on mice.
    *Use long cutting strokes to prevent tearing during the scraping process

*If you become unsure of sterilization of anything-put it back in EtOH!!!

12. Spread skin out with hair side down in 100mm plastic petri dish. Scrape fat and connective tissue away until skin is almost translucent. BE CAREFUL, it is very easy to tear a hole in the skin.
    IMPORTANT Epidermis will not separate if all fat is not removed.

13. Transfer skin to the cover of the plastic petri dish (the lid of the dish that the skin was scraped in) with **hair side up (this means that you have to flip the skins over)**, spread out completely, and let dry for less than 10min. Often 2-3 skins can be scaped and set to dry before the first one is ready to transfer to the 1X Trypsin.

14. Transfer semi-dried skin (hair side still up) to the glass petri dish (3 skins/dish) filled with a thin layer of 0.25% (1X) Trypsin (anywhere from 15-25mL is fine as long as it covers the bottom of the dish).
    *The skins need to be floating with no edges curled under.
    *Try to remove all large air bubbles.

15. Place the glass dishes in 37°C incubator for 45 min – 1 hour. Then transfer dishes to cell culture hood and let stand at RT for 1 hour.
    *Skins should not sit on trypsin for more than 3hrs total. I have found that even going past 2 hours seems to decrease viability.

16. If cells will be cultured after isolation, during this incubation coat dishes w/collegen mixture and allow to dry for 1hr in the hood; drying with the lids slightly open. Use ~0.5mL/dish; add all to first dish and coat, then transfer to next dish and coat, and transfer to next dish, etc.
    *Okay to leave for 2.25hrs; completely dry when you see crystals

17. Make EMEM#2 + 10% FBS: 5mL FBS + 45mL EMEM-2 per genotype, store at 4˚C.

18. Prop up one edge of a small glass petri dish and add 3 mL of cold EMEM#2 + 10% FBS. Place a piece of incubated skin (hair side up) on the dish **above** the medium, and hold it about the medium with forceps.

19. Using a scalpel (perpendicular to the skin) and forceps, lightly scrape epidermis into the medium. The epidermis should come off as a sheet of tissue. You do not want to contaminate the media in the dish with fibroblasts, so do not let the piece of skin fall down into the media; keep at top of tilted dish.
    *Don't force the scape if the epidermis won't come off easily or the fibroblasts will be pushed out and they will destroy the culture
    *Be careful. The epidermis will "roll up" at the end of the scrape
    *Use the same plate for all skins from the same genotype.

20. Carefully transfer the epidermal scrapings to a 50mL beaker. Don't pipette because the tissue will all just get stuck in the pipette or tip, it is better to just pour from the petri dish directly

into the beaker. Rinse the dish with 7 mL EMEM#2 + 10% FBS, and transfer that to beaker as well (total volume in beaker should be 10 mL media).

21. Mince the epidermis slightly with dissecting scissors for 5 min. Set a timer, you will want to stop early and the tissue will not be completely dissociated. Add medium up to ~30mL total.

22. Add the sterile stir bar and stir gently for 30 min. Stir as slow as possible, but make sure that it doesn't stop.

23. When samples are done stirring, take the mesh out of the EtOH and shake, then (rinse in 1XPBS beaker, shake) twice until mostly dry. Place mesh in the glass funnel on top of a 50mL conical tube and strain cells through nylon mesh.

24. Spin cells at 1000rpm (~250g) for 10min at 4C. While samples are spinning, prepare Percoll tubes: 20 mL of 22.5% Percoll/6 mice/50 mL conical tube.

25. Suck off supernatant and re-suspend each pellet in 2 mL cold EMEM#2 + 10% FBS per Percoll gradient to be loaded from this cell pellet. So, if you started with ~12 mice then re-suspend in 4 mL total because you need to split it between 2 Percoll gradient tubes. Make sure cells are very well re-suspended; you want a single cell suspension before the Percoll gradient.

26. Slowly add 2 mL cell suspension per Percoll gradient tube. Swirl Percoll well before using in order to distribute colloidal particles. Tilt the tube at a 30˚ angle and break the surface tension with the pipetter tip. Release the cell suspension about ½ inch above the Percoll and release slowly so that the solution runs down the side of the conical tube and layers on top of the Percoll. Be careful since the cells have a tendency to clump. Do not make bubbles.

27. Spin up to 1000 rpm with slow acceleration & no brake for 15min total at 4˚C. For this Mills lab centrifuge this is done by setting the accel and decel to 1 (the lowest setting).

28. When samples are done spinning, quickly remove ALL the Percoll with a pipet from the top to the bottom. Don't let them sit in the Percoll.

29. Re-suspend cell pellet(s) in 10 mL EMEM#2 +1% FBS and transfer all the cells to a new 15 mL conical tube. If you have split samples of the same genotype across multiple tubes for the Percoll gradient, you can recombine them at this step.

30. Spin at 1000rpm for 10 min at 4˚C.

31. Suck off supernatant with a pipet and resuspend cell pellet in 5-10 mL EMEM#2 + 1% FBS. I like to use the # of mL equal to the number of mice I started with for each genotype so it is easy to figure out how many cells I harvested per mouse.

32. Count the cells using a hemacytometer or Coulter counter

33. For convenience you can adjust the cell suspension to 1 or 2 million cells/mL. Normally 8-10 million cells are plated per 10 cm dish, or 2-3 million per well of a 6-well plate.

34. The cells can be transported back to Austin if the prep is done in Science Park. Cory had written down that they were fine at RT during the drive but I remember her doing it with them on ice, so keeping them cold might be better.

The Next Day:

35. Remove the plating medium and wash the plates twice with sterile 1x PBS.

36. Replace with fresh EMEM#2 + 1% FBS.

The cells should be ~90% confluent at day 3 or 4 depending on if 8-10million cells were originally plated. The EMEM-2 media allows the adult keratinocytes to sit down and grow properly.

Appendix 2: Neonatal Human Primary Keratinocyte Culture Protocol

Mediums and Buffers:

Keratinocyte Serum Free Media:

Add Bovine Pituitary Extract and EGF Supplement that come with the media, mix well. Store at 4°C.

HBSS + Na Bicarb + HEPES:

Dilute 50 mL of 10x stock of HBSS (w/o Bicarb, Gibco #14060-057) to 1x with 450 mL autoclaved Millipore water.
Add 5 mL of 7.5% Sodium Bicarbonate (tissue culture grade)
Add 5 mL of 1 M HEPES
Filter sterilize & store at 4°C.

Dispase Solution:

Place 50 mL of HBSS + Na Bicarb + HEPES in a conical tube and add 5 μL of 50 mg/mL Gentamicin, 2 μL of 250 μg/mL Fungizone, and 500 mg Dispase (Final concentrations = 5 μg/mL Gentamicin, 10 mg/mL Dispase).
Filter sterilize with a 0.2 μm syringe filter to exclude any bacterial remnants in Dispase. Store at 4°C.

Stop Media:
DMEM cell culture media
10% FBS (100 mL for 1 L media)
1% Pen-strep (10 mL for 1 L media)
0.1% Gentamicin (1 mL for 1 L media)

Preparation:

1.) Fill several 15 mL conical tubes with EMEM#2 media + 1:10,000 dilution of Gentamicin. For 20 tubes, I will make 100 mL media + 10 μL Gentamicin, and aliquot 5 mL per tube. If you are short on media, 3 mL per tube is ok.
2.) Take tubes to the hospital. The charge nurse will call when there are several specimens ready to pick up.

Procedure:

3.) Sterilize scissors and foreceps in beaker of 70% ethanol.
4.) Place 2-3 mL of Dispase solution in each well of a 6-well plate, or alternatively use 35 mm petri dishes.
5.) Use a 10 cm petri dish as a sterile surface to work with the foreskin.
6.) Flatten out foreskin by snipping open the ring of tissue. Trim the tissue to ensure that it lays flat and to remove extraneous fat/muscle that may still be attached to the underside of the tissue. If sample is big, it may help to cut it in half.
7.) Place sample skin side up in the well/dish with dispase solution.
8.) Cover and place at 4°C overnight (16-18 hours). Don't let them incubate too long or it will decrease cell viability.
9.) Clean hood WELL with bleach and then 70% ethanol. This is human tissue and is Biohazardous and potentially infectious. The hospital is not supposed to give us anything that is HIV+ or HepC+ but you can never be too careful.

The Next Day:

10.) Sterilize forceps and scissors in 70% ethanol.
11.) Place foreskin in culture dish and peel away epidermis. Place the epidermis in a 50 mL conical tube.
12.) Add 5 mL of Trypsin-EDTA (0.25% Trypsin, 1 mM EDTA). Swirl to immerse. Place in 37°C incubator for 5-7 minutes. Gently swirl half way through incubation.
13.) After incubation, add 30 mL Stop Media. Swirl to mix.
14.) Centrifuge at 3000 x g for 10 minutes.
15.) Aspirate media. At this point there may be particles floating in the media. These are not live cells but part of the cornified layer and can be aspirated with the media.
16.) Resuspend the cells in 10-30 mL of KSFM.
17.) Plate cells in 1-3 10 cm cell culture dishes or 1 T75 flask, depending on the size of the cell pellet and how dense you want the cells to be.
18.) Allow to grow 2-3 days at 37°C, or until cells are 80% confluent.

Continue to culture as you would with a normal cell line until cells are expanded enough to use for experiments.

References

Abel, E.L., Angel, J.M., Kiguchi, K., and DiGiovanni, J. (2009). Multi-stage chemical carcinogenesis in mouse skin: fundamentals and applications. Nature protocols *4*, 1350-1362.

Alonso, L., and Fuchs, E. (2003). Stem cells of the skin epithelium. Proc Natl Acad Sci U S A *100 Suppl 1*, 11830-11835.

Alonso, L., and Fuchs, E. (2006). The hair cycle. Journal of cell science *119*, 391-393.

Anderson, E.J., Yamazaki, H., and Neufer, P.D. (2007). Induction of endogenous uncoupling protein 3 suppresses mitochondrial oxidant emission during fatty acid-supported respiration. The Journal of biological chemistry *282*, 31257-31266.

Arsenijevic, D., Onuma, H., Pecqueur, C., Raimbault, S., Manning, B.S., Miroux, B., Couplan, E., Alves-Guerra, M.C., Goubern, M., Surwit, R., et al. (2000). Disruption of the uncoupling protein-2 gene in mice reveals a role in immunity and reactive oxygen species production. Nature genetics *26*, 435-439.

Ashcroft, F.M., and Gribble, F.M. (1999). ATP-sensitive K+ channels and insulin secretion: their role in health and disease. Diabetologia *42*, 903-919.

Barreiro, E., Garcia-Martinez, C., Mas, S., Ametller, E., Gea, J., Argiles, J.M., Busquets, S., and Lopez-Soriano, F.J. (2009). UCP3 overexpression neutralizes oxidative stress rather than nitrosative stress in mouse myotubes. FEBS letters *583*, 350-356.

Battalora, M.S., Spalding, J.W., Szczesniak, C.J., Cape, J.E., Morris, R.J., Trempus, C.S., Bortner, C.D., Lee, B.M., and Tennant, R.W. (2001). Age-dependent skin tumorigenesis and transgene expression in the Tg.AC (v-Ha-ras) transgenic mouse. Carcinogenesis *22*, 651-659.

Bauer, D.E., Hatzivassiliou, G., Zhao, F., Andreadis, C., and Thompson, C.B. (2005). ATP citrate lyase is an important component of cell growth and transformation. Oncogene *24*, 6314-6322.

Beis, I., and Newsholme, E.A. (1975). The contents of adenine nucleotides, phosphagens and some glycolytic intermediates in resting muscles from vertebrates and invertebrates. The Biochemical journal *152*, 23-32.

Benitah, S.A., Frye, M., Glogauer, M., and Watt, F.M. (2005). Stem cell depletion through epidermal deletion of Rac1. Science *309*, 933-935.

Bensaad, K., Tsuruta, A., Selak, M.A., Vidal, M.N., Nakano, K., Bartrons, R., Gottlieb, E., and Vousden, K.H. (2006). TIGAR, a p53-inducible regulator of glycolysis and apoptosis. Cell *126*, 107-120.

Berg, J.M., Tymoczko, J.L., and Stryer, L. (2002). Biochemistry, Fifth Edition. (W.H. Freeman).

Bergstrom, J., Furst, P., Noree, L.O., and Vinnars, E. (1974). Intracellular free amino acid concentration in human muscle tissue. Journal of applied physiology *36*, 693-697.

Bernardi, P., Paradisi, V., Pozzan, T., and Azzone, G.F. (1984). Pathway for uncoupler-induced calcium efflux in rat-liver mitochondria - inhibition by rutheium red. Biochemistry *23*, 1645-1651.

Berwick, D.C., Hers, I., Heesom, K.J., Moule, S.K., and Tavare, J.M. (2002). The identification of ATP-citrate lyase as a protein kinase B (Akt) substrate in primary adipocytes. The Journal of biological chemistry *277*, 33895-33900.

Bezaire, V., Hofmann, W., Kramer, J.K., Kozak, L.P., and Harper, M.E. (2001). Effects of fasting on muscle mitochondrial energetics and fatty acid metabolism in Ucp3(-/-) and wild-type mice. American journal of physiology. Endocrinology and metabolism *281*, E975-982.

Bezaire, V., Spriet, L.L., Campbell, S., Sabet, N., Gerrits, M., Bonen, A., and Harper, M.-E. (2005). Constitutive UCP3 overexpression at physiological levels increases mouse skeletal muscle capacity for fatty acid transport and oxidation. The FASEB Journal.

Biswas, G., Adebanjo, O.A., Freedman, B.D., Anandatheerthavarada, H.K., Vijayasarathy, C., Zaidi, M., Kotlikoff, M., and Avadhani, N.G. (1999). Retrograde Ca2+ signaling in C2C12 skeletal myocytes in response to mitochondrial genetic and metabolic stress: a novel mode of inter-organelle crosstalk. The EMBO journal *18*, 522-533.

Boland, M.L., Chourasia, A.H., and Macleod, K.F. (2013). Mitochondrial Dysfunction in Cancer. Frontiers in Oncology *3*.

Bollag, W.B. (2009). Protein kinase Calpha puts the hand cuffs on epidermal keratinocyte proliferation. The Journal of investigative dermatology *129*, 2330-2332.

Boss, O., Samec, S., Paoloni-Giacobino, A., Rossier, C., Dulloo, A., Seydoux, J., Muzzin, P., and Giacobino, J.P. (1997). Uncoupling protein-3: a new member of the mitochondrial carrier family with tissue-specific expression. FEBS letters *408*, 39-42.

Bouillaud, F., Ricquier, D., Thibault, J., and Weissenbach, J. (1985). Molecular approach to thermogenesis in brown adipose tissue: cDNA cloning of the mitochondrial uncoupling protein. Proc Natl Acad Sci U S A *82*, 445-448.

Bourdon, A., Minai, L., Serre, V., Jais, J.P., Sarzi, E., Aubert, S., Chretien, D., de Lonlay, P., Paquis-Flucklinger, V., Arakawa, H., et al. (2007). Mutation of RRM2B, encoding p53-controlled ribonucleotide reductase (p53R2), causes severe mitochondrial DNA depletion. Nature genetics *39*, 776-780.

Bowser, D.N., Minamikawa, T., Nagley, P., and Williams, D.A. (1998). Role of mitochondria in calcium regulation of spontaneously contracting cardiac muscle cells. Biophysical journal *75*, 2004-2014.

Boyer, P.D. (1993). The binding change mechanism for ATP synthase--some probabilities and possibilities. Biochimica et biophysica acta *1140*, 215-250.

Brand, M.D., Brindle, K.M., Buckingham, J.A., Harper, J.A., Rolfe, D.F., and Stuart, J.A. (1999). The significance and mechanism of mitochondrial proton conductance. Int J Obes Relat Metab Disord *23 Suppl 6*, S4-11.

Brand, M.D., Pakay, J.L., Ocloo, A., Kokoszka, J., Wallace, D.C., Brookes, P.S., and Cornwall, E.J. (2005). The basal proton conductance of mitochondria depends on adenine nucleotide translocase content. The Biochemical journal *392*, 353-362.

Brazil, D.P., Yang, Z.Z., and Hemmings, B.A. (2004). Advances in protein kinase B signalling: AKTion on multiple fronts. Trends in biochemical sciences *29*, 233-242.

Bricker, D.K., Taylor, E.B., Schell, J.C., Orsak, T., Boutron, A., Chen, Y.C., Cox, J.E., Cardon, C.M., Van Vranken, J.G., Dephoure, N., et al. (2012). A mitochondrial pyruvate carrier required for pyruvate uptake in yeast, Drosophila, and humans. Science *337*, 96-100.

Brookes, P.S., Parker, N., Buckingham, J.A., Vidal-Puig, A., Halestrap, A.P., Gunter, T.E., Nicholls, D.G., Bernardi, P., Lemasters, J.J., and Brand, M.D. (2008). UCPs - unlikely calcium porters. Nature Cell Biology *10*, 1235-1237.

Buzzai, M., Bauer, D.E., Jones, R.G., Deberardinis, R.J., Hatzivassiliou, G., Elstrom, R.L., and Thompson, C.B. (2005). The glucose dependence of Akt-transformed cells can be reversed by pharmacologic activation of fatty acid beta-oxidation. Oncogene *24*, 4165-4173.

Cannon, B., Hedin, A., and Nedergaard, J. (1982). Exclusive occurrence of thermogenin antigen in brown adipose tissue. FEBS letters *150*, 129-132.

Caspary, F., Elliott, G., Nave, B.T., Verzaal, P., Rohrbach, M., Das, P.K., Nagelkerken, L., and Nieland, J.D. (2005). A new therapeutic approach to treat psoriasis by inhibition of fatty acid oxidation by Etomoxir. The British journal of dermatology *153*, 937-944.

Chan, C.B., Saleh, M.C., Koshkin, V., and Wheeler, M.B. (2004a). Uncoupling protein 2 and islet function. Diabetes *53 Suppl 1*, S136-142.

Chan, K.S., Carbajal, S., Kiguchi, K., Clifford, J., Sano, S., and DiGiovanni, J. (2004b). Epidermal growth factor receptor-mediated activation of Stat3 during multistage skin carcinogenesis. Cancer research *64*, 2382-2389.

Chan, S.L., Liu, D., Kyriazis, G.A., Bagsiyao, P., Ouyang, X., and Mattson, M.P. (2006). Mitochondrial uncoupling protein-4 regulates calcium homeostasis and sensitivity to store depletion-induced apoptosis in neural cells. The Journal of biological chemistry *281*, 37391-37403.

Chen, N., Ma, W.Y., She, Q.B., Wu, E., Liu, G., Bode, A.M., and Dong, Z. (2001). Transactivation of the epidermal growth factor receptor is involved in 12-O-tetradecanoylphorbol-13-acetate-induced signal transduction. The Journal of biological chemistry *276*, 46722-46728.

Cheng, T., Sudderth, J., Yang, C., Mullen, A.R., Jin, E.S., Mates, J.M., and DeBerardinis, R.J. (2011). Pyruvate carboxylase is required for glutamine-independent growth of tumor cells. Proc Natl Acad Sci U S A *108*, 8674-8679.

Cheranov, S.Y., and Jaggar, J.H. (2004). Mitochondrial modulation of Ca2+ sparks and transient KCa currents in smooth muscle cells of rat cerebral arteries. The Journal of physiology *556*, 755-771.

Cho, Y.M., Kwon, S., Pak, Y.K., Seol, H.W., Choi, Y.M., Park do, J., Park, K.S., and Lee, H.K. (2006). Dynamic changes in mitochondrial biogenesis and antioxidant

enzymes during the spontaneous differentiation of human embryonic stem cells. Biochemical and biophysical research communications *348*, 1472-1478.

Chowdhury, H.H., Rebolj, K., Kreft, M., Zorec, R., Macek, P., and Sepcic, K. (2008). Lysophospholipids prevent binding of a cytolytic protein ostreolysin to cholesterol-enriched membrane domains. Toxicon : official journal of the International Society on Toxinology *51*, 1345-1356.

Christofk, H.R., Vander Heiden, M.G., Harris, M.H., Ramanathan, A., Gerszten, R.E., Wei, R., Fleming, M.D., Schreiber, S.L., and Cantley, L.C. (2008a). The M2 splice isoform of pyruvate kinase is important for cancer metabolism and tumour growth. Nature *452*, 230-233.

Christofk, H.R., Vander Heiden, M.G., Wu, N., Asara, J.M., and Cantley, L.C. (2008b). Pyruvate kinase M2 is a phosphotyrosine-binding protein. Nature *452*, 181-186.

Chung, S., Arrell, D.K., Faustino, R.S., Terzic, A., and Dzeja, P.P. (2010). Glycolytic network restructuring integral to the energetics of embryonic stem cell cardiac differentiation. Journal of molecular and cellular cardiology *48*, 725-734.

Clark, J., Anderson, K.E., Juvin, V., Smith, T.S., Karpe, F., Wakelam, M.J., Stephens, L.R., and Hawkins, P.T. (2011). Quantification of PtdInsP3 molecular species in cells and tissues by mass spectrometry. Nature methods *8*, 267-272.

Claudinot, S., Nicolas, M., Oshima, H., Rochat, A., and Barrandon, Y. (2005). Long-term renewal of hair follicles from clonogenic multipotent stem cells. Proc Natl Acad Sci U S A *102*, 14677-14682.

Coburn, C.T., Knapp, F.F., Jr., Febbraio, M., Beets, A.L., Silverstein, R.L., and Abumrad, N.A. (2000). Defective uptake and utilization of long chain fatty acids in muscle and adipose tissues of CD36 knockout mice. The Journal of biological chemistry *275*, 32523-32529.

Cohen, A.L., Holmen, S.L., and Colman, H. (2013). IDH1 and IDH2 mutations in gliomas. Current neurology and neuroscience reports *13*, 345.

Cornelissen, L.H., Oomens, C.W., Huyghe, J.M., and Baaijens, F.P. (2007). Mechanisms that play a role in the maintenance of the calcium gradient in the epidermis. Skin research and technology : official journal of International Society for Bioengineering and the Skin *13*, 369-376.

Corradetti, M.N., Inoki, K., Bardeesy, N., DePinho, R.A., and Guan, K.L. (2004). Regulation of the TSC pathway by LKB1: evidence of a molecular link between tuberous sclerosis complex and Peutz-Jeghers syndrome. Genes & development *18*, 1533-1538.

Cory, J.G., and Cory, A.H. (2006). Critical roles of glutamine as nitrogen donors in purine and pyrimidine nucleotide synthesis: asparaginase treatment in childhood acute lymphoblastic leukemia. In vivo (Athens, Greece) *20*, 587-589.

Cotsarelis, G., Sun, T.T., and Lavker, R.M. (1990). Label-retaining cells reside in the bulge area of pilosebaceous unit: implications for follicular stem cells, hair cycle, and skin carcinogenesis. Cell *61*, 1329-1337.

Cox, B., and Emili, A. (2006). Tissue subcellular fractionation and protein extraction for use in mass-spectrometry-based proteomics. Nature protocols *1*, 1872-1878.

Dang, C.V., Lewis, B.C., Dolde, C., Dang, G., and Shim, H. (1997). Oncogenes in tumor metabolism, tumorigenesis, and apoptosis. Journal of bioenergetics and biomembranes *29*, 345-354.

Dang, C.V., and Semenza, G.L. (1999). Oncogenic alterations of metabolism. Trends in biochemical sciences *24*, 68-72.

de Koning, T.J., Duran, M., Dorland, L., Gooskens, R., Van Schaftingen, E., Jaeken, J., Blau, N., Berger, R., and Poll-The, B.T. (1998). Beneficial effects of L-serine and glycine in the management of seizures in 3-phosphoglycerate dehydrogenase deficiency. Annals of neurology *44*, 261-265.

DeBerardinis, R.J., and Cheng, T. (2010). Q's next: the diverse functions of glutamine in metabolism, cell biology and cancer. Oncogene *29*, 313-324.

DeBerardinis, R.J., Lum, J.J., Hatzivassiliou, G., and Thompson, C.B. (2008). The biology of cancer: metabolic reprogramming fuels cell growth and proliferation. Cell metabolism *7*, 11-20.

Deberardinis, R.J., Lum, J.J., and Thompson, C.B. (2006). Phosphatidylinositol 3-kinase-dependent modulation of carnitine palmitoyltransferase 1A expression regulates lipid metabolism during hematopoietic cell growth. The Journal of biological chemistry *281*, 37372-37380.

DeBerardinis, R.J., Mancuso, A., Daikhin, E., Nissim, I., Yudkoff, M., Wehrli, S., and Thompson, C.B. (2007). Beyond aerobic glycolysis: transformed cells can engage in glutamine metabolism that exceeds the requirement for protein and nucleotide synthesis. Proc Natl Acad Sci U S A *104*, 19345-19350.

Deprez, J., Vertommen, D., Alessi, D.R., Hue, L., and Rider, M.H. (1997). Phosphorylation and activation of heart 6-phosphofructo-2-kinase by protein kinase B and other protein kinases of the insulin signaling cascades. The Journal of biological chemistry *272*, 17269-17275.

Derdak, Z., Fulop, P., Sabo, E., Tavares, R., Berthiaume, E.P., Resnick, M.B., Paragh, G., Wands, J.R., and Baffy, G. (2006). Enhanced colon tumor induction in uncoupling protein-2 deficient mice is associated with NF-kappaB activation and oxidative stress. Carcinogenesis *27*, 956-961.

Derdak, Z., Mark, N.M., Beldi, G., Robson, S.C., Wands, J.R., and Baffy, G. (2008). The mitochondrial uncoupling protein-2 promotes chemoresistance in cancer cells. Cancer research *68*, 2813-2819.

DiGiovanni, J., Bol, D.K., Wilker, E., Beltran, L., Carbajal, S., Moats, S., Ramirez, A., Jorcano, J., and Kiguchi, K. (2000). Constitutive expression of insulin-like growth factor-1 in epidermal basal cells of transgenic mice leads to spontaneous tumor promotion. Cancer research *60*, 1561-1570.

Dombrauckas, J.D., Santarsiero, B.D., and Mesecar, A.D. (2005). Structural basis for tumor pyruvate kinase M2 allosteric regulation and catalysis. Biochemistry *44*, 9417-9429.

Eagle, H. (1955). Nutrition needs of mammalian cells in tissue culture. Science *122*, 501-514.

Eaton, S. (2002). Control of mitochondrial beta-oxidation flux. Progress in lipid research *41*, 197-239.

Echtay, K.S., Murphy, M.P., Smith, R.A., Talbot, D.A., and Brand, M.D. (2002a). Superoxide activates mitochondrial uncoupling protein 2 from the matrix side. Studies using targeted antioxidants. The Journal of biological chemistry *277*, 47129-47135.

Echtay, K.S., Roussel, D., St-Pierre, J., Jekabsons, M.B., Cadenas, S., Stuart, J.A., Harper, J.A., Roebuck, S.J., Morrison, A., Pickering, S., et al. (2002b). Superoxide activates mitochondrial uncoupling proteins. Nature *415*, 96-99.

Elstrom, R.L., Bauer, D.E., Buzzai, M., Karnauskas, R., Harris, M.H., Plas, D.R., Zhuang, H., Cinalli, R.M., Alavi, A., Rudin, C.M., et al. (2004). Akt stimulates aerobic glycolysis in cancer cells. Cancer research *64*, 3892-3899.

Enerback, S., Jacobsson, A., Simpson, E.M., Guerra, C., Yamashita, H., Harper, M.E., and Kozak, L.P. (1997). Mice lacking mitochondrial uncoupling protein are cold-sensitive but not obese. Nature *387*, 90-94.

Esteves, T.C., and Brand, M.D. (2005). The reactions catalysed by the mitochondrial uncoupling proteins UCP2 and UCP3. Biochimica et biophysica acta *1709*, 35-44.

Ezashi, T., Das, P., and Roberts, R.M. (2005). Low O2 tensions and the prevention of differentiation of hES cells. Proceedings of the National Academy of Sciences of the United States of America *102*, 4783-4788.

Fantin, V.R., St-Pierre, J., and Leder, P. (2006). Attenuation of LDH-A expression uncovers a link between glycolysis, mitochondrial physiology, and tumor maintenance. Cancer cell *9*, 425-434.

Faurschou, A., Haedersdal, M., Poulsen, T., and Wulf, H.C. (2007). Squamous cell carcinoma induced by ultraviolet radiation originates from cells of the hair follicle in mice. Exp Dermatol *16*, 485-489.

Febbraio, M., Abumrad, N.A., Hajjar, D.P., Sharma, K., Cheng, W., Pearce, S.F., and Silverstein, R.L. (1999). A null mutation in murine CD36 reveals an important role in fatty acid and lipoprotein metabolism. The Journal of biological chemistry *274*, 19055-19062.

Fedorenko, A., Lishko, P.V., and Kirichok, Y. (2012). Mechanism of fatty-acid-dependent UCP1 uncoupling in brown fat mitochondria. Cell *151*, 400-413.

Feldmann, H.M., Golozoubova, V., Cannon, B., and Nedergaard, J. (2009). UCP1 ablation induces obesity and abolishes diet-induced thermogenesis in mice exempt from thermal stress by living at thermoneutrality. Cell metabolism *9*, 203-209.

Fleury, C., Neverova, M., Collins, S., Raimbault, S., Champigny, O., Levi-Meyrueis, C., Bouillaud, F., Seldin, M.F., Surwit, R.S., Ricquier, D., et al. (1997). Uncoupling protein-2: a novel gene linked to obesity and hyperinsulinemia. Nature genetics *15*, 269-272.

Frauwirth, K.A., Riley, J.L., Harris, M.H., Parry, R.V., Rathmell, J.C., Plas, D.R., Elstrom, R.L., June, C.H., and Thompson, C.B. (2002). The CD28 signaling pathway regulates glucose metabolism. Immunity *16*, 769-777.

Fuchs, E., and Green, H. (1980). Changes in keratin gene expression during terminal differentiation of the keratinocyte. Cell *19*, 1033-1042.

Gao, P., Tchernyshyov, I., Chang, T.C., Lee, Y.S., Kita, K., Ochi, T., Zeller, K.I., De Marzo, A.M., Van Eyk, J.E., Mendell, J.T., et al. (2009). c-Myc suppression of miR-23a/b enhances mitochondrial glutaminase expression and glutamine metabolism. Nature *458*, 762-765.

Garcia-Martinez, C., Sibille, B., Solanes, G., Darimont, C., Mace, K., Villarroya, F., and Gomez-Foix, A.M. (2001). Overexpression of UCP3 in cultured human muscle lowers mitochondrial membrane potential, raises ATP/ADP ratio, and favors fatty acid vs. glucose oxidation. FASEB journal : official publication of the Federation of American Societies for Experimental Biology *15*, 2033-2035.

Gates, A.C., Bernal-Mizrachi, C., Chinault, S.L., Feng, C., Schneider, J.G., Coleman, T., Malone, J.P., Townsend, R.R., Chakravarthy, M.V., and Semenkovich, C.F. (2007). Respiratory uncoupling in skeletal muscle delays death and diminishes age-related disease. Cell metabolism *6*, 497-505.

Golozoubova, V., Hohtola, E., Matthias, A., Jacobsson, A., Cannon, B., and Nedergaard, J. (2001). Only UCP1 can mediate adaptive nonshivering thermogenesis in the cold. FASEB journal : official publication of the Federation of American Societies for Experimental Biology *15*, 2048-2050.

Gong, D.W., Monemdjou, S., Gavrilova, O., Leon, L.R., Marcus-Samuels, B., Chou, C.J., Everett, C., Kozak, L.P., Li, C., Deng, C., et al. (2000). Lack of obesity and normal response to fasting and thyroid hormone in mice lacking uncoupling protein-3. The Journal of biological chemistry *275*, 16251-16257.

Gottlob, K., Majewski, N., Kennedy, S., Kandel, E., Robey, R.B., and Hay, N. (2001). Inhibition of early apoptotic events by Akt/PKB is dependent on the first committed step of glycolysis and mitochondrial hexokinase. Genes & development *15*, 1406-1418.

Grzelczyk, A., and Gendaszewska-Darmach, E. (2013). Novel bioactive glycerol-based lysophospholipids: new data -- new insight into their function. Biochimie *95*, 667-679.

Gu, Z., Wu, J., Wang, S., Suburu, J., Chen, H., Thomas, M.J., Shi, L., Edwards, I.J., Berquin, I.M., and Chen, Y.Q. (2013). Polyunsaturated fatty acids affect the localization and signaling of PIP3/AKT in prostate cancer cells. Carcinogenesis *34*, 1968-1975.

Guigal, N., Rodriguez, M., Cooper, R.N., Dromaint, S., Di Santo, J.P., Mouly, V., Boutin, J.A., and Galizzi, J.P. (2002). Uncoupling protein-3 (UCP3) mRNA expression in reconstituted human muscle after myoblast transplantation in RAG2-/-/gamma c/C5(-) immunodeficient mice. The Journal of biological chemistry *277*, 47407-47411.

Gwinn, D.M., Shackelford, D.B., Egan, D.F., Mihaylova, M.M., Mery, A., Vasquez, D.S., Turk, B.E., and Shaw, R.J. (2008). AMPK phosphorylation of raptor mediates a metabolic checkpoint. Molecular cell *30*, 214-226.

Hanahan, D., and Weinberg, R.A. (2000). The hallmarks of cancer. Cell *100*, 57-70.

Hanahan, D., and Weinberg, R.A. (2011). Hallmarks of cancer: the next generation. Cell *144*, 646-674.

Hanai, J., Doro, N., Sasaki, A.T., Kobayashi, S., Cantley, L.C., Seth, P., and Sukhatme, V.P. (2012). Inhibition of lung cancer growth: ATP citrate lyase knockdown and statin treatment leads to dual blockade of mitogen-activated protein kinase (MAPK) and phosphatidylinositol-3-kinase (PI3K)/AKT pathways. Journal of cellular physiology *227*, 1709-1720.

Hatzivassiliou, G., Zhao, F., Bauer, D.E., Andreadis, C., Shaw, A.N., Dhanak, D., Hingorani, S.R., Tuveson, D.A., and Thompson, C.B. (2005). ATP citrate lyase inhibition can suppress tumor cell growth. Cancer cell *8*, 311-321.

Hedeskov, C.J. (1968). Early effects of phytohaemagglutinin on glucose metabolism of normal human lymphocytes. The Biochemical journal *110*, 373-380.

Herrlich, A., Klinman, E., Fu, J., Sadegh, C., and Lodish, H. (2008). Ectodomain cleavage of the EGF ligands HB-EGF, neuregulin1-beta, and TGF-alpha is specifically triggered by different stimuli and involves different PKC isoenzymes. FASEB journal : official publication of the Federation of American Societies for Experimental Biology *22*, 4281-4295.

Himms-Hagen, J., and Harper, M.E. (2001). Physiological role of UCP3 may be export of fatty acids from mitochondria when fatty acid oxidation predominates: an hypothesis. Experimental biology and medicine (Maywood, N.J.) *226*, 78-84.

Hirasaka, K., Lago, C.U., Kenaston, M.A., Fathe, K., Nowinski, S.M., Nikawa, T., and Mills, E.M. (2011). Identification of a redox-modulatory interaction between uncoupling protein 3 and thioredoxin 2 in the mitochondrial intermembrane space. Antioxidants & redox signaling *15*, 2645-2661.

Holley, R.W., and Kiernan, J.A. (1974). Control of the Initiation of DNA Synthesis in 3T3 Cells: Low-Molecular-Weight Nutrients. Proceedings of the National Academy of Sciences *71*, 2942-2945.

Horimoto, M., Resnick, M.B., Konkin, T.A., Routhier, J., Wands, J.R., and Baffy, G. (2004). Expression of Uncoupling Protein-2 in Human Colon Cancer. Clinical Cancer Research *10*, 6203-6207.

Hudson, C.C., Liu, M., Chiang, G.G., Otterness, D.M., Loomis, D.C., Kaper, F., Giaccia, A.J., and Abraham, R.T. (2002). Regulation of hypoxia-inducible factor 1alpha expression and function by the mammalian target of rapamycin. Mol Cell Biol *22*, 7004-7014.

Ishikawa, K., Takenaga, K., Akimoto, M., Koshikawa, N., Yamaguchi, A., Imanishi, H., Nakada, K., Honma, Y., and Hayashi, J. (2008). ROS-generating mitochondrial DNA mutations can regulate tumor cell metastasis. Science *320*, 661-664.

Ito, M., Liu, Y., Yang, Z., Nguyen, J., Liang, F., Morris, R.J., and Cotsarelis, G. (2005a). Stem cells in the hair follicle bulge contribute to wound repair but not to homeostasis of the epidermis. Nat Med *11*, 1351-1354.

Ito, M., Liu, Y., Yang, Z., Nguyen, J., Liang, F., Morris, R.J., and Cotsarelis, G. (2005b). Stem cells in the hair follicle bulge contribute to wound repair but not to homeostasis of the epidermis. Nature medicine *11*, 1351-1354.

Jerome-Morais, A., Rahn, H.R., Tibudan, S.S., and Denning, M.F. (2009). Role for protein kinase C-alpha in keratinocyte growth arrest. The Journal of investigative dermatology *129*, 2365-2375.

Kaplan, R.S., Mayor, J.A., and Wood, D.O. (1993). The mitochondrial tricarboxylate transport protein. cDNA cloning, primary structure, and comparison with other mitochondrial transport proteins. The Journal of biological chemistry *268*, 13682-13690.

Kessler, R.J., Tyson, C.A., and Green, D.E. (1976). Mechanism of uncoupling in mitochondria: uncouplers as ionophores for cycling cations and protons. Proceedings of the National Academy of Sciences of the United States of America *73*, 3141-3145.

Kiguchi, K., Beltran, L., Rupp, T., and DiGiovanni, J. (1998). Altered expression of epidermal growth factor receptor ligands in tumor promoter-treated mouse epidermis and in primary mouse skin tumors induced by an initiation-promotion protocol. Molecular carcinogenesis *22*, 73-83.

Klingenberg, M., and Appel, M. (1989). The uncoupling protein dimer can form a disulfide cross-link between the mobile C-terminal SH groups. European journal of biochemistry / FEBS *180*, 123-131.

Kopec, B., and Fritz, I.B. (1971). Properties of a purified carnitine palmitoyltransferase, and evidence for the existence of other carnitine acyltransferases. Canadian journal of biochemistry *49*, 941-948.

Kopec, B., and Fritz, I.B. (1973). Comparison of properties of carnitine palmitoyltransferase I with those of carnitine palmitoyltransferase II, and preparation of antibodies to carnitine palmitoyltransferases. The Journal of biological chemistry *248*, 4069-4074.

Kovacevic, Z., and Morris, H.P. (1972). The role of glutamine in the oxidative metabolism of malignant cells. Cancer research *32*, 326-333.

Krauss, S., Zhang, C.-Y., and Lowell, B.B. (2005). The mitochondrial uncoupling-protein homologues. Nature Reviews Molecular Cell Biology *6*, 248-261.

Kretschmer, M., Klose, J., and Kronstad, J.W. (2012). Defects in mitochondrial and peroxisomal beta-oxidation influence virulence in the maize pathogen Ustilago maydis. Eukaryotic cell *11*, 1055-1066.

Lago, C.U., Nowinski, S.M., Rundhaug, J.E., Pfeiffer, M.E., Kiguchi, K., Hirasaka, K., Yang, X., Abramson, E.M., Bratton, S.B., Rho, O., et al. (2012). Mitochondrial respiratory uncoupling promotes keratinocyte differentiation and blocks skin carcinogenesis. Oncogene *31*, 4725-4731.

Launonen, V., Vierimaa, O., Kiuru, M., Isola, J., Roth, S., Pukkala, E., Sistonen, P., Herva, R., and Aaltonen, L.A. (2001). Inherited susceptibility to uterine leiomyomas and renal cell cancer. Proc Natl Acad Sci U S A *98*, 3387-3392.

Lawley, P.D. (1994). Historical origins of current concepts of carcinogenesis. Advances in cancer research *65*, 17-111.

Leder, A., Kuo, A., Cardiff, R.D., Sinn, E., and Leder, P. (1990). v-Ha-ras transgene abrogates the initiation step in mouse skin tumorigenesis: effects of phorbol esters and retinoic acid. Proc Natl Acad Sci U S A *87*, 9178-9182.

Li, L., and Clevers, H. Coexistence of quiescent and active adult stem cells in mammals. Science (New York, N.Y *327*, 542-545.

Li, L., Ren, C.H., Tahir, S.A., Ren, C., and Thompson, T.C. (2003). Caveolin-1 Maintains Activated Akt in Prostate Cancer Cells through Scaffolding Domain Binding Site Interactions with and Inhibition of Serine/Threonine Protein Phosphatases PP1 and PP2A. Molecular and Cellular Biology *23*, 9389-9404.

Li, X., Monks, B., Ge, Q., and Birnbaum, M.J. (2007). Akt/PKB regulates hepatic metabolism by directly inhibiting PGC-1alpha transcription coactivator. Nature *447*, 1012-1016.

Liang, C.C., You, L.R., Chang, J.L., Tsai, T.F., and Chen, C.M. (2009). Transgenic mice exhibiting inducible and spontaneous Cre activities driven by a bovine keratin 5 promoter that can be used for the conditional analysis of basal epithelial cells in multiple organs. Journal of biomedical science *16*, 2.

Lin, C.S., Hackenberg, H., and Klingenberg, E.M. (1980). The uncoupling protein from brown adipose tissue mitochondria is a dimer. A hydrodynamic study. FEBS letters *113*, 304-306.

Liu, Y., Lyle, S., Yang, Z., and Cotsarelis, G. (2003). Keratin 15 promoter targets putative epithelial stem cells in the hair follicle bulge. The Journal of investigative dermatology *121*, 963-968.

Liu, Y.C., Li, F., Handler, J., Huang, C.R., Xiang, Y., Neretti, N., Sedivy, J.M., Zeller, K.I., and Dang, C.V. (2008). Global regulation of nucleotide biosynthetic genes by c-Myc. PloS one *3*, e2722.

Lockshon, D., Surface, L.E., Kerr, E.O., Kaeberlein, M., and Kennedy, B.K. (2007). The sensitivity of yeast mutants to oleic acid implicates the peroxisome and other processes in membrane function. Genetics *175*, 77-91.

Lunt, S.Y., and Vander Heiden, M.G. (2011). Aerobic glycolysis: meeting the metabolic requirements of cell proliferation. Annual review of cell and developmental biology *27*, 441-464.

Luo, Y., Bond, J.D., and Ingram, V.M. (1997). Compromised mitochondrial function leads to increased cytosolic calcium and to activation of MAP kinases. Proceedings of the National Academy of Sciences of the United States of America *94*, 9705-9710.

Macheda, M.L., Rogers, S., and Best, J.D. (2005). Molecular and cellular regulation of glucose transporter (GLUT) proteins in cancer. Journal of cellular physiology *202*, 654-662.

MacLellan, J.D., Gerrits, M.F., Gowing, A., Smith, P.J., Wheeler, M.B., and Harper, M.E. (2005). Physiological increases in uncoupling protein 3 augment fatty acid oxidation and decrease reactive oxygen species production without uncoupling respiration in muscle cells. Diabetes *54*, 2343-2350.

Majumder, P.K., Febbo, P.G., Bikoff, R., Berger, R., Xue, Q., McMahon, L.M., Manola, J., Brugarolas, J., McDonnell, T.J., Golub, T.R., et al. (2004). mTOR inhibition reverses Akt-dependent prostate intraepithelial neoplasia through regulation of apoptotic and HIF-1-dependent pathways. Nature medicine *10*, 594-601.

Mannava, S., Grachtchouk, V., Wheeler, L.J., Im, M., Zhuang, D., Slavina, E.G., Mathews, C.K., Shewach, D.S., and Nikiforov, M.A. (2008). Direct role of nucleotide metabolism in C-MYC-dependent proliferation of melanoma cells. Cell cycle *7*, 2392-2400.

Manning, B.D., and Cantley, L.C. (2007). AKT/PKB signaling: navigating downstream. Cell *129*, 1261-1274.

Mardis, E.R., Ding, L., Dooling, D.J., Larson, D.E., McLellan, M.D., Chen, K., Koboldt, D.C., Fulton, R.S., Delehaunty, K.D., McGrath, S.D., et al. (2009). Recurring mutations found by sequencing an acute myeloid leukemia genome. The New England journal of medicine *361*, 1058-1066.

Masui, K., Cavenee, W.K., and Mischel, P.S. (2014). mTORC2 in the center of cancer metabolic reprogramming. Trends in endocrinology and metabolism: TEM.

Matoba, S., Kang, J.G., Patino, W.D., Wragg, A., Boehm, M., Gavrilova, O., Hurley, P.J., Bunz, F., and Hwang, P.M. (2006). p53 regulates mitochondrial respiration. Science *312*, 1650-1653.

Mazurek, S. (2011). Pyruvate kinase type M2: a key regulator of the metabolic budget system in tumor cells. The international journal of biochemistry & cell biology *43*, 969-980.

Medina, R.A., and Owen, G.I. (2002). Glucose transporters: expression, regulation and cancer. Biological research *35*, 9-26.

Menon, G.K., Grayson, S., and Elias, P.M. (1985). Ionic calcium reservoirs in mammalian epidermis: ultrastructural localization by ion-capture cytochemistry. The Journal of investigative dermatology *84*, 508-512.

Mills, E.M., Banks, M.L., Sprague, J.E., and Finkel, T. (2003). Pharmacology: uncoupling the agony from ecstasy. Nature *426*, 403-404.

Mills, E.M., Xu, D., Fergusson, M.M., Combs, C.A., Xu, Y., and Finkel, T. (2002). Regulation of cellular oncosis by uncoupling protein 2. The Journal of biological chemistry *277*, 27385-27392.

Miyamoto, S., Murphy, A.N., and Brown, J.H. (2008). Akt mediates mitochondrial protection in cardiomyocytes through phosphorylation of mitochondrial hexokinase-II. Cell death and differentiation *15*, 521-529.

Moreno-Sanchez, R., Rodriguez-Enriquez, S., Marin-Hernandez, A., and Saavedra, E. (2007). Energy metabolism in tumor cells. The FEBS journal *274*, 1393-1418.

Mori, S., Yoshizuka, N., Takizawa, M., Takema, Y., Murase, T., Tokimitsu, I., and Saito, M. (2008a). Expression of uncoupling proteins in human skin and skin-derived cells. Journal of Investigative Dermatology *128*, 1894-1900.

Mori, S., Yoshizuka, N., Takizawa, M., Takema, Y., Murase, T., Tokimitsu, I., and Saito, M. (2008b). Expression of Uncoupling Proteins in Human Skin and Skin-Derived Cells. The Journal of investigative dermatology.

Morris, R.J. (2000). Keratinocyte stem cells: targets for cutaneous carcinogens. The Journal of clinical investigation *106*, 3-8.

Morris, R.J., Fischer, S.M., Klein-Szanto, A.J., and Slaga, T.J. (1990). Subpopulations of primary adult murine epidermal basal cells sedimented on density gradients. Cell and tissue kinetics *23*, 587-602.

Morris, R.J., Tryson, K.A., and Wu, K.Q. (2000). Evidence that the epidermal targets of carcinogen action are found in the interfollicular epidermis of infundibulum as well as in the hair follicles. Cancer Res *60*, 226-229.

Mullen, A.R., Wheaton, W.W., Jin, E.S., Chen, P.H., Sullivan, L.B., Cheng, T., Yang, Y., Linehan, W.M., Chandel, N.S., and DeBerardinis, R.J. (2012). Reductive carboxylation supports growth in tumour cells with defective mitochondria. Nature *481*, 385-388.

Murata, H., Ihara, Y., Nakamura, H., Yodoi, J., Sumikawa, K., and Kondo, T. (2003). Glutaredoxin exerts an antiapoptotic effect by regulating the redox state of Akt. The Journal of biological chemistry *278*, 50226-50233.

Naito, M., Naito, Y., and DiGiovanni, J. (1987). Comparison of the histological changes in the skin of DBA/2 and C57BL/6 mice following exposure to various promoting agents. Carcinogenesis *8*, 1807-1815.

Navarro, P., Gomez, M., Pizarro, A., Gamallo, C., Quintanilla, M., and Cano, A. (1991). A role for the E-cadherin cell-cell adhesion molecule during tumor progression of mouse epidermal carcinogenesis. The Journal of cell biology *115*, 517-533.

NCI (2014). SEER Cancer Statistics Factsheets: All Cancer Sites. National Cancer Institute. Bethesda, MD.

Neumann, H.P., Pawlu, C., Peczkowska, M., Bausch, B., McWhinney, S.R., Muresan, M., Buchta, M., Franke, G., Klisch, J., Bley, T.A., et al. (2004). Distinct clinical features of paraganglioma syndromes associated with SDHB and SDHD gene mutations. Jama *292*, 943-951.

Nicholls, D.G. (1976). The bioenergetics of brown adipose tissue mitochondria. FEBS letters *61*, 103-110.

Nicholls, D.G., and Ward, M.W. (2000). Mitochondrial membrane potential and neuronal glutamate excitotoxicity: mortality and millivolts. Trends in neurosciences *23*, 166-174.

Okamura, S., Ng, C.C., Koyama, K., Takei, Y., Arakawa, H., Monden, M., and Nakamura, Y. (1999). Identification of seven genes regulated by wild-type p53 in a colon cancer cell line carrying a well-controlled wild-type p53 expression system. Oncology research *11*, 281-285.

Osthus, R.C., Shim, H., Kim, S., Li, Q., Reddy, R., Mukherjee, M., Xu, Y., Wonsey, D., Lee, L.A., and Dang, C.V. (2000). Deregulation of glucose transporter 1 and glycolytic gene expression by c-Myc. The Journal of biological chemistry *275*, 21797-21800.

Owen, O.E., Kalhan, S.C., and Hanson, R.W. (2002). The key role of anaplerosis and cataplerosis for citric acid cycle function. The Journal of biological chemistry *277*, 30409-30412.

Pardee, A.B. (1974). A Restriction Point for Control of Normal Animal Cell Proliferation. Proceedings of the National Academy of Sciences *71*, 1286-1290.

Parlo, R.A., and Coleman, P.S. (1984). Enhanced rate of citrate export from cholesterol-rich hepatoma mitochondria. The truncated Krebs cycle and other metabolic ramifications of mitochondrial membrane cholesterol. The Journal of biological chemistry *259*, 9997-10003.

Pecqueur, C., Alves-Guerra, M.C., Gelly, C., Levi-Meyrueis, C., Couplan, E., Collins, S., Ricquier, D., Bouillaud, F., and Miroux, B. (2001). Uncoupling protein 2, in vivo distribution, induction upon oxidative stress, and evidence for translational regulation. The Journal of biological chemistry *276*, 8705-8712.

Pedersen, P.L. (1978). Tumor mitochondria and the bioenergetics of cancer cells. Progress in experimental tumor research. Fortschritte der experimentellen Tumorforschung *22*, 190-274.

Pedersen, P.L., Greenawalt, J.W., Chan, T.L., and Morris, H.P. (1970). A comparison of some ultrastructural and biochemical properties of mitochondria from Morris hepatomas 9618A, 7800, and 3924A. Cancer research *30*, 2620-2626.

Pelicano, H., Xu, R.H., Du, M., Feng, L., Sasaki, R., Carew, J.S., Hu, Y.M., Ramdas, L., Hu, L.M., Keating, M.J., et al. (2006). Mitochondrial respiration defects in cancer cells cause activation of Akt survival pathway through a redox-mediated mechanism. Journal of Cell Biology *175*, 913-923.

Petros, J.A., Baumann, A.K., Ruiz-Pesini, E., Amin, M.B., Sun, C.Q., Hall, J., Lim, S., Issa, M.M., Flanders, W.D., Hosseini, S.H., et al. (2005). mtDNA mutations increase tumorigenicity in prostate cancer. Proc Natl Acad Sci U S A *102*, 719-724.

Pfeiffer, M., Kayzer, E.B., Yang, X., Abramson, E., Kenaston, M.A., Lago, C.U., Lo, H.H., Sedensky, M.M., Lunceford, A., Clarke, C.F., et al. (2011). Caenorhabditis elegans UCP4 protein controls complex II-mediated oxidative phosphorylation through succinate transport. The Journal of biological chemistry *286*, 37712-37720.

Pfeiffer, T., Schuster, S., and Bonhoeffer, S. (2001). Cooperation and competition in the evolution of ATP-producing pathways. Science *292*, 504-507.

Pinton, P., Tsuboi, T., Ainscow, E.K., Pozzan, T., Rizzuto, R., and Rutter, G.A. (2002). Dynamics of glucose-induced membrane recruitment of protein kinase C beta II in living pancreatic islet beta-cells. The Journal of biological chemistry *277*, 37702-37710.

Polyak, K., Li, Y., Zhu, H., Lengauer, C., Willson, J.K., Markowitz, S.D., Trush, M.A., Kinzler, K.W., and Vogelstein, B. (1998). Somatic mutations of the mitochondrial genome in human colorectal tumours. Nature genetics *20*, 291-293.

Portais, J.C., Voisin, P., Merle, M., and Canioni, P. (1996). Glucose and glutamine metabolism in C6 glioma cells studied by carbon 13 NMR. Biochimie *78*, 155-164.

Pozzan, T., Bragadin, M., and Azzone, G.F. (1977). Disequilibrium between steady-state Ca2+ accumulation ratio and membrane potential in mitochondria. Pathway and role of Ca2+ efflux. Biochemistry *16*, 5618-5625.

Rao, S., and Coleman, P.S. (1989). Control of DNA replication and cell growth by inhibiting the export of mitochondrially derived citrate. Experimental cell research *180*, 341-352.

Rathmell, J.C., Fox, C.J., Plas, D.R., Hammerman, P.S., Cinalli, R.M., and Thompson, C.B. (2003). Akt-Directed Glucose Metabolism Can Prevent Bax Conformation Change and Promote Growth Factor-Independent Survival. Molecular and Cellular Biology *23*, 7315-7328.

Reinacher, M., and Eigenbrodt, E. (1981). Immunohistological demonstration of the same type of pyruvate kinase isoenzyme (M2-Pk) in tumors of chicken and rat. Virchows Archiv. B, Cell pathology including molecular pathology *37*, 79-88.

Reitzer, L.J., Wice, B.M., and Kennell, D. (1979). Evidence that glutamine, not sugar, is the major energy source for cultured HeLa cells. The Journal of biological chemistry *254*, 2669-2676.

Rhee, S.G., Bae, Y.S., Lee, S.R., and Kwon, J. (2000). Hydrogen peroxide: a key messenger that modulates protein phosphorylation through cysteine oxidation. Science's STKE : signal transduction knowledge environment *2000*, pe1.

Rial, E., and Nicholls, D.G. (1984). The mitochondrial uncoupling protein from guinea-pig brown adipose tissue. Synchronous increase in structural and functional parameters during cold-adaptation. The Biochemical journal *222*, 685-693.

Rice, R.H., and Green, H. (1979). Presence in human epidermal cells of a soluble protein precursor of the cross-linked envelope: activation of the cross-linking by calcium ions. Cell *18*, 681-694.

Rodriguez-Puebla, M.L., Robles, A.I., Johnson, D.G., LaCava, M., and Conti, C.J. (1998). Synchronized proliferation induced by 12-O-tetradecanoylphorbol-13-acetate treatment of mouse skin: an in vivo model for cell cycle regulation. Cell growth & differentiation : the molecular biology journal of the American Association for Cancer Research *9*, 31-39.

Rundhaug, J.E., Gimenez-Conti, I., Stern, M.C., Budunova, I.V., Kiguchi, K., Bol, D.K., Coghlan, L.G., Conti, C.J., DiGiovanni, J., Fischer, S.M., et al. (1997a). Changes in protein expression during multistage mouse skin carcinogenesis. Mol Carcinog *20*, 125-136.

Rundhaug, J.E., Gimenez-Conti, I., Stern, M.C., Budunova, I.V., Kiguchi, K., Bol, D.K., Coghlan, L.G., Conti, C.J., DiGiovanni, J., Fischer, S.M., et al. (1997b). Changes in protein expression during multistage mouse skin carcinogenesis. Molecular carcinogenesis *20*, 125-136.

Rundhaug, J.E., Park, J., Pavone, A., Opdenakker, G., and Fischer, S.M. (1997c). Opposite effect of stable transfection of bioactive transforming growth factor-beta 1 (TGF beta 1) versus exogenous TGF beta 1 treatment on expression of 92-kDa type IV collagenase in mouse skin squamous cell carcinoma CH72 cells. Molecular carcinogenesis *19*, 122-136.

Rundhaug, J.E., Pavone, A., Kim, E., and Fischer, S.M. (2007). The effect of cyclooxygenase-2 overexpression on skin carcinogenesis is context dependent. Molecular carcinogenesis *46*, 981-992.

Sancak, Y., Bar-Peled, L., Zoncu, R., Markhard, A.L., Nada, S., and Sabatini, D.M. (2010). Ragulator-Rag complex targets mTORC1 to the lysosomal surface and is necessary for its activation by amino acids. Cell *141*, 290-303.

Sancak, Y., Peterson, T.R., Shaul, Y.D., Lindquist, R.A., Thoreen, C.C., Bar-Peled, L., and Sabatini, D.M. (2008). The Rag GTPases bind raptor and mediate amino acid signaling to mTORC1. Science *320*, 1496-1501.

Sanchis, D., Fleury, C., Chomiki, N., Goubern, M., Huang, Q., Neverova, M., Gregoire, F., Easlick, J., Raimbault, S., Levi-Meyrueis, C., et al. (1998). BMCP1, a novel mitochondrial carrier with high expression in the central nervous system of humans and rodents, and respiration uncoupling activity in recombinant yeast. The Journal of biological chemistry *273*, 34611-34615.

Sandoval, M.E. (1980). Studies on the relationship between Ca2+ efflux from mitochondria and the release of amino acid neurotransmitters. Brain research *181*, 357-367.

Saraste, M. (1999). Oxidative phosphorylation at the fin de siecle. Science *283*, 1488-1493.

Schieke, S.M., Ma, M., Cao, L., McCoy, J.P., Jr., Liu, C., Hensel, N.F., Barrett, A.J., Boehm, M., and Finkel, T. (2008). Mitochondrial metabolism modulates differentiation and teratoma formation capacity in mouse embryonic stem cells. The Journal of biological chemistry *283*, 28506-28512.

Schuppel, M., Kurschner, U., Kleuser, U., Schafer-Korting, M., and Kleuser, B. (2008). Sphingosine 1-phosphate restrains insulin-mediated keratinocyte proliferation via inhibition of Akt through the S1P(2) receptor subtype. Journal of Investigative Dermatology *128*, 1747-1756.

Segrelles, C., Lu, J., Hammann, B., Santos, M., Moral, M., Cascallana, J.L., Lara, M.F., Rho, O., Carbajal, S., Traag, J., et al. (2007). Deregulated activity of Akt in epithelial basal cells induces spontaneous tumors and heightened sensitivity to skin carcinogenesis. Cancer research *67*, 10879-10888.

Selak, M.A., Armour, S.M., MacKenzie, E.D., Boulahbel, H., Watson, D.G., Mansfield, K.D., Pan, Y., Simon, M.C., Thompson, C.B., and Gottlieb, E. (2005). Succinate links TCA cycle dysfunction to oncogenesis by inhibiting HIF-alpha prolyl hydroxylase. Cancer cell *7*, 77-85.

Semenza, G.L. (2000). HIF-1 and human disease: one highly involved factor. Genes & development *14*, 1983-1991.

Semenza, G.L., Roth, P.H., Fang, H.M., and Wang, G.L. (1994). Transcriptional regulation of genes encoding glycolytic enzymes by hypoxia-inducible factor 1. The Journal of biological chemistry *269*, 23757-23763.

Senapedis, W.T., Kennedy, C.J., Boyle, P.M., and Silver, P.A. (2011). Whole genome siRNA cell-based screen links mitochondria to Akt signaling network through uncoupling of electron transport chain. Molecular biology of the cell *22*, 1791-1805.

Senese, R., Valli, V., Moreno, M., Lombardi, A., Busiello, R.A., Cioffi, F., Silvestri, E., Goglia, F., Lanni, A., and de Lange, P. (2011). Uncoupling protein 3 expression levels influence insulin sensitivity, fatty acid oxidation, and related signaling pathways. Pflugers Archiv : European journal of physiology *461*, 153-164.

Shim, H., Dolde, C., Lewis, B.C., Wu, C.S., Dang, G., Jungmann, R.A., Dalla-Favera, R., and Dang, C.V. (1997). c-Myc transactivation of LDH-A: implications for tumor metabolism and growth. Proc Natl Acad Sci U S A *94*, 6658-6663.

Sokolova, I.M., and Sokolov, E.P. (2005). Evolution of mitochondrial uncoupling proteins: novel invertebrate UCP homologues suggest early evolutionary divergence of the UCP family. FEBS letters *579*, 313-317.

Spitkovsky, D., Sasse, P., Kolossov, E., Bottinger, C., Fleischmann, B.K., Hescheler, J., and Wiesner, R.J. (2004). Activity of complex III of the mitochondrial electron transport chain is essential for early heart muscle cell differentiation. Faseb J *18*, 1300-1302.

Sprague, J.E., Yang, X., Sommers, J., Gilman, T.L., and Mills, E.M. (2007). Roles of norepinephrine, free Fatty acids, thyroid status, and skeletal muscle uncoupling protein 3 expression in sympathomimetic-induced thermogenesis. The Journal of pharmacology and experimental therapeutics *320*, 274-280.

Srere, P.A. (1972). The citrate enzymes: their structures, mechanisms, and biological functions. Current topics in cellular regulation *5*, 229-283.

St John, J.C., Ramalho-Santos, J., Gray, H.L., Petrosko, P., Rawe, V.Y., Navara, C.S., Simerly, C.R., and Schatten, G.P. (2005). The expression of mitochondrial DNA transcription factors during early cardiomyocyte in vitro differentiation from human embryonic stem cells. Cloning and stem cells *7*, 141-153.

Steck, T.L., Kaufman, S., and Bader, J.P. (1968). Glycolysis in chick embryo cell cultures transformed by Rous sarcoma virus. Cancer research *28*, 1611-1619.

Stout, A.K., Raphael, H.M., Kanterewicz, B.I., Klann, E., and Reynolds, I.J. (1998). Glutamate-induced neuron death requires mitochondrial calcium uptake. Nature neuroscience *1*, 366-373.

Su, W.P., Lo, Y.C., Yan, J.J., Liao, I.C., Tsai, P.J., Wang, H.C., Yeh, H.H., Lin, C.C., Chen, H.H., Lai, W.W., et al. (2012). Mitochondrial uncoupling protein 2 regulates the effects of paclitaxel on Stat3 activation and cellular survival in lung cancer cells. Carcinogenesis *33*, 2065-2075.

Sullivan, A.C., Triscari, J., Hamilton, J.G., Miller, O.N., and Wheatley, V.R. (1974). Effect of (-)-hydroxycitrate upon the accumulation of lipid in the rat. I. Lipogenesis. Lipids *9*, 121-128.

Sundqvist, A., Bengoechea-Alonso, M.T., Ye, X., Lukiyanchuk, V., Jin, J., Harper, J.W., and Ericsson, J. (2005). Control of lipid metabolism by phosphorylation-dependent degradation of the SREBP family of transcription factors by SCF(Fbw7). Cell metabolism *1*, 379-391.

Taha, C., Liu, Z., Jin, J., Al-Hasani, H., Sonenberg, N., and Klip, A. (1999). Opposite translational control of GLUT1 and GLUT4 glucose transporter mRNAs in response to insulin. Role of mammalian target of rapamycin, protein kinase b, and phosphatidylinositol 3-kinase in GLUT1 mRNA translation. The Journal of biological chemistry *274*, 33085-33091.

Tamiji, S., Beauvillain, J.C., Mortier, L., Jouy, N., Tual, M., Delaporte, E., Formstecher, P., Marchetti, P., and Polakowska, R. (2005). Induction of apoptosis-like mitochondrial impairment triggers antioxidant and Bcl-2-dependent keratinocyte differentiation. The Journal of investigative dermatology *125*, 647-658.

Taylor, G., Lehrer, M.S., Jensen, P.J., Sun, T.T., and Lavker, R.M. (2000). Involvement of follicular stem cells in forming not only the follicle but also the epidermis. Cell *102*, 451-461.

Teshima, Y., Akao, M., Jones, S.P., and Marban, E. (2003). Uncoupling protein-2 overexpression inhibits mitochondrial death pathway in cardiomyocytes. Circulation research *93*, 192-200.

Theriot, C.M., Koenigsknecht, M.J., Carlson, P.E., Jr., Hatton, G.E., Nelson, A.M., Li, B., Huffnagle, G.B., J, Z.L., and Young, V.B. (2014). Antibiotic-induced shifts in the mouse gut microbiome and metabolome increase susceptibility to Clostridium difficile infection. Nature communications *5*, 3114.

Thomas, S.A., and Palmiter, R.D. (1997). Thermoregulatory and metabolic phenotypes of mice lacking noradrenaline and adrenaline. Nature *387*, 94-97.

Tomlinson, I.P., Alam, N.A., Rowan, A.J., Barclay, E., Jaeger, E.E., Kelsell, D., Leigh, I., Gorman, P., Lamlum, H., Rahman, S., et al. (2002). Germline mutations in FH predispose to dominantly inherited uterine fibroids, skin leiomyomata and papillary renal cell cancer. Nature genetics *30*, 406-410.

Tong, X., Zhao, F., and Thompson, C.B. (2009). The molecular determinants of de novo nucleotide biosynthesis in cancer cells. Current opinion in genetics & development *19*, 32-37.

Trempus, C.S., Morris, R.J., Bortner, C.D., Cotsarelis, G., Faircloth, R.S., Reece, J.M., and Tennant, R.W. (2003). Enrichment for living murine keratinocytes from the hair follicle bulge with the cell surface marker CD34. The Journal of investigative dermatology *120*, 501-511.

Trempus, C.S., Morris, R.J., Ehinger, M., Elmore, A., Bortner, C.D., Ito, M., Cotsarelis, G., Nijhof, J.G., Peckham, J., Flagler, N., et al. (2007). CD34 expression by hair follicle stem cells is required for skin tumor development in mice. Cancer Res *67*, 4173-4181.

Trenker, M., Malli, R., Fertschai, I., Levak-Frank, S., and Graier, W.F. (2007). Uncoupling proteins 2 and 3 are fundamental for mitochondrial Ca2+ uniport. Nature Cell Biology *9*, 445-U156.

Tu, C.L., Oda, Y., Komuves, L., and Bikle, D.D. (2004). The role of the calcium-sensing receptor in epidermal differentiation. Cell calcium *35*, 265-273.

Turrens, J.F. (2003). Mitochondrial formation of reactive oxygen species. The Journal of physiology *552*, 335-344.

Turrens, J.F., Freeman, B.A., Levitt, J.G., and Crapo, J.D. (1982). The effect of hyperoxia on superoxide production by lung submitochondrial particles. Archives of biochemistry and biophysics *217*, 401-410.

Vander Heiden, M.G., Cantley, L.C., and Thompson, C.B. (2009). Understanding the Warburg effect: the metabolic requirements of cell proliferation. Science *324*, 1029-1033.

Vander Heiden, M.G., Lunt, S.Y., Dayton, T.L., Fiske, B.P., Israelsen, W.J., Mattaini, K.R., Vokes, N.I., Stephanopoulos, G., Cantley, L.C., Metallo, C.M., et al. (2011). Metabolic pathway alterations that support cell proliferation. Cold Spring Harbor symposia on quantitative biology *76*, 325-334.

Vander Heiden, M.G., Plas, D.R., Rathmell, J.C., Fox, C.J., Harris, M.H., and Thompson, C.B. (2001). Growth factors can influence cell growth and survival through effects on glucose metabolism. Mol Cell Biol *21*, 5899-5912.

Vidal-Puig, A., Solanes, G., Grujic, D., Flier, J.S., and Lowell, B.B. (1997). UCP3: an uncoupling protein homologue expressed preferentially and abundantly in skeletal muscle and brown adipose tissue. Biochemical and biophysical research communications *235*, 79-82.

Vidal-Puig, A.J., Grujic, D., Zhang, C.Y., Hagen, T., Boss, O., Ido, Y., Szczepanik, A., Wade, J., Mootha, V., Cortright, R., et al. (2000). Energy metabolism in uncoupling protein 3 gene knockout mice. The Journal of biological chemistry *275*, 16258-16266.

Villegas-Comonfort, S., Castillo-Sanchez, R., Serna-Marquez, N., Cortes-Reynosa, P., and Salazar, E.P. (2014). Arachidonic acid promotes migration and invasion through a PI3K/Akt-dependent pathway in MDA-MB-231 breast cancer cells. Prostaglandins, leukotrienes, and essential fatty acids *90*, 169-177.

Wallace, D.C. (2005). Mitochondria and cancer: Warburg addressed. Cold Spring Harbor symposia on quantitative biology *70*, 363-374.

Wang, J.B., Erickson, J.W., Fuji, R., Ramachandran, S., Gao, P., Dinavahi, R., Wilson, K.F., Ambrosio, A.L., Dias, S.M., Dang, C.V., et al. (2010). Targeting mitochondrial glutaminase activity inhibits oncogenic transformation. Cancer cell *18*, 207-219.

Wang, T., Marquardt, C., and Foker, J. (1976). Aerobic glycolysis during lymphocyte proliferation. Nature *261*, 702-705.

Warburg, O. (1925). Über den Stoffwechsel der Carcinomzelle. Klin. Wochenschr *4*, 534-536.

Warburg, O. (1926). On the effect of hydrocyanic acid ethyl ester (ethyl-carbylamine) on the Pasteur reaction. Biochemische Zeitschrift *172*, 432-441.

Warburg, O. (1956a). On respiratory impairment in cancer cells. Science *124*, 269-270.

Warburg, O. (1956b). On the origin of cancer cells. Science *123*, 309-314.

Ward, P.S., Patel, J., Wise, D.R., Abdel-Wahab, O., Bennett, B.D., Coller, H.A., Cross, J.R., Fantin, V.R., Hedvat, C.V., Perl, A.E., et al. (2010). The common feature of leukemia-associated IDH1 and IDH2 mutations is a neomorphic enzyme activity converting alpha-ketoglutarate to 2-hydroxyglutarate. Cancer cell *17*, 225-234.

Ward, P.S., and Thompson, C.B. (2012). Signaling in control of cell growth and metabolism. Cold Spring Harbor perspectives in biology *4*, a006783.

Watt, F.M. (1984). Selective migration of terminally differentiating cells from the basal layer of cultured human epidermis. The Journal of cell biology *98*, 16-21.

Welter, J.F., Crish, J.F., Agarwal, C., and Eckert, R.L. (1995). Fos-related antigen (Fra-1), junB, and junD activate human involucrin promoter transcription by binding to proximal and distal AP1 sites to mediate phorbol ester effects on promoter activity. The Journal of biological chemistry *270*, 12614-12622.

Wise, D.R., DeBerardinis, R.J., Mancuso, A., Sayed, N., Zhang, X.Y., Pfeiffer, H.K., Nissim, I., Daikhin, E., Yudkoff, M., McMahon, S.B., et al. (2008). Myc regulates a transcriptional program that stimulates mitochondrial glutaminolysis and leads to glutamine addiction. Proc Natl Acad Sci U S A *105*, 18782-18787.

Wise, D.R., and Thompson, C.B. (2010). Glutamine addiction: a new therapeutic target in cancer. Trends in biochemical sciences *35*, 427-433.

Wu, M.C., Arimura, G.K., and Yunis, A.A. (1978). Mechanism of sensitivity of cultured pancreatic carcinoma to asparaginase. International journal of cancer. Journal international du cancer *22*, 728-733.

Wu, W.Y., and Morris, R.J. (2005). Method for the harvest and assay of in vitro clonogenic keratinocytes stem cells from mice. Methods Mol Biol *289*, 79-86.

Xian, W., Kiguchi, K., Imamoto, A., Rupp, T., Zilberstein, A., and DiGiovanni, J. (1995). Activation of the epidermal growth factor receptor by skin tumor promoters and in skin

tumors from SENCAR mice. Cell growth & differentiation : the molecular biology journal of the American Association for Cancer Research *6*, 1447-1455.

Yecies, J.L., Zhang, H.H., Menon, S., Liu, S., Yecies, D., Lipovsky, A.I., Gorgun, C., Kwiatkowski, D.J., Hotamisligil, G.S., Lee, C.H., et al. (2011). Akt stimulates hepatic SREBP1c and lipogenesis through parallel mTORC1-dependent and independent pathways. Cell metabolism *14*, 21-32.

Yoshida, K., Furuya, S., Osuka, S., Mitoma, J., Shinoda, Y., Watanabe, M., Azuma, N., Tanaka, H., Hashikawa, T., Itohara, S., et al. (2004). Targeted disruption of the mouse 3-phosphoglycerate dehydrogenase gene causes severe neurodevelopmental defects and results in embryonic lethality. The Journal of biological chemistry *279*, 3573-3577.

Yuneva, M., Zamboni, N., Oefner, P., Sachidanandam, R., and Lazebnik, Y. (2007). Deficiency in glutamine but not glucose induces MYC-dependent apoptosis in human cells. The Journal of cell biology *178*, 93-105.

Zenisek, D., and Matthews, G. (2000). The role of mitochondria in presynaptic calcium handling at a ribbon synapse. Neuron *25*, 229-237.

Zhang, C.Y., Baffy, G., Perret, P., Krauss, S., Peroni, O., Grujic, D., Hagen, T., Vidal-Puig, A.J., Boss, O., Kim, Y.B., et al. (2001). Uncoupling protein-2 negatively regulates insulin secretion and is a major link between obesity, beta cell dysfunction, and type 2 diabetes. Cell *105*, 745-755.

Zhang, H., Gao, P., Fukuda, R., Kumar, G., Krishnamachary, B., Zeller, K.I., Dang, C.V., and Semenza, G.L. (2007). HIF-1 inhibits mitochondrial biogenesis and cellular respiration in VHL-deficient renal cell carcinoma by repression of C-MYC activity. Cancer cell *11*, 407-420.

Zhao, S., Lin, Y., Xu, W., Jiang, W., Zha, Z., Wang, P., Yu, W., Li, Z., Gong, L., Peng, Y., et al. (2009). Glioma-derived mutations in IDH1 dominantly inhibit IDH1 catalytic activity and induce HIF-1alpha. Science *324*, 261-265.

Zhong, H., Chiles, K., Feldser, D., Laughner, E., Hanrahan, C., Georgescu, M.M., Simons, J.W., and Semenza, G.L. (2000). Modulation of hypoxia-inducible factor 1alpha expression by the epidermal growth factor/phosphatidylinositol 3-kinase/PTEN/AKT/FRAP pathway in human prostate cancer cells: implications for tumor angiogenesis and therapeutics. Cancer research *60*, 1541-1545.

Zhong, H., De Marzo, A.M., Laughner, E., Lim, M., Hilton, D.A., Zagzag, D., Buechler, P., Isaacs, W.B., Semenza, G.L., and Simons, J.W. (1999). Overexpression of hypoxia-inducible factor 1alpha in common human cancers and their metastases. Cancer research *59*, 5830-5835.

Zu, X.L., and Guppy, M. (2004). Cancer metabolism: facts, fantasy, and fiction. Biochemical and biophysical research communications *313*, 459-465.

Vita

Sara Marie Nowinski was born in Royal Oak, Michigan and raised in Sterling Heights, Michigan. Sara attended Henry Ford II High School and the Utica Center for Mathematics, Science, and Technology in Sterling Heights, Michigan and graduated *summa cum laude* in 2004. She then attended Carleton College in Northfield, Minnesota from 2004-2008, where she worked as a part time research assistant in the laboratory of Dr. Matt Rand, studying thermoregulatory and mating behavioral physiology in *Scleoporus consobrinus* and *Anolis carolinensis* lizards. Sara graduated from Carleton College *magna cum laude* with a Bachelor of Arts degree in Biology and a concentration in Biochemistry in June 2008. She entered the Graduate School in the Division of Pharmacology and Toxicology, College of Pharmacy at The University of Texas at Austin in July of the same year, and completed the work described in this body of literature under the mentorship of Dr. Ted Mills.

Permanent email address: sara.nowinski@gmail.com

This dissertation was typed by the author.